DISSERTATION

Titel der Dissertation

Mechanisms of transcriptional repression by EWS-FLI1 in Ewing Sarcoma

Verfasser

Mag.rer.nat. Stephan Niedan

angestrebter akademischer Grad

Doctor of Philosophy (PhD)

Wien, 2012

Table of contents

List of figures

Abstract

The EWS-FLI1 chimeric oncoprotein characterizing Ewing Sarcoma (ES) is a prototypic aberrant ETS transcription factor with activating and repressive gene regulatory functions. Mechanisms of transcriptional regulation, especially transcriptional repression by EWS-FLI1, are poorly understood. We report that EWS-FLI1 repressed promoters are enriched in forkhead box recognition motifs, and identify FOXO1 as a EWS-FLI1 suppressed master regulator responsible for a significant subset of EWS-FLI1 repressed genes. In addition to transcriptional FOXO1 regulation by direct promoter binding of EWS-FLI1, its subcellular localization and activity is regulated by CDK2 and AKT mediated phosphorylation downstream of EWS-FLI1. Functional restoration of nuclear FOXO1 expression in ES cells impaired proliferation and significantly reduced clonogenicity. Gene-expression profiling revealed a significant overlap between EWS-FLI1 repressed and FOXO1-activated genes. Treatment of ES cell lines with Methylseleninic acid (MSA) evoked reactivation of endogenous FOXO1 in the presence of EWS-FLI1 in a dose- and time-dependent manner and induced massive cell death which was found to be partially FOXO1-dependent. In an orthotopic xenograft mouse model, MSA increased FOXO1 expression in the tumor paralleled by a significant decrease in ES tumor growth. Together, these data suggest that a repressive sub-signature of EWS-FLI1 repressed genes precipitates suppression of FOXO1. FOXO1 re-activation by small molecules may therefore constitute a novel therapeutic strategy in the treatment of ES.

Zusammenfassung

Ewing Sarkome (ES), die am zweithäufigst auftretenden Tumore der Knochen und Weichteile bei Kindern und Jugendlichen, werden genetisch durch die Genfusion EWS-FLI1 als Folge einer chromosomalen Translokation charakterisiert. EWS-FLI1 kodiert für einen äusserst potenten Transkriptionsfaktor, welcher sowohl Gen aktivierende als auch Gen repremierende Eigenschaften besitzt. Obwohl EWS-FLI1 als transkriptioneller Hauptregulator in ES fungiert, ist dennoch nur sehr wenig über Mechanismen der Genregulation und im Speziellen, der transkriptionellen Repression bekannt. In dieser Arbeit konnte gezeigt werden, dass Promotoren von EWS-FLI1 reprimierten Genen eine Anreicherung von Motiven für Bindung von Forkhead Box Transkriptionsfaktoren zeigen. Des Weiteren konnte FOXO1 als ein EWS-FLI1 reprimierter transkriptioneller Meisterregulator identifiziert werden, welcher signifikant zur repressiven transkriptionellen Signatur von EWS-FLI1 beiträgt. FOXO1 wird dabei einerseits direkt durch Bindung von EWS-FLI1 an dessen Promotor transkriptionell, aber auch post-transkriptionell über inhibitorische Phosphorylierung durch CDK2 und AKT unterdrückt, welche die sub-zelluläre Lokalisation und somit die transkriptionelle Aktivität von FOXO1 regulieren. Durch die funktionelle Re-Expression von nukleärem FOXO1 konnte eine signifikant reduzierte Proliferation, als auch Klonogenizität in ES Zelllinien *in vitro* gezeigt werden. Profile von Experimenten zur Genexpression konnten zeigen, dass es eine signifikante Überlappung zwischen EWS-FLI1 reprimierten und FOXO1 aktivierten Genen gibt. Eine Reaktivierung von endogenen FOXO1 durch Verwendung von Methylselen Säure (MSA), im Beisein von EWS-FLI1, konnte eine Zeit- und Konzentrations-Abhängigkeit sowie Induktion von Zelltod, welcher zumindest teilweise auf die Reaktivierung von FOXO1 zurückzuführen ist, *in vitro* bewirken. Durch Verwendung eines orthotopen Maus Xenograft Modells konnte gezeigt werden, dass MSA behandelte Mäuse ein signifikant verringertes Tumor Wachstum und gleichzeitig erhöhte FOXO1 Expression aufweisen.

Zusammenfassend konnte gezeigt werden, dass eine EWS-FLI1 vermittelt repressive Sub-Signatur durch die Unterdrückung des Tumorsuppressors FOXO1 ausgelöst ist. Deshalb könnte die Reaktivierung von FOXO1 durch niedermolekulare Substanzen eine neue therapeutische Strategie zur Behandlung von ES Patienten darstellen.

1   Introduction

1.1   Cancer evolution

1.1.1 The progression model of cancer development

The current model of cancer development is based on the central tenet that it is a genetic disease (Figure 1). Tumors evolve as a consequence of somatically acquired mutations, including base substitution, insertions and deletions of bases, rearrangements and changes in the copy number of DNA segments, leading to clonal expansion of cells in an unregulated fashion (1). However, somatic mutations are believed to be essentially random and accumulate throughout the lifespan of an individual. The effect of such mutations can be potentially accelerated by exogenous carcinogens or DNA repair defects (2). Functionally, somatic mutations can be classified into 'passenger' or 'driver' mutations based on their capability to promote cancer development. Whereas passenger mutations do not contribute to cancer development because they are neither subject to genetic selection nor they confer growth advantage, driver mutations are causally implicated in oncogenesis. Driver mutations confer growth advantage on the cancer cell, are further positively selected through Darwinian competition and thus enhance the cell's evolutionary fitness to promote clonal out-growth and progression towards cancer (2).
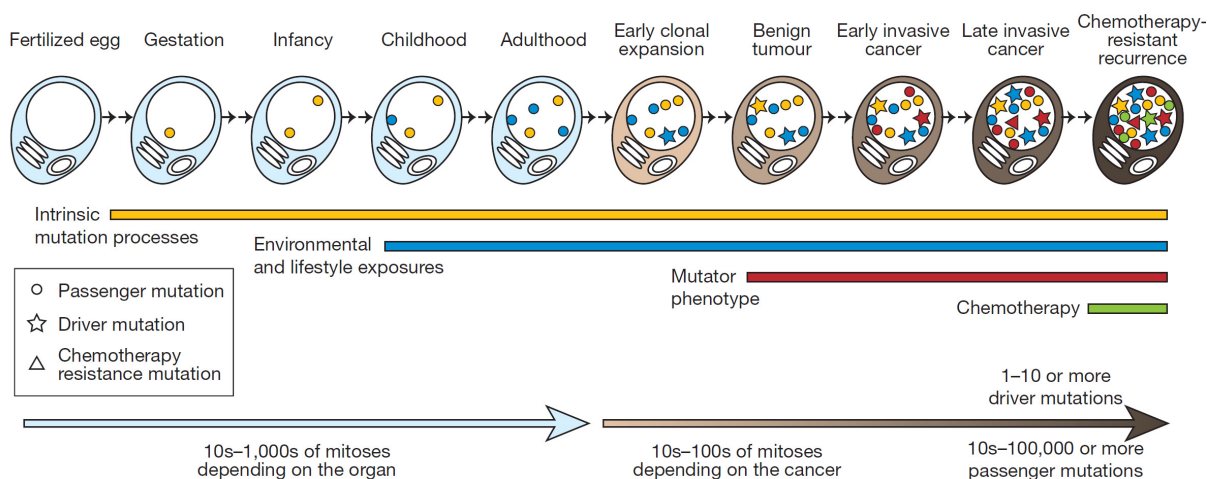
Figure 1: A multistep process of cancer evolution, from the fertilized egg to a single cell within a cancer (2).

Passenger mutations that evolve and accumulate during an individual's lifespan may be acquired while the cell lineage is phenotypically normal. This reflects both intrinsic mutations arising from

normal cell division and mutations caused by exogenous mutagens. Driver mutations will cause clonal expansion and tumor formation which may be supported by other processes such as DNA repair defects.

Driver mutations reside, by definition, in the subset of genes known as 'cancer genes' and have thus subverted known hallmarks of cancer such as control of cell proliferation, differentiation, apoptosis and other homeostatic interactions with the tissue microenvironment (1, 3). The number of driver mutations and, hence, the number of cancer genes they alter varies between cancer types but probably lies around 5-7 as shown for breast, colorectal and prostate cancer (2) or by in vitro studies (4). However, genomic studies of cancer cells have shown that the number of drivers might be much higher than expected (5, 6). Interestingly, so far around 350 of the ~22.000 protein-coding genes (1.6%) have been reported to show somatic mutations in cancer with strong evidence to act as driver mutations (7).

1.1.2 The 'punctuated equilibrium' evolutionary model

The prevailing dogma of cancer development is characterized by the acquisition of driver mutations (described in section 1.1.1) in a cumulative manner over years and decades, resulting in a step-wise progression towards cancer development through increasingly malignant phenotypes (8). In contrast, there is experimental evidence that a more 'punctuated equilibrium' model may also apply to cancer development.

For example, genome-wide telomere attrition in somatic cells that are already defective in DNA checkpoint response genes e.g. *TP53* may lead to genomic instability followed by breakage of chromosomes, thus naked DNA ends serve as source for chromosomal rearrangements (9, 10). The resulting chromosomal end-to-end fusions due to telomere loss can lead to cycles of dsDNA breaks followed by aberrant repair and further chromosomal damage in both daughter cells (11, 12). If these cycles of repair and breakage iterate, extensive genomic rearrangements that occur in only few cell cycles may arise in multiple sub-clones (13).

In addition, it has been reported that massive chromosomal rearrangements, involving single or more chromosomes, can be acquired in one catastrophic event, a phenomenon called chromothripsis (Figure 2). This model proposes that a chromosome can shatter into hundreds to thousands of pieces in a single catastrophic event. Non-homologous end-joining stitches the pieces back together haphazardly, therefore generating hundreds of chromosomal rearrangements (14).
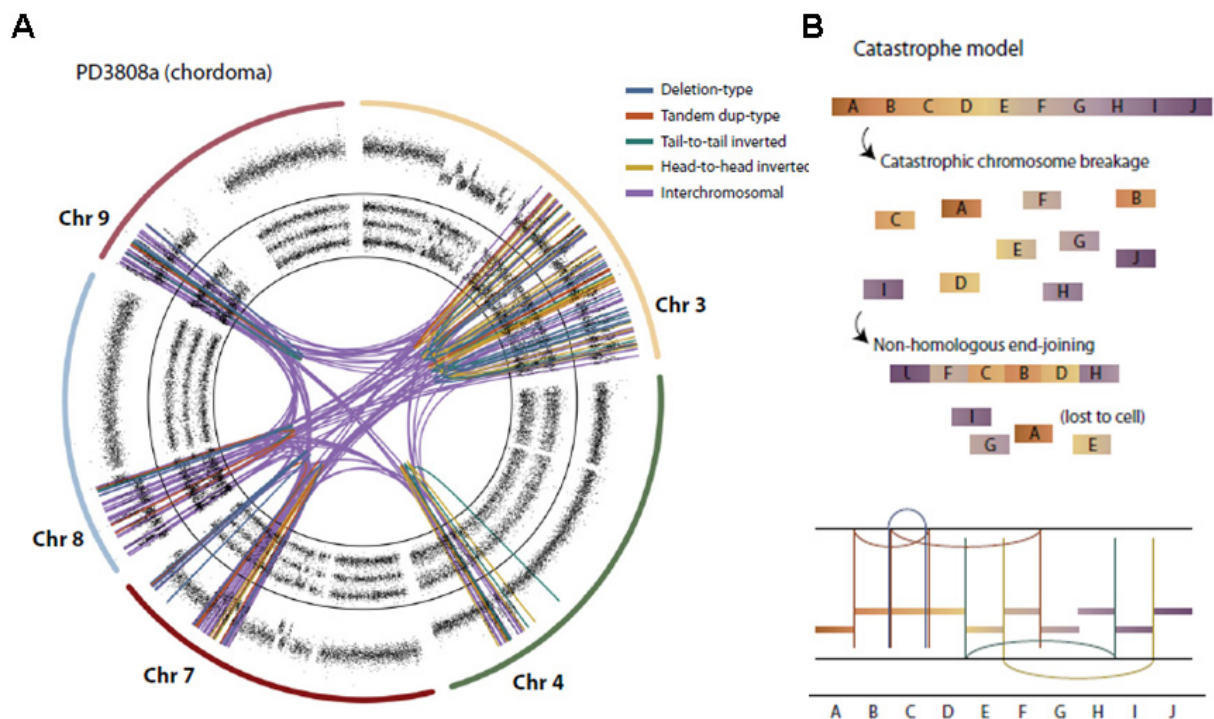
Figure 2: Chromosomes can break into hundreds of pieces that are stitched back together randomly to create highly aberrant chromosomes, a phenomenon called chromothripsis (14).
(A) A patient with chordoma, exhibits 147 rearrangements that are inter- and intra-chromosomal. (B) Model of chromothripsis: a catastrophic event breaks the chromosome into many pieces that are randomly put together thereafter.

Taken together, the progressive cancer development model may be complemented by a more 'punctuated equilibrium' model where bursts of somatic mutations accrue in a relatively short period of chronological time leading to massive genomic changes (e.g. intra- and inter-chromosomal rearrangements, deletions, formation of Double Minute Chromosomes) that further provoke cancer development.

1.1.3 Cancer genes – the role of tumor suppressors and oncogenes

All afore-mentioned genetic aberrations, whether they accumulate over time or they are generated throughout a single catastrophic event commonly can affect the expression and function of cancer genes, which can be divided into tumor suppressor

and oncogenes. Since tumor suppressor genes function in a recessive manner, mutation of both alleles is required to abrogate protein function thus increasing the probability of tumor formation. In contrast, oncogenes are dominantly acting, that is, mutation of just one allele can cause the development of a neoplasm (2, 15). The actual number of human cancer genes is still a matter of speculation but based on mice studies more than 2000 genes, when appropriately altered, can potentially contribute to cancer development (16). Approximately 90% of the known cancer genes are acting as oncogenes, whereas around 10% function as tumor suppressors (2).

The mechanisms and patterns of mutations differ between oncogenes and tumor suppressors. Whereas tumor suppressors can arise from different mutations ranging from single base substitutions to whole deletions, which commonly result in abrogation of protein function, oncogenes are mainly activated by genomic rearrangements, missense amino acid changes, in-frame insertions, deletions or gene amplifications (2). Genomic rearrangements may involve two different genes leading to oncogenic fusion proteins or may position genes adjacent to other regulatory elements. Interestingly, rearranged oncogenic fusion genes were discovered in lung adenocarcinomas (17) and in more than half of the prostate cancer cases (18).

However, cancer genes cluster on certain signaling pathways that control cell cycle, genome integrity, morphogenetic reactions, cell differentiation and apoptosis thus subverting biological pathways and processes towards cancer development (15).

1.2 The forkhead box O (FOXO) family of transcription factors

FOX transcription factors are a superfamily of proteins with a conserved 100-residue DNA-binding domain, the forkhead (FKH) domain. Since the original identification of the forkhead gene in Drosophila melanogaster more than 100 structurally related FOX proteins and 19 human subgroups named FOXA to FOXS have been discovered (19, 20). The O class includes FOXO1, FOXO3, FOXO4 and FOXO6 (21). FOXO transcription factors have been shown to be involved in many cellular processes. They can induce cell cycle arrest (22-24), apoptosis and DNA repair (25-27) or can modulate expression of genes involved in oxidative stress and cell differentiation (27) (see Figure 4).

1.2.1 Structure of FOXO proteins

FOXO proteins function primarily in the nucleus where they either activate or repress target gene transcription (21).
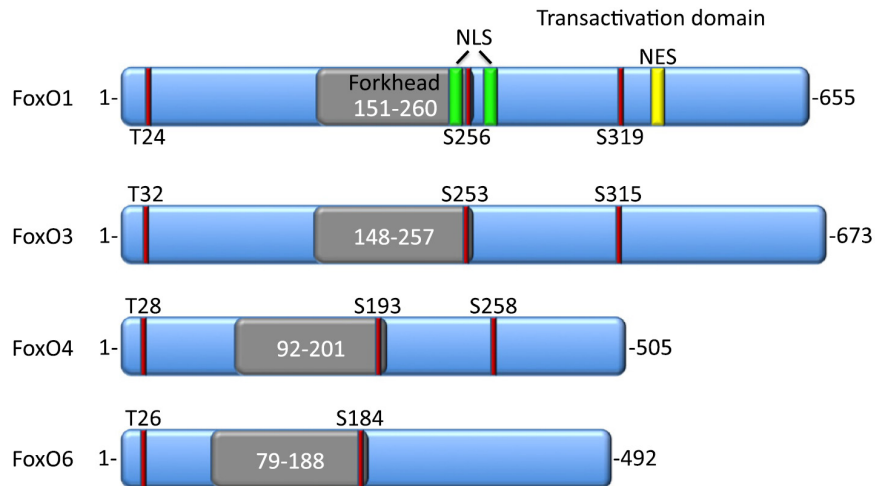
Figure 3: Structure of the FoxO family of transcription factors (28).
FOXO proteins share common structural features: transactivation domain, nuclear export and nuclear import signals (NLS, NES), a forkhead domain which enables DNA binding as well as conserved AKT phosphorylation sites.

FOXO proteins bind their cognate DNA targeting sequences as monomers through their conserved forkhead domain that relies on fourteen protein-DNA contacts (29). The forkhead domain consists of three major α-helices, three β-sheets and two large loops resulting in a butterfly-like appearance that is described as 'winged helix' structure (29, 30). However, even though both winged loops make important interactions with DNA, it is the second loop that can influence the stability of DNA binding. Furthermore, it has been shown that the α-helix H3 serves as the primary DNA recognition site. Notably, most post-translational modifications, such as phosphorylation or acetylation that block FOXO activity, occur in these C-terminal basic regions of the forkhead domain to prevent transcriptional activity (Figure 3) (29, 31). High affinity DNA binding studies have revealed that FOXO transcription factors specifically bind at a consensus FOXO-recognized element (FRE) with the core sequence motif (G/C)(T/A)AA(C/T)AA (32-34). FRE sites have been identified in promoters of canonical FOXO targets such as Fas ligand (FasL), insulin-like growth factor binding protein 1 (IGFBP1) or the apoptotic regulator BIM (25, 35). Furthermore, putative FOXO-target genes and their potential binding sites that have been identified by systematic bioinformatic approaches (36) suggest that FOXO

transcription factors are involved in various signaling pathways and thus, control a wide range of biochemical processes.

1.2.2 Regulation of FOXO activity by post-translational modifications

The FOXO transcriptional activity is tightly regulated on a post-translational level via phosphorylation, acetylation or ubiquitylation (summarized in Figure 4).

1.2.2.1 Phosphorylation

Insulin signaling regulates FOXO activity via Ras- and phosphatidylinositol-3-kinase (PI3K)-dependent pathways which activate protein kinase B (AKT). AKT subsequently translocates into the nucleus where it phosphorylates FOXO on three conserved serine/threonine (Figure 4) residues.
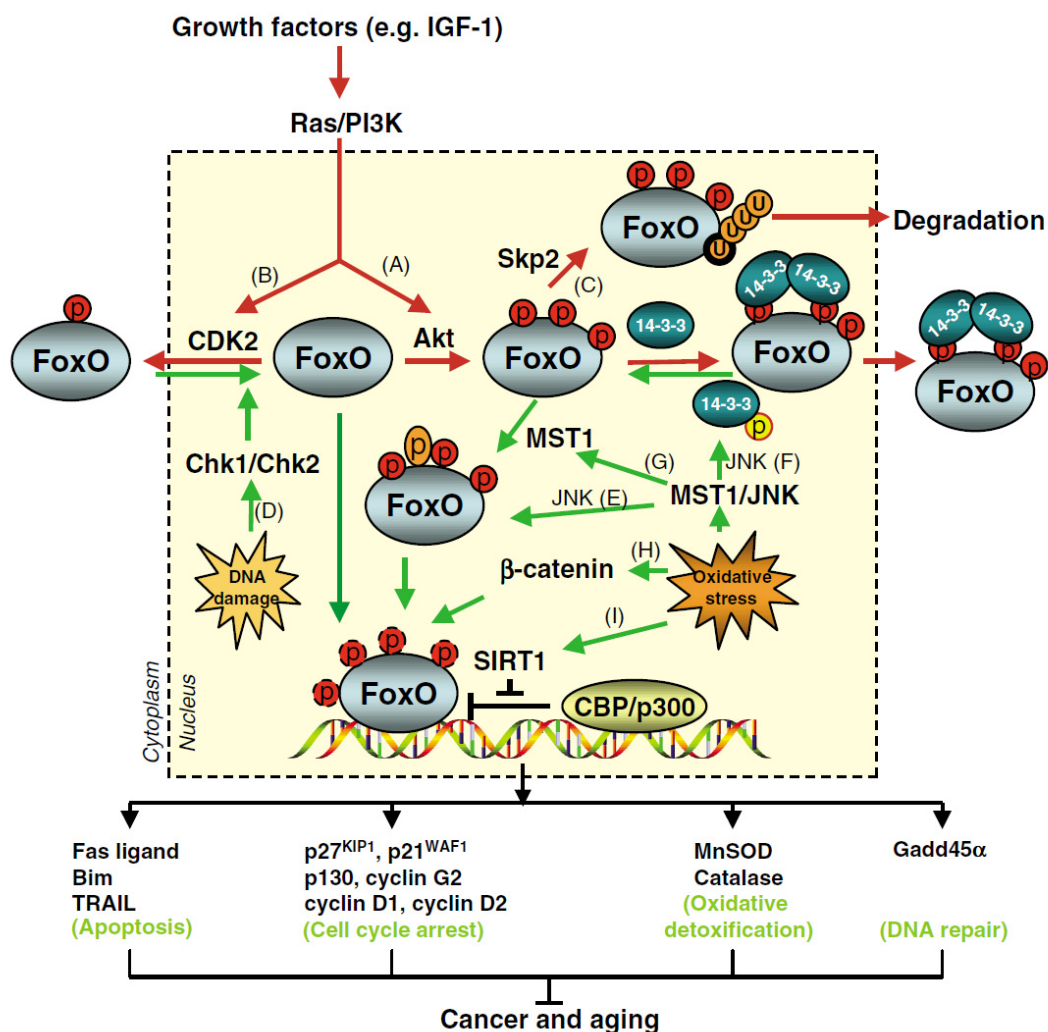
Figure 4: Regulation of FOXO proteins by post-translational modifications (27).
Growth factors induce Ras or PI3K signaling leading to AKT- or CDK2- mediated phosphorylation resulting in transcriptional inactivation of FOXO proteins by nuclear exclusion or Skp2 mediated

ubiquitylation and proteasomal degradation (A-C). CDK2-dependent phosphorylation is negatively regulated by DNA damage induced checkpoint kinases Chk1/Chk2 (D). On the other hand, oxidative stress has been shown to promote nuclear FOXO due to phosphorylation by JNK (E), JNK-dependent phosphorylation of 14-3-3 protein (F) or direct phosphorylation of FOXO protein by MST1 (G). Oxidative stress also favours the interaction of FOXO proteins with β-catenin (H). Histone acetyl-transferases CBP and p300 inhibit the transcriptional activity of FOXO proteins but activation of SIRT1 deacetylase can overcome this effect under oxidative stress (I).

These posttranslational modifications allow FOXO proteins to bind the chaperone protein 14-3-3, resulting in the FOXO release from DNA and nuclear export in a CRM-1 dependent manner. The association between FOXO and the exportin CRM-1 is regulated by the small GTPase Ran. Bound 14-3-3 protein prevents re-entry of cytosolic FOXO by masking the nuclear localization signal (NLS) and inhibits importin binding (37).

In addition, CDK2 has been shown to phosphorylate FOXO1 at specific serine residues (S249/S298). This phosphorylation seems to be independent from AKT-mediated phosphorylation events and also leads to FOXO1 nuclear exclusion through a mechanism that appears not to be affected by 14-3-3 binding (38).

This CDK2 phosphorylation site lies in a CDK2 consensus phosphorylation sequence (K/R)(S/T)PX(K/R) which has been also found in human and mouse FOXO1 and FOXO6 but not in other FOXO family members (38).

Besides AKT and CDK2, FOXO proteins are also phosphorylated by serum- and glucocorticoid-inducible kinases (SGKs) which act similar to AKT. SGKs are also activated by the PI3K pathway and translocate to the nucleus where they phosphorylate FOXO3 at the same residues that are recognized by AKT. However, SGKs preferentially phosphorylate serine 319 whereas AKT mainly phosphorylates serine 256 (39).

In addition, FOXO1 can be phosphorylated by a dual-specificity tyrosine-phosphorylated and regulated kinase (DYRK) at a novel phosphorylation site, serine 329. When this site is mutated to alanine, the resulting mutant FOXO1 becomes predominantly nuclear in 90% of the cells whereas wild-type protein is only found nuclear in 75% of cells (40).

In contrast to signaling pathways which drive FOXO proteins out of the nucleus, stress conditions such as oxidative stress or genotoxic stress consistently reconstitute nuclear FOXO proteins, even in the presence of growth factors. For example, CDK2-mediated phosphorylation of FOXO1 is abolished by activation of

checkpoint kinases Chk1 and Chk2 (38) (Figure 4). On the other hand, oxidative stress activates c-Jun N-terminal kinase (JNK) which in turn phosphorylates and activates FOXO4 at threonine 447 and threonine 451 (41). The JNK mediated nuclear FOXO activation seems to be evolutionary conserved since JNK antagonizes insulin/IGF-1 signaling in *Drosophila* and promotes nuclear localization of FOXO proteins (42). However, it seems that the JNK phosphorylation sites in FOXO4 are not very conserved throughout the FOXO family (43), thus, additional mechanisms might mediate the JNK dependent nuclear localization of FOXO proteins. One possibility for JNK directed nuclear FOXO regulation might be the observation that JNK can phosphorylate 14-3-3ξ at serine 184, causing dissociation of 14-3-3 from FOXO3 in the cytoplasm and finally triggers nuclear localization of FOXO3 (44) (Figure 4). Another JNK-related mechanism for the nuclear localization of FOXO3 has been suggested, involving the mammalian Ste20 (yeast protein kinase Sterile 20)-like kinase-1 (MST1) that phosphorylates FOXO3 at serine 207 (45). This phosphorylation blocks the interaction of FOXO3 with 14-3-3β and induces nuclear localization (Figure 4). However, the serine 207 site within the forkhead domain is conserved throughout the FOXO family and MST-FOXO interactions are also observed in *C. elegans* (45). In addition, MST1 might regulate FOXO activity through JNK-dependent pathways since it has been shown that MST1 can activate the JNK pathway in mammalian cells (46).

1.2.2.2 Ubiquitylation

As shown in Figure 4, FOXO proteins can be degraded by the ubiquitin proteasome system. FOXO1, for example, has been shown to be degraded via proteosomal degradation in response to AKT mediated phosphorylation. This process requires the interaction of FOXO1 with the F-box protein Skp2, the substrate-binding component of the Skp1/culin 1/F-box protein (SCF^{Skp2}) E3 ligase complex. Interestingly, Skp2 dependent polyubiquitylation requires preceding phosphorylation at serine 256 by AKT (47). Since Skp2 is a nuclear protein (48) and FOXO1 is phosphorylated by AKT in the nucleus as well (49), Skp2-dependent polyubiquitylation probably occurs in the nucleus. In contrast, FOXO4 can be monoubiquitylated in response to oxidative stress, leading to nuclear localization of FOXO4 and thus, increased transcriptional activity (50). The conserved lysine residues K199 and K211 within the C-terminus of the FKH domain of FOXO4 are targeted by monoubiquitylation and can be deubiquitylated by the herpesvirus associated ubiquitin-specific protease

(HAUSP/USP7) (50). Deubiquitylation of FOXO4 results in cytoplasmic localization and abolished transcriptional activity. Therefore, monoubiquitylation, at least for FOXO4, represents another important post-translational modification in cells that regulates the transcriptional activity of FOXO proteins.

1.2.2.3 Acetylation

The nuclear proteins CBP and p300 posess intrinsic histone acetyl-transferase (HAT) activity and, thus, have been implicated to play essential roles in promoting transcription. They acetylate histones and/or integrate signals from enhancer to promoter regions. Furthermore, it has been shown that they can directly acetylate transcription factors through a transcription factor acetyl-transferase (FAT) activity (51). CBP, on the one hand, can acetylate chromosomal histones and therefore facilitates FOXO-mediated gene transcription, but on the other hand promotes acetylation and regulation of FOXO proteins themselves.

In response to oxidative stress, acetylation of FOXO proteins within the nucleus increases (52, 53), leading to accumulation and association with Pml bodies, which hinders FOXO activity (54). This acetylation and nuclear accumulation can be abrogated by a nicotinamide adenine dinucleotide (NAD)-dependent histone deacetylase, SIRT1. Upon stress stimuli, nuclear SIRT1 forms a complex with FOXO proteins followed by FOXO-deacetylation and transcriptional reactivation (52).

Interestingly, expression of SIRT1 increases FOXO3 induced cell cycle arrest via induction of p27^{KIP1} (52), which is consistent with the negative regulatory role of CPB on the FOXO transcriptional activity (55). In addition, by blocking SIRT1 activity using class I/II and III histone deacetylase (HDAC) inhibitors, FOXO3 induced expression of the apoptotic gene *BIM* is further enhanced (52). Thus, SIRT1 appears to function as fine-tuner, shifting FOXO function from cell death to survival.

1.2.3 FOXO transcription factors function as tumor suppressors

The ability of FOXO transcription factors to regulate the cell cycle, stress repair, oxidative detoxification and cell death has long suggested that they function as tumor suppressors (Figure 4). In line with this assumption, in most human cancers that have very high levels of AKT due to mutations in *RAS*, *PTEN* or *PI3K*, FOXO function is inhibited (56). As explained in the following section, recent *in vivo* approaches have shown that FOXO proteins are bona fide tumor suppressors.

Initially the FOXO transcription factors were discovered in some forms of leukemia and alveolar rhabdomyosarcoma where they evolve as fusion proteins, resulting from chromosomal translocations (myeloid/lymphoid or mixed lineage leukemia (*MLL*)-*FOXO4* and *MLL-FOXO3*; *PAX3-FOXO1*, *PAX7-FOXO1*) (57). In these cases, the FOXO transactivation domain (see Figure 3) is fused to PAX3/7 or MLL, resulting in maintainance of the transcriptional program of these genes, thus, leading to permanently active transcription factors that drive proliferation even at times when they should be inactive (58). Since FOXO proteins can induce cell cycle arrest and apoptosis, it was suggested that the fusion proteins function, to some extent, dependent on (partial) FOXO loss-of-function as shown for the MLL-FOXO4 fusion (58). Thus, the function of the afore-mentioned fusion proteins could be delineated to uncontrolled proliferation mediated through PAX3, PAX7 or MLL function and loss of the tumor suppressor function of the remaining intact *FOXO* allele (56).

In vitro assays have demonstrated that mutations of specific FOXO residues that are required for inactivation by AKT-mediated phosphorylation can block colony formation in RAS-transformed cells or cells deficient for the phosphatase and tensin homolog (PTEN) (59).

Furthermore, a dominant negative form of FOXO (dnFOXO) which comprises the DNA-binding domain, but lacks the transactivation domain, has been shown to substitute RAS expression in classical combinatorial RAS and MYC transformation studies (60). Forced expression of FOXO transcription factors can also reduce tumor growth in vivo using a xenograft model in nude mice (61, 62). Taken together, *in vitro* and *in vivo* studies indicate that FOXO proteins could function as tumor suppressors.

The first orthotopic in vivo evidence that FOXO proteins can function as negative regulators of uncontrolled cell-growth came from studies performed in *C. elegans*. Since the activity of the abnormal dauer formation protein 16 (DAF-16), the *C.elegans* ortholog of FOXO, is also negatively regulated by PI3K/AKT signaling, it seems that the molecular mechanisms that control FOXO expression and activity have been conserved during evolution. Consistent with activation of mammalian FOXO proteins during stress by JNK-mediated phosphorylation, DAF-16 is also positively regulated by JNK in C. elegans. In addition, DAF-16 or FOXO (D. melanogaster) have been shown to extend life span (63, 64). It is likely that FOXO also possibly affects the life span in mammals since the mechanism of DAF-16 and FOXO activity seems to be evolutionary conserved. In this respect, a tumor

suppressor role of FOXO proteins seems plausible because escape from cancer (an age-related disease) is likely to prolong at least median life span (56). Further experimental evidence that FOXO transcription factors function as genuine tumor suppressors came from studies where three FOXO genes (*FOXO1*, *FOXO3* and *FOXO4*) were simultaneously conditionally deleted (triple *FOXO*-knockout). This caused spontaneous tumor formation in mice (65). Using dominant negative FOXO (dnFOXO), which, in principle, should inhibit all FOXO isoforms, enhanced lymphomagenesis in the E-μ-*MYC* mouse model (66). It is believed that FOXO can counterbalance MYC-induced proliferation by induction of p27^{KIP1} and lead to a lowered apoptotic threshold in MYC-transformed cells via upregulation of BIM and FasL (56). FOXO can also directly affect MYC-induced protein translation in Drosophila as a consequence of ribosome biogenesis interference (67).

Taken together, it has been shown that FOXO proteins can counteract both spontaneous as well as MYC-induced tumor formation and, furthermore, that FOXO transcription factors can interfere with the oncogenic functions of MYC (56).

The p53 protein mediates one of its tumor-suppressive functions through induction of the DNA-damage-repair response. Also FOXO proteins have been implicated in DNA repair via regulation of GADD45 and involvement in the ATM-mediated DNA-damage response (68, 69).

FOXO transcription factors also regulate the cellular antioxidant capacity through the induction of genes encoding enzymes such as the manganese superoxide dismutase (MnSOD) or catalase. These enzymes are important to scavenge respiration-derived reactive oxygen species (ROS). Thus, loss of FOXO function contributes to an increase in cellular ROS. Even though tumor cells are more sensitive to increased levels of ROS than untransformed cells, they have acquired means to cope with higher ROS levels in the absence of FOXO by switching to glycolysis rather than mitochondrial respiration even in the presence of sufficient oxygen supply (Warburg effect) (70).

Interestingly, FOXO transcription factors have been shown to be also involved in the positive regulation of autophagy during nutrient starvation through transcriptional regulation of BNIP3 (BCL2/adenovirus E1B 19kDa-interacting protein 3), LC3 (microtubule-associated protein 1A/B-light chain 3), ATG12 (autophagy-related 12 homolog) and GABA(A)-receptor associated protein-like 1 (GBRL1) (71). Autophagy has long been regarded as a catabolic process involving the degradation of damaged

or surplus organelles by the lysosomal machinery or as an alternative source of amino acids in times of nutrient deprivation. However, it has now become clear that autophagy can contribute to cancer formation and moreover that, for example, by blocking p53-induced autophagy using chloroquine, the oncogenic potential of MYC is greatly limited (72). Blocking autophagy might serve as promising strategy for enhancing cancer therapies because cell death through inhibition of autophagy is not dependent on proteins such as Bax (Bcl-2 associated X), Bak (Bcl2 homologous antagonist/killer) or caspase activation or ATM signaling, which are often mutated in cancer (73).

The loss of FOXO protein can perturb the proliferation-apoptosis balance in homeostasis and provides one of many explanations on how cells can become tumorigenic, but for cancer to become malignant, angiogenesis is required. Tumor vascularization under hypoxic conditions is normally provided by up-regulation of the hypoxia inducible factor 1 alpha transcription factor (HIF-1α) that in turn activates the transcription of the secreted vascular endothelial growth factor-A (VEGF-A) (74). The resulting expression of VEGF functions to attract endothelial cells for the formation of new blood vessels (75). Interestingly, a study using the triple *FOXO*-knockout mouse (previously explained) revealed that loss of FOXO function leads to aberrant vascular growth and widespread hemangiomas. This indicates that FOXO transcription factors are obviously involved in the regulation of homeostasis of the vasculature (76). Furthermore, FOXO1-knockout mice die at day 10.5 due to incomplete vascular development (77).

The FOXO transcription factors have been shown to also regulate HIF activity. Initially, HIF-1α levels where shown to be down-regulated by FOXO4 in a VHL-independent manner (78) but two more recent studies have shed light on a molecular mechanism of FOXO-dependent HIF-1α transcriptional inhibition. On the one hand, FOXO indirectly prevents the HIF-1α-induced apoptosis by up-regulation of its target CBP/p300-interacting transactivator 2 (CITED2) (79). On the other hand, PTEN mediated activation of FOXO facilitated the titration of p300 away from HIF-1α (80).

So far, it is not clear to what extent the role of FOXO in the regulation of angiogenesis under hypoxic conditions contributes to its tumor-suppressive functions. However, re-activation of suppressed FOXO proteins in cancer might not only control tumor growth via anti-proliferative or pro-apoptotic functions but could possibly also be beneficial by abrogating tumor angiogenesis (56).

1.3   Ewing Sarcoma

Ewing Sarcoma (ES) is a very aggressive primary tumor of the bone, characterized by its small round cell phenotype (81, 82). ES is a malignancy of children and young adults with a peak incidence of ~ 15 years, making it the second most common bone tumor following osteosarcoma (83, 84). The primary tumor location typically is in the bone but in a small portion (<15%) of patients the tumor arises in soft tissue (85, 86). ES belongs to a group referred to as Ewing sarcoma family tumors, including Askin's tumors and primitive neuroectodermal tumors, which harbour the same set of translocations (87-90).
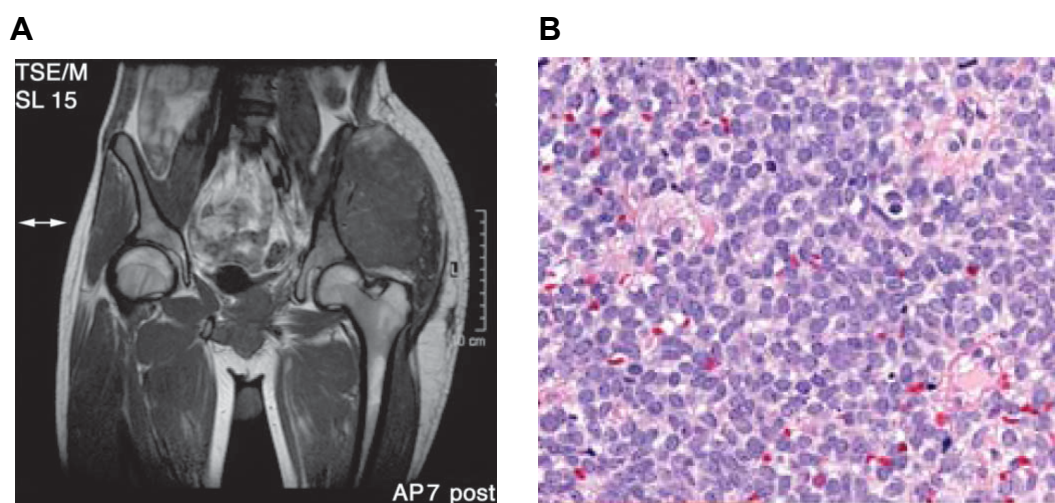
Figure 5: Characteristics of Ewing sarcoma (91).
(A) Magnetic resonance image of a Ewing tumor (ET) (pelvis). (B) Typical small round cell phenotype of ES (H&E staining, resolution 200x).

Since ES are very aggressive tumors, the propensity to metastasize to the lung, bone or bone marrow is very high. The current standard to treat ES patients is a combination of systematic chemotherapy, surgery and/or radiation (86). Despite this multimodal aggressive treatment, the 5-years disease free survival rate of patients with metastasis at diagnosis (15-25%) (92) is very low (~ 10-30%) and increases up to 60-70% when the disease is localized (93, 94).

The poor prognosis for patients with metastasis and the high relapse rate for patients with surgically-resected ES tumors in the absence of chemotherapy (~90%) (95-97) clearly demonstrate the need for new treatment strategies and a better understanding of the biology underlying the pathogenesis of ES.

A major question that needs to be addressed is from which cell-of-origin the disease arises. Currently there is no definite answer to this question. However, there are two main hypothesis on the precursor cell type for ES. On the one hand, there is a growing body of evidence that mesenchymal stem or progenitor cells represent the cellular origin for Ewing sarcoma (98-101), but on the other hand, neural crest cells have been shown to fulfil the criteria to function as a precursor cell type for ES (102-104). Interestingly, a recent idea suggests that maybe both hypothesis are valid to some extent. Either ES arise from a neural crest stem cell with mesenchymal features or from a mesenchymal stem cell, derived from a neural progenitor cell (105, 106).

The problem that the cellular origin of ES is not yet clarified is further demonstrated by a number of attempts to generate a mouse model for Ewing sarcoma. In one study, the underlying strategy to express EWS-FLI1 (see section 1.3.1), which is embryonic lethal when constitutively expressed, was to knock-in the gene-fusion under the Rosa-26 locus. The EWS-FLI1 expression was then targeted to bone marrow progenitor cells by crossing to mice that express the cre recombinase (*Mx1-cre*) (107). However, neither these mice, nor mice from other studies, e.g. lymphocyte specific expression of *Rag-1 cre* recombinase to drive EWS-ERG expression (108, 109), or expression of EWS-FLI1 in the primitive mesenchyme of the early limb bud using the *Prx-cre* driver (110), developed spontaneously sarcomas or only when the *Tp53* gene was simultaneously mutated.

In addition, it has been reported that human mesenchymal stem cells that express EWS-FLI1 did not form tumors in immunodeficient mice, suggesting that not only the cellular context but also the existence of cooperating mutations enable normal cells to transform to cancer cells (86).

Another highly speculative possibility, why no other organism except humans has ever been reported to develop ES, is the lack of EWS-FLI1 specific GGAA-microsatellites in non-primates (e.g. the mouse). EWS-FLI1 is supposed to bind these GGAA arrays to activate specific target genes which are required for the oncogenic phenotype of ES. If these sequences are lacking, EWS-FLI1, even though it's expressed, may not be able to induce target gene promoters and, thus, formation of Ewing sarcoma is abrogated (86).

1.3.1 EWS-FLI1

ES is genetically characterized by chromosomal translocations that result in EWS-ETS gene rearrangements. The most frequently observed gene fusion combines EWS with FLI1, leading to the expression of an aberrantly active ETS transcription factor, EWS-FLI1 (111). About 85% of ES tumors harbor this specific t(11;22)(q24;q12) translocation (89, 112) involving the Ewing sarcoma break point region 1 (*EWSR1*) gene on chromosome 22 and the Friend leukemia virus integration site 1 (*FLI1*) gene on chromosome 11 (Figure 6).
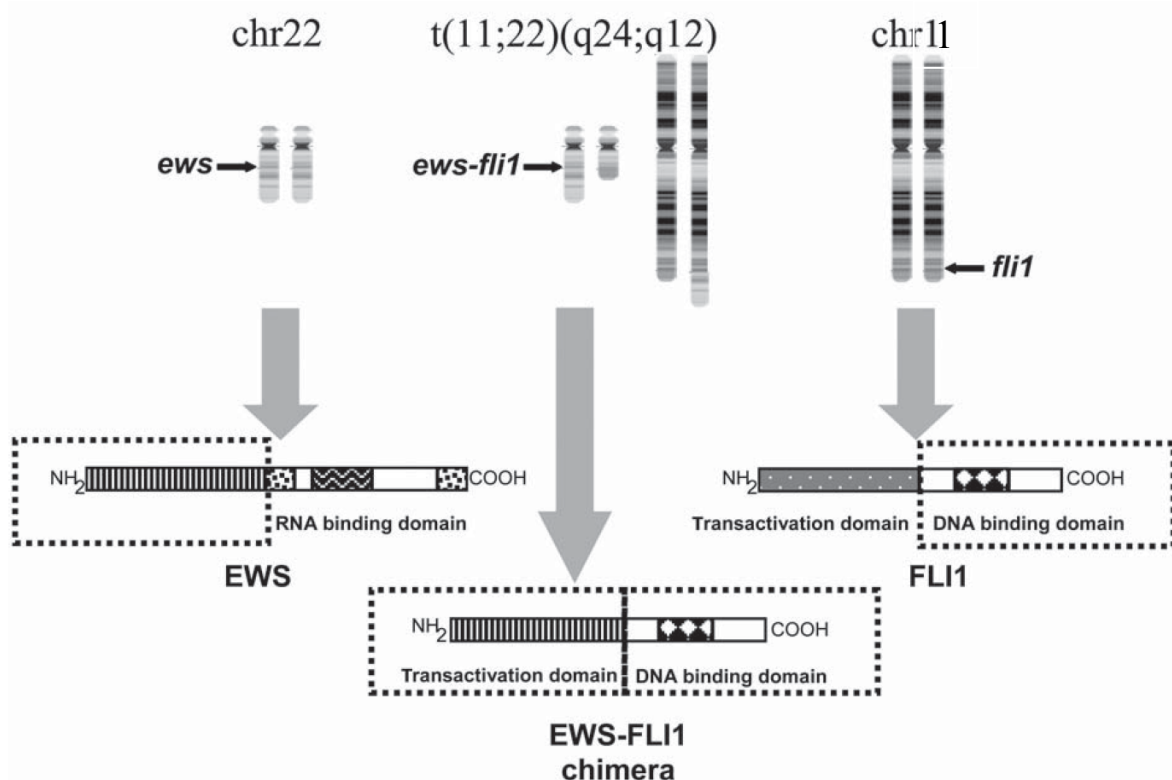
Figure 6: The EWS-FLI1 chimeric transcription factor characteristic of Ewing sarcoma (91).
The N-terminal transactivation domain of the *EWSR1* gene fuses to the DNA-binding domain of the *FLI1* gene leading to formation of an aberrantly active transcription factor.

The EWS protein, belonging to the TET family of proteins, normally associates with the transcriptional machinery including RNA polymerase II, TFIID and CPB/p300, suggesting a role in transcriptional activation (113-116). In contrast, the FLI1 protein belongs to the afore-mentioned ETS family of transcription factors and normally functions in vascular, neural-crest and hematopoietic development (117-119). As shown in Figure 6, the chimeric EWS-FLI1 protein consists of the amino-terminus of

EWS (contains the transactivation domain) and the carboxy-terminus of FLI1 (contains the DNA binding domain) which recognizes purine-rich sequences containing a GGAA/T core motif (120, 121), thus representing a typical aberrant transcription factor that functions as an oncogene (122, 123). However, the reciprocal FLI/EWS fusion is not expressed in ES tumors (89).

The EWS-FLI1 protein is constitutively expressed from the *EWSR1* promoter, whereas the *FLI1* promoter is not functional in ES cells (86). Rearrangement of EWS-FLI1 leads to disruption of one wild-type copy of *EWSR1* and one wild-type copy of *FLI1* in Ewing tumors (ET) (89). Since the latter is not expressed in ES it might not be of any importance (86), but the role or function of the EWSR1 haploinsufficiency is yet not well understood.

The EWS-FLI1 protein is considered an ideal tumor specific therapeutic target (124) due to its exclusive presence in ES and its proven rate-limiting role in the pathogenesis of this disease (125). For instance, interference with EWS-FLI1 expression or function results in tumor regression in vivo and dysregulates ES tumor cell growth in vitro (126-128). Since EWS-FLI1 functions as a very potent transcription factor, RNA-interference (RNAi) based approaches in combination with microarray technology revealed a number of EWS-FLI1 dysregulated genes downstream of the fusion protein (129-131). There is a growing list of EWS-FLI1 regulated target genes involved in cellular processes that sustain tumorigenesis through regulation of the cell cycle, evasion of apoptosis, cell proliferation, drug resistance, evasion of growth inhibition, angiogenesis, adhesion, immortalization and maintainance of pluripotency (e.g. *CCND1*, *IGFBP3*, GSTM4, *TGFBRII*, *p21*, *hTERT*, *VEGF*, *CAV* and *EZH2*) (130, 132-137). These examples demonstrate that EWS-FLI1 obviously regulates a whole network of downstream effector genes in a direct or indirect manner.

1.3.2 Mechanisms of transcriptional regulation by EWS-FLI1

The mechanism of transcriptional regulation by EWS-FLI1 is a growing area of research in the field. Whereas some studies have shown that EWS-FLI1 can regulate gene-expression in a DNA-binding independent manner (138, 139), there is clear experimental evidence that the DNA-binding property of EWS-FLI1 is indispensable to its oncogenic potential (140). EWS-FLI1 has been shown to up-regulate transcription of specific target genes by binding to a high affinity ETS binding site (ACCGGAAGTG) or by binding to GGAA-microsatellite repeat sequences in target

gene promoters (86). Experimental evidence suggests that the EWS domain confers transcription activating properties to the chimeric transcription factor (122, 141). However, knockdown of EWS-FLI1 uncovers similar numbers of EWS-FLI1 repressed and activated genes (129).

Kinetic studies of gene expression, using an inducible EWS-FLI1 knockdown model in ES cell lines (our unpublished data), revealed that CGGAAT motifs are particularly enriched in early down-regulated genes (EWS-FLI1 activated). Interestingly, this presumably directly activated target genes also show enrichment for other transcription factor binding motifs such as E2F, NRF1 and NFY, suggesting a model of transcription factor cooperation to activate gene transcription. Furthermore, a ChIP-seq study has shown that combinations of two ETS binding sites were frequently found in non-microsatellite EWS-FLI1 binding regions, suggesting that, for at least some promoters, EWS-FLI1 homo- or hetero-dimerizes with other ETS transcription factors to activate target gene transcription (142).

This model is further supported by a study showing that cooperative DNA binding of EWS-FLI1 with Fos-Jun (AP-1) is required to activate the expression of uridine phosphorylase (UPP) mRNA and to transform 3T3 fibroblasts *in vitro*. In contrast, a C-terminally truncated mutant version of EWS-FLI1 failed to activate UPP transcription and 3T3 fibroblast transformation as a consequence of a deficient cooperative DNA binding ability (143).

Direct protein interactions represent another intriguing mode of transcriptional regulation by EWS-FLI1. It has been shown that EWS-FLI1 not only binds to DNA but also directly interacts and binds to proteins of the transcriptional apparatus such as the hRBP7 subunit of RNA polymerase holoenzyme II (Pol II) (114) or the Creb-binding protein (CBP) (144). Another interesting binding partner of EWS-FLI1 is the RNA helicase A (RHA). RHA functions as part of the basal transcriptional apparatus (145) and is also involved in the posttranscriptional RNA metabolism (146). It has been shown that the interaction of EWS-FLI1 with RHA is required for optimal transformation of murine fibroblasts (147). In contrast, reduced EWS-FLI1 activity and tumorigenesis was observed when binding of EWS-FLI1 to RHA was blocked (126).

Interestingly, it has been shown that EWS-FLI1 can form ternary complexes with serum response factors (SRFs) to recognize and bind serum response elements (SREs) within promoters of target genes such as *c-fos* or *Erg1* (148, 149).

In addition, components of the splicing machinery such as U1C protein were identified as binding partners of EWS-FLI1, suggesting an important posttranscriptional regulatory role of the chimeric oncoprotein (150). Interestingly, EWS-FLI1 showed altered splice site selection of the E1A (151) as well as cyclin D transcript, the latter giving rise to a more stable cell cycle agonist (152). Other proteins that are associated with the EWS-FLI1 spliceosome, but not identified as directly binding to EWS-FLI1, are TASR proteins (153) and YB-1 (154).

Furthermore, protein-protein interactions can be influenced by posttranslational modifications such as *O*-GlcNAcylation, a modification that has been shown to enhance the transcriptional activity of EWS-FLI1 and seems to be reciprocally related to phosphorylation (155). However, the effects of posttranslational modifications on protein-protein interactions and on overall ES cellular growth remain elusive.

1.3.2.1 Transcriptional repression

The mechanisms of transcriptional regulation by EWS-FLI1 are only partially understood. So far, very little is known about mechanisms of EWS-FLI1 mediated gene repression, even though there is evidence that a subset of genes is indirectly repressed by EWS-FLI1.

On the one hand, EWS-FLI1 repressed genes (activated upon inducible knockdown of EWS-FLI1) did not show any enrichment of ETS binding motifs in our *in silico* analysis (129) or in the afore-mentioned ChIP-seq study (142). On the other hand, binding motifs for a large number of other transcription factors were identified in proximal promoter regions of EWS-FLI1 repressed genes, suggesting an indirect mechanism of EWS-FLI1 mediated gene repression in ES.

Experimental evidence for such indirect repressive mechanisms evolved by a study showing that part of the EWS-FLI1 repressive signature can be assigned to the activation of transcriptional repressors such as NKX2.2 or NR0B1 (156, 157). EWS-FLI1 directly activates NKX2.2, which encodes for a dual-function homeodomain transcription factor whose repressive function is mediated by recruiting Groucho-family co-repressors. The NKX2.2 repressed gene-set highly overlapped with the EWS-FLI1 downregulated signature. Furthermore, NKX2.2 functionally mediated oncogenic transformation via transcriptional repression since structure-function analysis revealed that the DNA binding and repressor domains of NKX2.2 were required for oncogenesis in ES cells (156). Whereas NKX2.2 represents a

downstream target of EWS-FLI1, NR0B1 was found to physically interact with EWS-FLI1 and to coordinately modulate gene-expression (157).

Another interesting study has shown that EWS-FLI1 can mediate gene repression via both transcriptional and posttranscriptional mechanisms (158). Whereas one EWS-FLI1 mediated repressive mechanism functioned via decreased levels of Pol II at promotors of repressed genes, EWS-FLI1 was also found to decrease the half-life of insulin-like growth factor binding protein 3 (IGFBP3), a down-regulated direct target of EWS-FLI1. These findings suggest that EWS-FLI1 can modulate both transcript synthesis and degradation, leading to a steady-state target gene expression.

Another mode of EWS-FLI1 induced gene repression may involve epigenetic mechanisms, since several genes whose gene products function in histone-modification are among EWS-FLI1 activated targets. For example, the histone methyl transferase Enhancer of Zeste homolog 2 (EZH2) gene-promoter was found to be bound by EWS-FLI1 *in vivo* and, furthermore, that down-regulation of EZH2 by RNA interference suppressed oncogenic transformation by inhibiting clonogenicity *in vitro* (136). EZH2 is part of the enzymatic subunit of the polycomb PRC2 complex and mediates gene silencing by methylation of histone H3 Lys27. Interestingly, silencing of EZH2 in ES cells revealed a general loss of H3 Lys27 methylation and increased H3 acetylation, leading to gene activation (159).

Other mechanisms of gene repression mediated by EWS-FLI1 may evolve from the identification of microRNAs (miRNAs) that are regulated by the oncogenic fusion protein. Our group has recently identified mir-145 as a top EWS-FLI1-repressed miRNA, whose ectopic re-expression dramatically decreased expression of EWS-FLI1 protein and also reduced growth of ES cell lines *in vitro* (160). Another study revealed that a group of miRNAs, strongly repressed by EWS-FLI1, can negatively regulate the expression of IGF-1 and IGF-1R, suggesting that EWS-FLI1 utilizes repression of tumor-suppressive miRNAs to de-repress IGF signaling (161).

However, to fully appreciate the role of miRNAs in the context of ES-specific gene expression, large-scale proteomic studies for ES will be required, since miRNAs rather affect protein translation than mRNA levels (162).

Since the mechanisms and mediators of transcriptional regulation by EWS-FLI1 are poorly understood, a better understanding of how the fusion protein mediates transcriptional activation and/or repression will help to identify novel opportunities for

therapeutic intervention since it has been difficult to directly target nuclear transcription factors.

1.4   Aim of the thesis

The mechanisms of transcriptional repression by EWS-FLI1 are poorly understood. Based on time-course experiments following EWS-FLI1 knockdown in combination with expression analysis in different ES cell lines, a subset of EWS-FLI1 activated and EWS-FLI1 repressed genes was identified. Interestingly, in-silico motif analysis revealed enrichment of recognition motifs for forkhead box (FOX) proteins within promoters of EWS-FLI1 repressed genes. In contrast, EWS-FLI1 activated promoters exhibited enrichment for ETS binding sites that were not over-represented in EWS-FLI1 repressed promoters.

The aim of this thesis, therefore, was to investigate whether FOX transcription factors are involved in the EWS-FLI1 mediated gene repression.

2 Materials and Methods

2.1 Materials

2.1.1 Media

RPMI 1640 with GlutaMAX^{Tm}-I

Invitrogen, Groningen, Netherlands

Add 10% fetal calf serum (FCS Gold, PAA Laboratories, Linz, Austria) and 100.000

Units/l penicillin / streptomycin (PAA Laboratories, Linz, Austria)

DMEM

Invitrogen, Groningen, Netherlands

1000 mg/L glucose, 4mM L-glutamine and 110 mg/L sodium pyruvate

Add 10% fetal calf serum (FCS Gold, PAA Laboratories, Linz, Austria) and 100.000

Units/l penicillin / streptomycin (PAA Laboratories, Linz, Austria)

Luria Broth (LB)

1% Trypton,

1% NaCl,

0,5% Yeast-extract; LB was autoclaved

Opti-MEM: Invitrogen, Groningen, Netherlands

Trypsin / EDTA: PAA Laboratories, Linz, Austria

FCS/Accutase: PAA Laboratories, Linz, Austria

2.1.2 Buffers

TBS-T: 50mM Tris, 150mM NaCl, 0,1% Tween 20; pH 7,5

TBS: 50mM Tris, 150mM NaCl, pH 7,5

PBS: 137mM NaCl; 3mM KCl; 6,5mM Na_2HPO_4-$2H_2O$; 1,5mM KH_2PO_4

Laemmli buffer

15,1g Tris

72g glycine

25ml 20% SDS

per 1 liter

4% Paraformaldehyde (PFA) (100ml)

25ml of 16% ultra pure Formaldehyde

+ 75ml ddH2O

PBS/5%TritonX-100 & PBS/2%FCS (100ml)

5ml Triton X100, 2ml FCS

+ corresponding volume of PBS

Transfer buffer

14g glycine

3g Tris

20% methanol

per 1 liter

2x sample buffer

20% (v/v) glycerol

6% ß-mercaptoethanol

3% SDS

125mM Tris-Cl pH 6,8

small amount of bromphenol blue crystals

Ponceau S staining solution (10x stock)

2g Ponceau S

30g trichloroacetic acid

30g 5-sulfosalicylic acid

fill up to 100ml with dH_20

Loading Dye

4M Urea

80mM EDTA

10% Saccharose

0,25% BPB

TBE

5,4g Tris Base

2,75g Boric Acid

2ml 0,5M EDTA/pH8

per 1 liter

Blocking solution

10% (v/v) blocking reagent (Roche, Basel, Switzerland) in maleic acid buffer (100mM Maleic Acid, 150 mM NaCl, pH= 7.5, sterile).

2.1.3 Chemicals

Probidium Iodide (PI): (P4170) Sigma, St. Louis, USA

DAPI: Sigma-Aldrich, St.Louis, MO, USA

Roscovitine: Sigma-Aldrich, St.Louis, MO, USA

Methylseleninic Acid (MSA): Sigma-Aldrich, St.Louis, MO, USA

LY294002: Merck, Darmstadt, Germany

Doxycycline: Sigma, St. Louis, USA

Puromycin : Sigma, St. Louis, USA

Zeocin: Cayla, Toulouse, France

Blasticidin: Invitrogen, Groningen, Netherlands

Ampicillin: Biomol, Hamburg, Germany

Trypan blue: Sigma, St. Louis, USA

2.1.4 Ewing tumor cell lines

TC252
Established by T. Triche (Dep. of Pathology, Children's hospital, Los Angeles, USA); p53 wild type, expresses the type I (Exon 7 [EWS]/ Exon 6 [FLI1]) EWS-FLI1 fusion.

SK-N-MC
Established by J. Biedler (Memorial Sloan Ketternig Cancer Center, New York, USA); truncated p53, expresses the type I EWS-FLI1 fusion, derived from pPNET localized within the rib.

A673 and A673sh (ASP14)
The A673 ES cell line (purchased at American Type Culture Collection) expressing type I EWS-FLI1 fusion and doxycycline-inducible short hairpin RNA against EWS-FLI1 (A673sh) was previously described (133) and kindly provided by Javier Alonso (Departamento de Biología Molecular y Celular del Cáncer, Instituto de Investigaciones Biomédicas, Madrid, Spain).

2.1.5 Antibodies

- **α-FOXO1** (rabbit monoclonal, Cell Signalling, C29H4) [WB,1:1000] detects endogenous levels of total FOXO1 protein: 78-82 kDa. The antibody does not detect exogenously expressed family members FOXO3 or FOXO4.

- **α-Phospho-FoxO1** (Ser256) (rabbit polyclonal, Cell Signaling, # 9461) [WB,1:1000] detects phosphorylated Serin 256 (major AKT p-site): 82kDa

- **α-CDK2** (rabbit polyclonal, Santa Cruz, sc-163) [WB,1:500] detects human CDK2: 34 kDa

- **α-ERK2** (mouse monoclonal, Santa Cruz, sc-65981) [WB,1:200] detects ERK2 full length: 42 kDa

- **α-DYKDDDDK Tag Antibody** (Anti-FLAG) (rabbit polyclonal, Cell Signaling, #2368) [WB: 1:1000, for IF:1:800] recognizes FLAG-Tag

- **α-FOXO3a** (FKHRL1; rabbit polyclonal, Santa Cruz, sc-11351 (H-144)) [WB,1:200] detects endogenous FOXO3a: 97kDa

- **α-Phospho-FoxO3a** (Ser253) (rabbit polyclonal, Cell Signaling, #9466) [WB,1:1000] detects phosphorylated Serin 253 (major AKT p-site): 97kDa

- **α- Tubulin** (mouse monoclonal (DM1A), #CP06) [WB,1:1000] detects tubulin: 50kDa

- **α-LAMIN A/C** (rabbit polyclonal, Cell Signaling, #2032) [WB,1:1000], Lamin A/C antibody detects endogenous levels of total full length lamin A (and lamin C) :70 kDa

- **α-p-AKT** (rabbit monoclonal, (244F9) Cell Signaling(Ser473), #4056) [WB,1:1000], Phospho-Akt (Thr308) (244F9) Rabbit mAb detects endogenous levels of Akt only when phosphorylated at threonine 308: 60kDa

- **α-AKT (**rabbit polyclonal, Cell Signaling, (#9272) [WB, 1:1000] detects endogenous levels of total Akt1, Akt2 and Akt3 proteins.

- **α-β-actin** to beta Actin, (mouse monoclonal, Abcam, Cambridge Science Park, Cambridge, UK, ab8226) [WB,1:10000]

- **α-POD-mouse** (product <u>no. 31430</u>, Pierce, Rockford Illinois, USA) Anti-Mouse IgG, (H+L), Peroxidase conjugated secondary antibody using chemiluminescence. [WB,1:10000]

- **α-POD-rabbit** (product <u>no. 31460</u>, Pierce, Rockford Illinois, USA) Anti-Rabbit IgG, (H+L), Peroxidase conjugated secondary antibody using chemiluminescence [WB,1:10000]

- **goat α-rabbit IgG secondary Ab** (red fluorescent Alexa 594, Molecular Probes, Eugene, OR) [IF,1:1000]

- **goat α-mouse IgG, DyLight^{TM} 800** (green fluorescent Ab) [WB, 1:10000]

2.1.6 Plasmids

- **pSuperΔRV:** pSUPER-based retroviral mammalian expression vector. (Gift from Reuven Agami, Division of Tumor Biology, Netherlands Cancer Institute, Amsterdam, Netherlands)

- **pCDNA3-FLAG-FOXO1wt:** was a gift from Dr. Guan (Department of Pharmacology, University of California, San Diego, CA).

- **pECE-FLAG-FOXO3a wt:** were purchased from Addgene (Cambridge, MA)

- **pBS/U6shCDK2** and **pBS/U6 empty** were kindly provided by Dr. Shi (Harvard Medical School, Boston, MA)

- **pCDNA3-FLAG-FOXO1-AAA(T24A/S256A/S319A)** were purchased from Addgene (Cambridge, MA)

- **pCDNA3.1-FLAG-FOXO1-S249A** and **pCDNA3.1-FLAG-FOXO1-S249A/S298A** was a gift from H.Huang & D.J.Tindall (Department of Biochemistry and Molecular Biology, Rochester, MI)

- **pRS-shFOXO1#1**(TGACTTGGATGGCATGTTCATTGAGCGCT)

  pRS-shFOXO1#2 (AATTCGGTCATGTCAACCTATGGCAGCCA)

  pRS-shFOXO1#3 (GAAGAGCTGCATCCATGGACAACAACAGT)

  pRS-shFOXO1#4 (CATCATTCGGAATGACCTCATGGATGGAG) and **pRS-sh-scrambled** were purchased from Origene (Rockville, MD)

- **MSCV-MIGR1:** MSCV-based retroviral construct expressing low levels of eGFP (described in (163)) was kindly provided by M. Busslinger (Institute of Molecular Pathology, Vienna, Austria).

2.1.7 Oligonucleotides

2.1.7.1 RT-PCR

BTG1:

forward primer CCGTGTCCTTCATCTCCAAG

reverse primer: TCGTTCTGCCCAAGAGAAGT

product size: 423 bp

GADD45a:

forward primer CAGAAGACCGAAAGGATGGA

reverse primer: TCCCGGCAAAAACAAATAAG

product size: 416 bp

CDKN1A:

forward primer: GAGGCCGGGATGAGTTGGGAGGAG

reverse primer: CAGCCGGCGTTTGGAGTGGTAGAA

product size: 197 bp

EWS-FLI1:

forward primer: TCCTACAGCCAAGCTCCAAGTC

reverse primer: ACTCCCCGTTGGTCCCCTCC

product size: 328 bp

FOXO1:

forward primer: AAGAGCGTGCCCTACTTCAA

reverse primer: CATCCCCTTCTCCAAGATCA

product size: 454 bp

FOXO3:

forward primer: TTCAAGGATAAGGGCGACAG

reverse primer: CAGGTCGTCCATGAGGTTTT

product size: 591 bp

LOX:

forward primer: CAGAGGAGAGTGGCTGAAGG

reverse primer: GTGAAATTGTGCAGCCTGAG

product size: 363 bp

DDIT4:

forward primer: AGACACGGCTTACCTGGATG

reverse primer: AGAGTTGGCGGAGCTAAACA

product size: 391 bp

PLAT:

forward primer: GCTACTTTGGGAATGGGTCA

reverse primer: ATGTTCTGCCCAAGATCACC

product size: 483 bp

HEY1:

forward primer: CGAGGTGGAGAAGGAGAGTG

reverse primer: CGAAATCCCAAACTCCGATA

product size: 339 bp

β-ACTIN:

forward primer: GCCGGGAAATCGTGCGTG

reverse primer: GGGTACATGGTGGTGCCG

product size: 305 bp

EPAS1:

forward primer: CGCCATCATCTCTCTGGATT

reverse primer: CTGGGTACTGCATTGGTCCT

product size: 328 bp

2.1.7.2 RT-qPCR

***EPAS1*:**

forward primer: AAGCCTTGGAGGGTTTCATT

reverse primer: TCATGAAGAAGTCCCGCTCT

Probe: TGACCCAAGATGGCGACATG

Product size: 234 bp

***MME*:**

forward primer: CCTTCTTTAGTGCCCAGCAG

reverse primer: CCAGTCAACGAGGTCTCCAT

Probe: CGGCATGGTCATAGGACACG

Product size: 131 bp

***OSMR*:**

forward primer: GTCATCTGGGTGGGGAATTA

reverse primer: CAAAGTGTGTGGCACATTCC

Probe: TTCTGCATTGGAGCTGGGAA

Product size: 100 bp

***B2M*:**

forward primer: TGAGTATGCCTGCCGTGTGA

reverse primer: TGATGCTGCTTACATGTCTCGAT

Probe: CCATGTGACTTTGTCACAGCCCAAGATAGTT

Product size: 82 bp

EWS-FLI1(typeI):

forward primer: CAGCCAAGCTCCAAGTCAATATAG

reverse primer: GCTCCTCTTCTGACTGAGTCATAAGA

Probe: CTGCCCGTAGCTGCTGCTCTGTTG

Product size: 84 bp

FOXO1:

forward primer: AAGAGCGTGCCCTACTTCAA

reverse primer: GTTGTTGTCCATGGATGCAG

Probe: CGGCGGGCTGGAAGAATTCA

Product size: 207 bp

2.1.7.3 ChIP-PCR

FOXO1 promoter (Chr.13): *covering ChIP seq. hit*

forward primer: GCCCGACTTACGGGATCT

reverse Primer: GAGAAAAACACCCCACTACCC

Product size: 197 bp at position -609/-412

FOXO1 promoter (Chr.13): *upstream of ChIP seq hit but probably also covered due to fragment size (shearing)*

forward primer: CCGGCGACACTTTGTTTACT

reverse Primer: CGTTCAGCAAAGACATCGTG

Product size: 225 bp at position -961/-736

FOXO1 control (Chr. 13): *~ 9kb upstream of TSS, predicted to contain no ETS sites (Consite)*

forward primer: CAGAGTCCCTCGGTCATCTC

reverse Primer: TGCGTTGTTGATTTTCTGCT

Product size: 183 bp at position -9071/-8888

2.1.8 Kits

MAGnify^{TM} Chromatin Immunoprecipation System Kit:

MAGnify^{TM} Chromatin Immunoprecipation System Kit (Invitrogen, Groningen, Netherlands) was used to perform ChIP experiments following the manufacturer's instructions. (see also, section 1.3 Methods, Chromatin immunoprecipitation assay)

SuperSignal® West Femto Maximum Sensitivity Substrate Kit:

SuperSignal® West Femto Maximum Sensitivity Substrate Kit is an extremely sensitive enhanced chemiluminescent substrate for detecting horseradish peroxidase (HRP) on western blots. (34096, Thermo Fisher Scientific, USA)

Nuclei EZ prep nuclei isolation Kit:

Nuclei EZ prep nuclei isolation Kit (NUC-101, Sigma, Saint Louis, MO) was used to prepare cytoplasmic/nuclear cell fractions according to the manufacturer's instructions.

Bright-Glo^{TM} Luciferase assay Kit:

Bright-Glo^{TM} Luciferase assay Kit (Promega, Madison, WI) was used for reporter gene assays according to the manufacturer's recommendations.

NE-PER Nuclear and Cytoplasmic Extraction Reagents:

NE-PER Nuclear and Cytoplasmic Extraction Reagents (Pierce Biotechnology, Rockford, USA; distributor Thermo Scientific, product no.78833) was used to separate nuclear and cytoplasmic protein fractions from fresh tumor tissues according to the manufacturer's recommendations.

2.2   Methods

2.2.1 DNA/RNA methods

2.2.1.1 RNA extraction

RNA extraction was performed using the RNAeasy Mini Kit (Qiagen, Austin, USA) according to the manufacturer's instructions.

2.2.1.2 cDNA synthesis

5µg of total RNA was denatured at 70°C for 10 minutes. After 2 min on ice, master mix, containing MMLV reverse transcriptase (Promega, Madison, USA), random hexamer primers and dNTP's were incubated for 90 min at 37°C. Subsequent addition of RNase free water was followed by incubation for 5 min at 70°C; cDNA was stored at -20°C.

2.2.1.3 RT-PCR

Standard RT-PCR was performed on 20-50ng cDNA template, mixed with a nucleotide mix, containing 2,5mM of dCTP, dATP, dTTP and dGTP (Promega, Madison, USA), 511 Reaction Buffer, (Finnzymes, Espoo, Finnland) containing 15mM $MgCl_2$, 0,4µM of each primer, and 0,5µl DyNAzyme DNA Polymerase (2U/µl, Finnzymes, Espoo, Finnland). The mix was filled up with ddH_2O to a total volume of 50µl per PCR reaction.

The polymerase chain reaction was performed by using the Dyad-Disciple thermal cycler (Biorad, California, USA) under following conditions:

Denaturation at 95°C for 2 min, 95°C for 1 min, specific annealing temperature, between 50-70°C, for 30 sec, elongation at 72°C for 1 min, all for the first 10 x cycles. This programme was slightly modified for the next 25 x cycles: 95°C for 30 sec, annealing temperature for 15 sec, elongation at 72°C for 1 min 30 sec, 72°C for 10 min and 15°C forever.

Following optimized PCR conditions could be obtained:

EPAS1

[20ng] cDNA; 10pmol/µl primer; annealing: 61.8°C; 1.5mM MgCl$_2$; x35cycles, elongation 1'-1'30''

HEY1

[20ng] cDNA; 10pmol/µl primer; annealing: 61.8°C; 3.0mM MgCl$_2$; 4% DMSO; x35cycles; elongation 1'-1'30''

PLAT

[20ng] cDNA; 10pmol/µl primer; annealing: 58.4°C; 1.5mM MgCl$_2$; x35cycles; elongation 1'-1'30''

DDIT4

[20ng] cDNA; 10pmol/µl primer; annealing: 61.8°C; 1.5mM MgCl$_2$; x35cycles; elongation
1'-1'30''

FOXO1

[20ng] cDNA; 20pmol/µl primer; annealing: 64.6°C; 1.5mM MgCl$_2$; x35cycles; elongation 1'-1'30''

EWS-FLI1

[20ng] cDNA; 20pmol/µl primer; annealing: 64.6°C; 1.5mM MgCl$_2$; x35cycles; elongation 1'-1'30''

β-actin

elong. 1'-1'30"; annealing: 58.4°C x 22cycles; 20pmol/µl; 1.5mM MgCl$_2$;

FOXO3

[20-50ng] cDNA; 20pmol/µl primer; annealing: 61.8°C; 1.5mM MgCl$_2$; x35cycles; elongation 1'-1'30''

GADD45a

[20-50ng]cDNA; 20pmol/µl primer; annealing: 61.8°C; 1.5mM MgCl$_2$; x35cycles; elongation 1'-1'30''

CDKN1A

[20-50ng]cDNA; 20pmol/μl primer; annealing: 61.8°C; 1.5mM MgCl$_2$; x35cycles; elongation 1'-1'30''

BTG1

[20-50ng]cDNA; 20pmol/μl primer; annealing: 61.8°C; 1.5mM MgCl$_2$; x35cycles; elongation 1'-1'30''

LOX

[20-50ng]cDNA; 20pmol/μl primer; annealing: 64.6°C; 1.5mM MgCl$_2$; x28cycles; elongation 1'-1'30''

2.2.1.4 RT-quantitative PCR (RT-qPCR)

5μg of total RNA was denatured at 70°C for 10 minutes. After 2 min on ice, master mix, containing MMLV reverse transcriptase (Promega, Madison, USA), random hexamer primers and dNTP's were incubated for 60 min at 37°C. Subsequent incubation for 30 min on 42°C and addition of RNase free water was followed by incubation for 5 min at 70°C; cDNA was stored at -20°C.

Reactions were set up in a total volume of 25μl containing 12,5μl 2x Universal PCR Master Mix (Applied Biosystems, Vienna, Austria) and 900nM (EWS-FLI1, β2M, EPAS1, OSMR, MME, FOXO1) of each primer and 250nM (EWS-FLI1, β2M, EPAS1, OSMR, MME, FOXO1) TaqMan probe (5'-FAM, 3'-TAMRA), and 2μl of cDNA template (5-10ng/reaction). The mixtures were prepared in 96-well optical microtiter plates and amplified on the ABI Prism 7900 Sequence Detection System (Applied Biosystems, Foster City, CA) using the following cycling parameters: 2 min at 50°C, 10 min a 95°C, and 40 cycles of 15s at 95°C and 60s at 60°C. The beta-2-microglobulin values were used for normalization.

2.2.1.5 Chromatin immunoprecipitation assay

ChIP experiments were carried out according to the manufacturer's instructions (MAGnifyTM Chromatin Immunoprecipitation System Kit, Invitrogen, Groningen, Netherlands). To cross-link DNA and protein, A673sh cells were treated with 1% formaldehyde for 10 min at room temperature. Cells were kept on ice and washed twice with ice-cold PBS. After centrifugation, 50μl of lysis buffer per million cells including protease inhibitors were applied. After sonication, using the Bioruptor UCD-

200 TM power up sonication system (Diagenode, Liège, Belgium), the lysates were cleared by centrifugation. For immunoprecipitation, 15µl of FLI1 Ab (MyBioSource, San Diego, CA) were used. PCR was performed using Phusion Hotstart II polymerase (Finnzymes, Espoo, Finland). Primers were used in 40 cycles of amplification.

2.2.1.6 Maxi Prep

The day prior to preparation, 250ml of LB (containing 10mg/ml ampicillin) were inoculated with a pre-culture of the corresponding plasmid and incubated at 37°C overnight. Qiagen Endotoxin free MaxiPrep kit (Qiagen, Austin, USA) was used for preparation according to the manufacturer's instructions.

2.2.1.7 Reporter gene assays

For firefly luciferase reporter assays, a CDK2 (-122/+458 from the TSS) promoter fragment was cloned into the pGL4.10 vector (Promega, Madison, WI). A673sh cells were co-transfected with the pGL4.10-based reporter constructs and pmaxEGFP (Amaxa GmbH, Cologne, Germany) using Lipofectamine Plus reagent (Invitrogen, Groningen, Netherlands) at 20% density. The cells were treated with doxycycline 48h after transfection, and gene reporter assays were carried out using Bright Glo Luciferase assay kit (Promega, Madison, WI) 96h after transfection (48h after doxycycline induction). To correct reporter activity for transfection efficiency, the number of EGFP positive cells was monitored by standard flow cytometry.

2.2.2 Protein methods

2.2.2.1 SDS- Polyacrylamide Gel Electrophoresis (PAGE)

The SDS- polyacrylamide gel consists of a stacking and a separating gel:

Seperating gel:

	6%	8,5%	12,5%
30%Acrylamid / 0,8% Bis	1,05ml	1,4ml	2,1ml
H_2O	2,625ml	2,275ml	1,575ml
1,5M Tris pH8,8	1,25ml	1,25ml	1,25ml
20% SDS	25µl	25µl	25µl
10% APS	50µl	50µl	50µl
TEMED	6µl	6µl	6µl

Stacking gel:

30%Acrylamid / 0,8% Bis	415µl
H_2O	1,7ml
1M Tris pH6,8	315µl
20% SDS	12,5µl
10% APS	25µl
TEMED	2,5µl

Cells were counted and adjusted to a concentration of 30.000 cells/ µl with PBS and the same volume of 2x sample buffer. Samples were boiled for 10 min at 96°C, followed by centrifugation at top speed, and finally loaded on the SDS-gel. The gel was run at 40mA for ~ 60 min, till the bromhenol blue front began to phase out.

2.2.2.2 Western Blot

The transfer was started by assembling the transfer unit, consisting of the typical sandwich conformation (sponge, 3x Whatman paper, gel, nitrocellulose membrane, 3x Whatman paper, sponge), which was put in the blotting tank. The transfer effected for 90 min at 400mA with blotting tank cooled on ice.

The nitrocellulose membrane was stained with 1x PonceauS solution for several minutes and scanned afterwards. To avoid unspecific binding of the primary antibody, the membrane was incubated in 1% blocking solution for 60 minutes at room temperature. The primary antibody was diluted in 0.5% blocking solution, added to the membrane and incubated overnight at 4°C. On the next day, the membrane was washed three times with TBST and once with 0.5x blocking solution for 10 minutes at room temperature. Again, the secondary antibody was diluted in 0.5% blocking solution and incubated with the membrane for 1h at room temperature, followed by three times washing with TBST. The membrane was then carefully rinsed once with deionized water and incubated, with appropriate dilution of SuperSignal® West Femto Maximum Sensitivity Substrate Kit (Thermo Fisher Scientific, USA), for 3- 5 minutes in the dark. Films were developed using a standard radiograph processor (AGFA, CP-1000).

For detection by LICOR, Odyssey® Infrared Imaging System, a green fluorescent labelled secondary antibody (goat α-mouse IgG, DyLight^{TM} 800) was diluted in Blocking Buffer (Odyssey infrared Imaging System, Part No.: 927-40000) and incubated for 1h at room temperature in the dark. The membrane was washed thrice with TBST and finally kept in PBS.

2.2.3 Cell culture techniques

ES cell lines SK-N-MC and TC252 used in this study have been previously described (164, 165). The A673 ES cell line expressing type I EWS-FLI1 fusion and doxycycline-inducible short hairpin RNA against EWS-FLI1 (A673sh) was previously described (133) and kindly provided by Javier Alonso (Departamento de Biología Molecular y Celular del Cáncer, Instituto de Investigaciones Biomédicas, Madrid, Spain). A673 (American Type Culture Collection), TC252 and SK-N-MC cells were maintained in RPMI 1640 (Invitrogen, Groningen, Netherlands) and supplemented with 10% FCS (PAA Laboratories, Linz, Austria). A673sh cells were maintained in DMEM (Invitrogen) supplemented with 10% FCS (PAA), 2µg/ml Blasticidine (Invitrogen) and 50µg/ml Zeocin (Cayla, France). EWS-FLI1 knockdown was induced by addition of 1µg/ml doxycycline (Sigma-Aldrich, St. Louis, MO). The CDK2 inhibitor roscovitine as well as methylseleninic acid (MSA) (Sigma-Aldrich) and the PI3K/AKT

inhibitor LY294002 (Merck, Darmstadt, Germany) were added to ES cells at concentrations and for time periods indicated in the figures.

2.2.3.1 Transfection

For plasmid transfections, A673sh, A673, SK-N-MC and TC252 ES cells were plated in 75-mm^2 culture flasks, or directly cultured on glass slides and grown to about 70% confluence. Cells were transfected using the Lipofectamine Plus reagent (Invitrogen, Groningen, Netherlands) in serum-free OptiMEM I medium (Invitrogen, Groningen, Netherlands) according to the manufacturer's recommendations.

Cells were incubated in OptiMEM I, including the transfection mix, for four hours at 37°C. Subsequently, the serum free medium was replaced by supplemented RPMI medium. Puromycin selection [1µg/ml] was initiated on the following day and cells were harvested after 72h.

2.2.4 Functional Assays

2.2.4.1 Proliferation Assay

ES cell lines were seeded (5x10^4 cells/ well) into 6-well plates, cultured in RPMI 1640 or DMEM medium with 50ng/µl puromycin for constant selection pressure. Proliferation of viable cells was monitored by cell counting using a Bürker-Türk chamber in combination with trypan blue exclusion test for 4 days. Cells were treated with Accutase (PAA Laboratories, Linz, Austria), for 10 minutes and 10µl of the cell suspension were mixed with the same volume of trypan blue.

2.2.4.2 Soft agar assay

Cells were seeded in triplicates at 2×10^4 cells/35-mm dish. After resuspension in 0.3% agar in 10% FCS and RPMI or DMEM, cells were plated in 0.6% agar-coated dishes. A top layer containing 0.6% agar was then added. Cells were fed every 5 days by placing ~ 200µl of medium on the top layer. Colonies were microscopically counted after 14 days. Colony formation was examined at seven sites per well for a total of 21 fields.

2.2.5 Immunofluorescence analysis

ES cells were fixed with 4% paraformaldehyde (PFA) for 10 min at room temperature (RT), washed with 1x PBS and permeabilized using 0.1-0.5% Triton X100/PBS for 10 minutes. Cells were blocked with 2%-FCS/PBS for another 10 minutes and stained with anti-FLAG antibody (DYKDDDDK, Cell Signaling Technology, Inc., Danvers, MA) diluted in 2%FCS/PBS for 1 hour in a humid chamber at RT. After extensive washing with PBS, cells were incubated with secondary antibody (red-fluorescent Alexa Fluor 594 goat anti–rabbit IgG, Molecular Probes, Eugene, OR,) for 30 minutes in the dark, subsequently washed with PBS and counterstained with DAPI.

2.2.6 Flow cytometric analysis

For testing ES sensitivity to different concentrations of MSA for 16h, a no-wash sample preparation was conducted in which cells were gently harvested using Accutase (PAA Laboratories, Linz, Austria) and finally mixed with the corresponding supernatant (SN) to ensure a cell suspension containing all cell populations (dead, apoptotic, living). Each cell suspension was stained for Annexin V using FITC Annexin V antibody (BD Biosciences). The cell suspensions were incubated for 15 min in the dark followed by addition of DAPI (0.03µg/ml; Sigma-Aldrich, St.Louis, MO) as a marker for cells referred to as non viable (166). After staining, cells were acquired on a BDTM LSRII flow cytometer.

For cell-death rescue experiments using sh-FOXO1 and sh-scrambled control, cells were co-transfected using the low-expression eGFP-Plasmid (MSCV-MIGR1). 48h post transfection, cells were treated or not with 5µM MSA for 24h and subjected to flow cytometric cell viability analysis following a no-wash sample preparation as described above. Cells were stained for Annexin V using the APC Annexin V antibody (BD Biosciences) for 15 min in the dark including all further steps as described above. The gating strategy was as follows: First, cells were gated on SSC-area versus FSC-width. Within this population the GFP-positive cells were identified using the FITC-A versus PerCP-A channel and the apoptotic and necrotic/dead cells were gated within the GFP-positive population on the APC-A versus DAPI-A channel. For data evaluation the FlowJo software (Version 7.6.3) was used. To validate the mRNA induction of FOXO1 by MSA as well as the knockdown of endogenous FOXO1, GFP pos. cells were sorted and RNA was extracted according to the manufacturer's instructions (TRIzol Reagent, Invitrogen, Groningen, Netherlands).

2.2.7 *In vivo* studies

An orthotopic xenotransplantation model, using the ES cell line SK-N-MC was used as described in (167). Briefly, 2×10^6 SK-N-MC Ewing sarcoma cells were directly injected into the M. gastrocnemius of 6-8 week-old female SCID/bg mice. Tumor formation was examined on a daily basis and MSA treatments begun when tumors reached measurable sizes. Two groups, consisting of 14 mice each, were either intraperitoneally injected with 2.5mg/kg MSA or PBS and treatments were conducted every second day for 2 weeks. Tumor dimensions were measured manually with a digital caliper obtaining 2 diameters of the tumor sphere to determine the total volume of the tumors. The lower extremity volume at the site of the tumor was determined by the formula (D x d2/6) x π, where D is the longer diameter and d is the shorter diameter. Experiments were terminated when tumors reached the critical volume of 1500mm^3. Mice studies were approved by the state regulatory board and all animals received human care in compliance with the respective guidelines.

2.2.8 Bioinformatic analysis

2.2.8.1 Microarray & in-silico motif analysis

Gene expression profiling was performed using Affymetrix HG-U133-PLUS2 arrays (Affymetrix, Inc., Santa Clara, CA). cRNA target synthesis and GeneChip® processing were performed at the Gene Expression Profiling Unit of the Medical University of Innsbruck (Innsbruck, Austria) according to standard protocols (Affymetrix, Inc., Santa Clara, CA). Microarray data were performed in compliance to MIAME guidelines and submitted to GEO - Accession number GSE37409. All further analyses were performed in R statistical environment using Bioconductor packages (168). Affymetrix CEL files were preprocessed as described previously (129), yielding a final number of 8154 probesets that were used for all further analyses. Differentially expressed genes were determined using a moderated t-test in the R package "limma" (169). All P-values were corrected for multiple testing using the "Benjamini-Hochberg" correction method.

Time-course analysis of gene expression in an ES cell line with a doxycycline inducible knockdown of EWS-FLI1 (A673sh) was performed on Affymetrix HGU-133A2 arrays as follows: At five timepoints, 0h, 18h, 36h, 53h, 72h, RNA was extracted and subjected to microarray analysis where 0h marks the time when doxycycline was added. Each experiment was reiterated at least twice and the EWS-

FLI1 protein was found to be consistently downregulated already at 18h in all replicate experiments. After filtering out probesets with very low expression values across all samples (R package "panp"), for every gene the most informative probeset (i.e. the one with the highest variance across all samples) was selected (R package "genefilter") yielding 8023 genes for further analysis. Differential expression for each gene at each later timepoint against 0h was determined using a moderated t-test from the R package "limma". The resulting p-values were corrected for multiple testing using the Benjamini-Hochberg method.

2.2.8.2 Promoter analysis for binding sites of known transcription factors

Coordinates of all conserved transcription factor binding sites (TFBS) were downloaded from the UCSC genome browser database (tfbsConsSites.txt) and hits for all sites within 1kb upstream of the TSS of all genes in the refGene.txt table were counted (both tables were downloaded from: http://hgdownload.cse.ucsc.edu/goldenPath/hg18/database/). Subsequently, the occurrence of each TFBS was correlated with gene expression change over time (all later time-points vs. h0 across all genes after the EWS-FLI1 knockdown. To count motifs in genes with similar time-course dynamics, genes were ordered by their logFC and binned into 100 equally sized bins (R-package "dr"). Within these bins motifs of all TFBS were counted and the counts plotted against the average logFC of the respective bin. Pearson correlation coefficients between number of motifs and mean logFC were recorded.

2.2.8.3 Statistical analysis of in-vitro and in-vivo assay

In-vitro data were analyzed by the unpaired t test with Welch's correction or with the one-sample t test using the Prism 5 for Windows (version 5.02) statistical software (GraphPad Prism Software, Inc.). Data shown in graphical format represent the means (±SEM), and a P value of <0.05 is considered statistically significant.

To test for overall differences in the growth curves of MSA treated vs. untreated mice a distribution free permutation test was utilized as described (170). Additionally, a mixed linear model analysis was performed on log-transformed values. To test for differences between treated and untreated groups on each day separately, a Wilcoxon signed rank test was performed. The mixed linear model analysis and Wilcoxon tests were done in SPPS. For the permutation test the implementation at http://www.stat.ucl.ac.be/ISpersonnel/lecoutre/Tgca/english/index3.html was used.

3 Results

3.1 EWS-FLI1 repressed genes show enrichment of recognition motifs for forkhead box (FOX) proteins.

To elucidate the transcriptional network downstream of EWS-FLI1, we analyzed time-resolved gene-expression profiles upon conditional EWS-FLI1 knockdown in A673sh cells. Promoter regions of knockdown responsive genes were analyzed for the presence of transcription factor binding motifs. Whereas EWS-FLI1 activated target gene promoters (suppressed upon modulation of EWS-FLI1) revealed strong enrichment of ETS binding motifs, EWS-FLI1 repressed gene promoters (activated upon EWS-FLI1 silencing) showed prominent over-representation of recognition motifs for forkhead box (FOX) transcription factors (i.e. FOXA2, FOXD1, FOXF2, FOXI1, FOXJ2, FOXL1, FOXO1, FOXO4) while lacking enrichment of ETS motifs (Figure 7). This result suggests a role for FOX family members in EWS-FLI1 mediated gene repression.
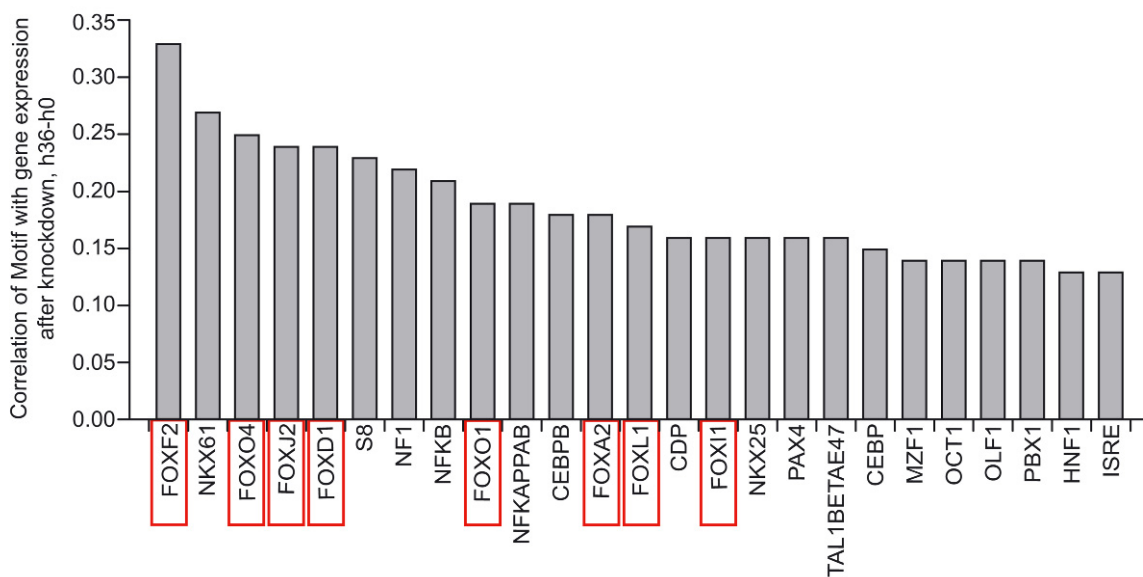

Figure 7: FOX motifs are enriched in EWS-FLI1 repressed genes.

Result from the correlation analysis of gene expression with motif occurence. X-Axis: DNA Motifs from Transfac ; Y-Axis: Pearson correlation of gene expression change at time-point h36 (against h0) of conditional EWS-FLI1 suppression in A673sh cells with the number of motifs. Forkhead-box motifs are marked by red squares.

3.2 Several FOX proteins, including FOXO1 and FOXO3, are regulated by EWS-FLI1 at the transcriptional level.

The enrichment of FOX motifs within EWS-FLI1 repressed promoters prompted us to investigate which FOX candidates are per se regulated by EWS-FLI1 in ES. Inspection of expression data of the inducible EWS-FLI1 knockdown as well as of 5 additional ES cell lines with transient EWS-FLI1 knockdown (previously described (129)) revealed consistently differential expression of FOXO1 and of the related FOXO3 between control and EWS-FLI1 knockdown conditions (Figure 8A and (129)).
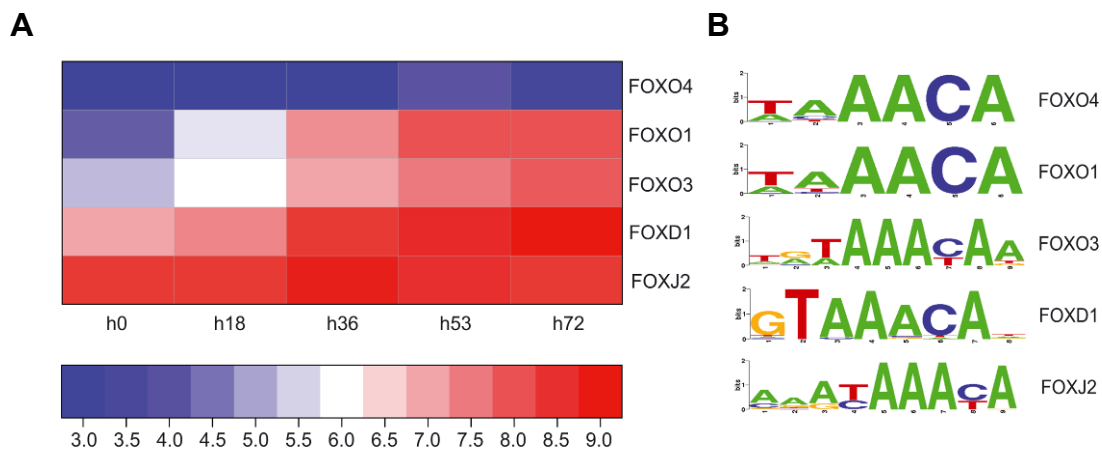

Figure 8: Various FOX proteins are transcriptionally repressed by EWS-FLI1

(A) Time resolved expression of FOX genes upon knockdown of EWS-FLI1 in A673sh cells. Only genes with probesets that passed quality filtering (see M&M section) are shown. (B) Sequence motifs of DNA motifs predicted to be specifically recognized by individual A673 expressed FOX-factors.

Furthermore, FOXO1 is expressed at lower levels in primary ES as compared to a wide variety of tissues (153) (Figure 9A) and its promoter is directly bound by EWS-FLI1 in ChIP-seq (our unpublished data) and ChIP-PCR experiments (Figure 10;(171)). The FOXO3 promoter, on the other hand, was not directly bound by EWS-FLI1 in ChIP-seq (data not shown) and shows higher expression in ES than in most other tissues (Figure 9B). Finally, position weight matrices (sequence logos, Figure 8B) of ES expressed FOX-factors (Figure 8A) were found to be very similar. Therefore, combining motif analysis with gene expression data, FOXO1 and FOXO3 were considered as the main candidate master regulatory transcription factors for a repressive transcriptional subsignature downstream of EWS-FLI1.
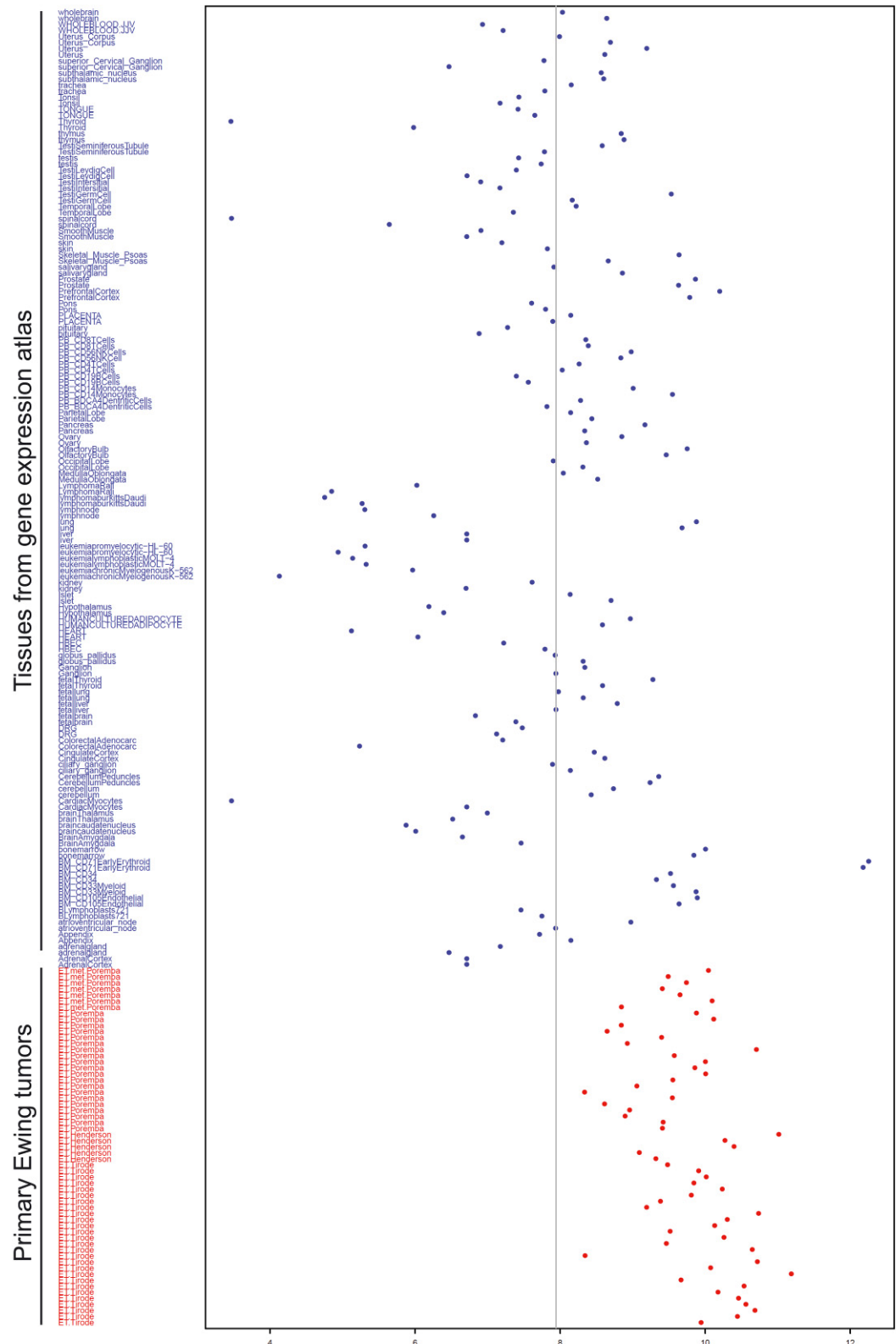
A

FOXO1 | 202723_s_at

Figure 9: Dot plot of normalized gene expression values

(A) FOXO1 (B) FOXO3. Data taken from (129). Blue: Reference tissues from (172). Red: primary Ewing Sarcoma samples. The comparison of A and B shows that FOXO1 is "off" in comparison to a wide variety of reference tissues, while FOXO3 is "on".
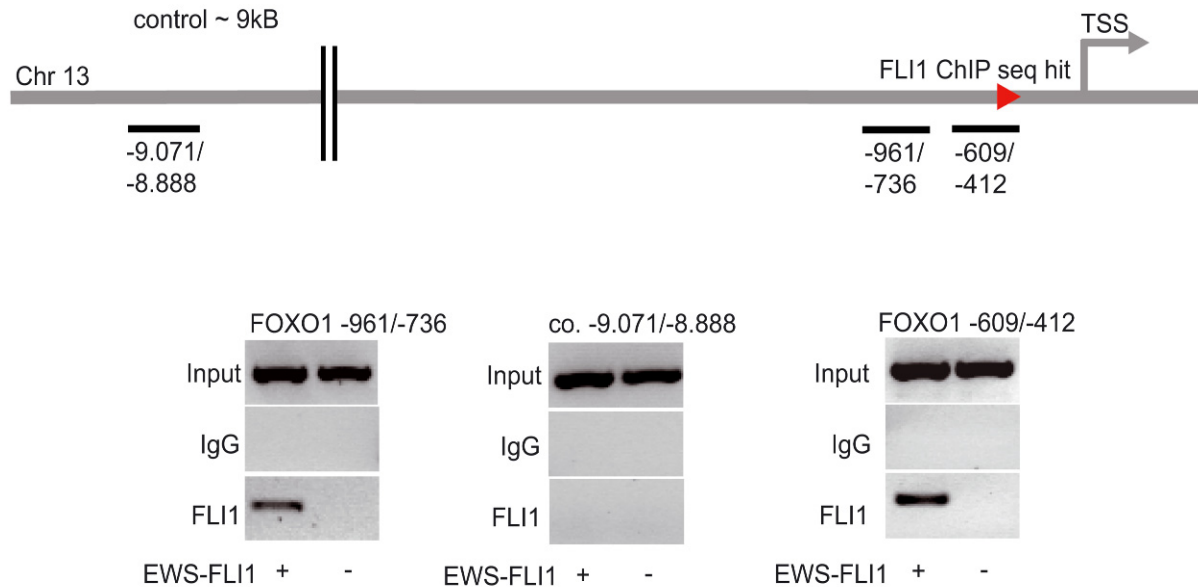
Figure 10: Representative ChIP-PCRs in A673sh cells.

Two different FOXO1 promoter fragments (from -961 to -736 and from -609 to -412 upstream of the transcription start site) including the ChIP-Seq hit at position -534 to -298, respectively and, for control, on a region further upstream (-9071 to -8888). Signals for EWS-FLI1 binding were obtained exclusively for the two promoter fragments in the presence of EWS-FLI1, but was completely abrogated upon 48h of doxycycline induced knockdown of EWS-FLI1. Input DNA and ChIPs using an IgG control antibody were used for specificity control.

3.3 Subcellular localization of FOXO1 is regulated by EWS-FLI1.

To test if reconstituted FOXO1 or FOXO3 can rescue expression of a subset of EWS-FLI1 repressed genes (induced mRNA expression upon EWS-FLI1 knockdown and predicted to have FOXO1/3 binding sites using ConSite (http://asp.ii.uib.no:8090/cgi-bin/CONSITE/consite)), we performed transient transfections to ectopically express these FOXO constructs as Flag-tagged proteins in A673sh cells. Following RNA extraction and subsequent cDNA synthesis, RT-PCR was performed and mRNA expression of 5 selected genes (*EPAS1*, *HEY1*, *PLAT*, *DDIT4*, *LOX*) was analysed (data not shown). No significant influence on the gene expression of these genes compared to EWS-FLI1 knockdown conditions was observed. However, since nuclear localization of FOXO proteins is a prerequisite for their transcriptional activity, we analysed whether the subcellular localization of ectopically expressed FOXO1 and FOXO3 was affected by EWS-FLI1.

In fact, in the presence of EWS-FLI1, both ectopic FOXO1 and FOXO3 were found excluded from the nucleus. Upon silencing of EWS-FLI1, however, Flag-FOXO1 but not Flag-FOXO3 readily translocated to the nucleus (Figure 11A).
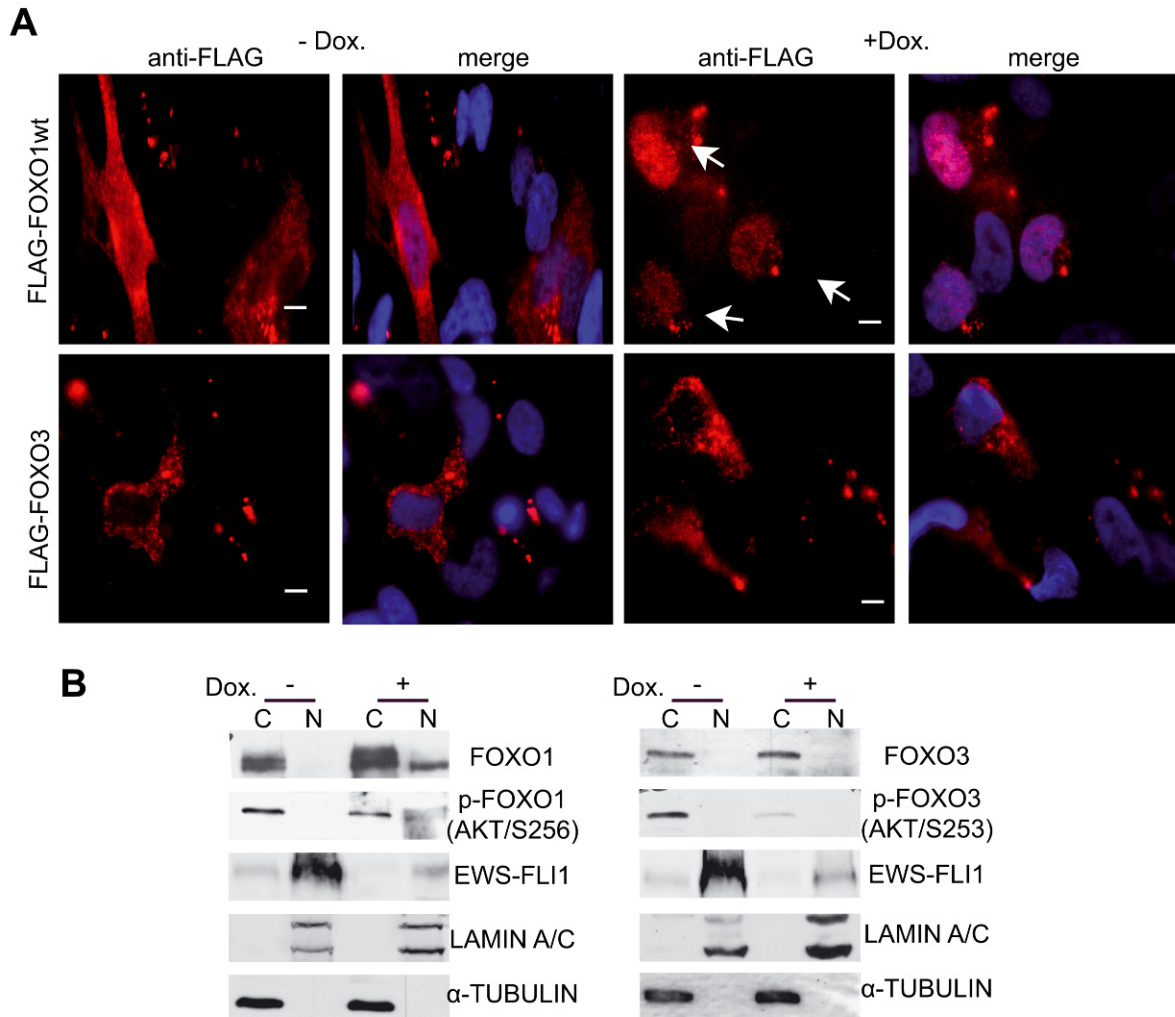
Figure 11: The subcellular localization of FOXO1 in A673sh cells is dependent on EWS-FLI1.
(A) Immunofluorescence analysis of FOXO1 and FOXO3 subcellular localization in the presence or absence of EWS-FLI1. Flag-tagged FOXO1 or FOXO3 was transfected into A673sh cells in the absence and presence of doxycycline induced EWS-FLI1 knockdown for 48 hours post transfection and subcellular localization was monitored by immunofluorescence using FLAG-tag specific antibody (red) with DAPI counterstain to delineate cell nuclei (blue). In the presence of EWS-FLI1, FOXO1 and FOXO3 stainings were confined exclusively to the cytoplasm. Upon EWS-FLI1 knockdown, only ectopically expressed FOXO1 but not FOXO3 translocated to the nucleus. (B) Immunoblot analysis of endogenous FOXO1 expression in cytoplasmic and nuclear cell fractions of A673sh cells. Basal expression of endogenous FOXO1 and FOXO3 in the presence of EWS-FLI1 was detectable exclusively in the cytoplasm. However, upon knockdown of EWS-FLI1 by doxycycline treatment for 48h, FOXO1 expression was significantly increased and also expressed in the nucleus, whereas

FOXO3 remained in the cytoplasm. In concordance with this observation, the levels of inactive phosphorylated FOXO1 and FOXO3 were reduced upon knockdown of EWS-FLI1. Scale bars: 10µM

We monitored endogenous FOXO1 and FOXO3 proteins upon doxycycline induced EWS-FLI1 knockdown by immunoblotting, and we observed strong FOXO1 induction and only weakly increased FOXO3 levels. FOXO1 was confined to the cytoplasm and the nucleus, whereas FOXO3 was exclusively retained in the cytoplasm (Figure 11B). While the cytoplasmic increase in FOXO1expression was already detectable at 16h of doxycycline treatment (the earliest time-point of EWS-FLI1 knockdown), nuclear FOXO1 was first observed at 36h (Figure. 12).
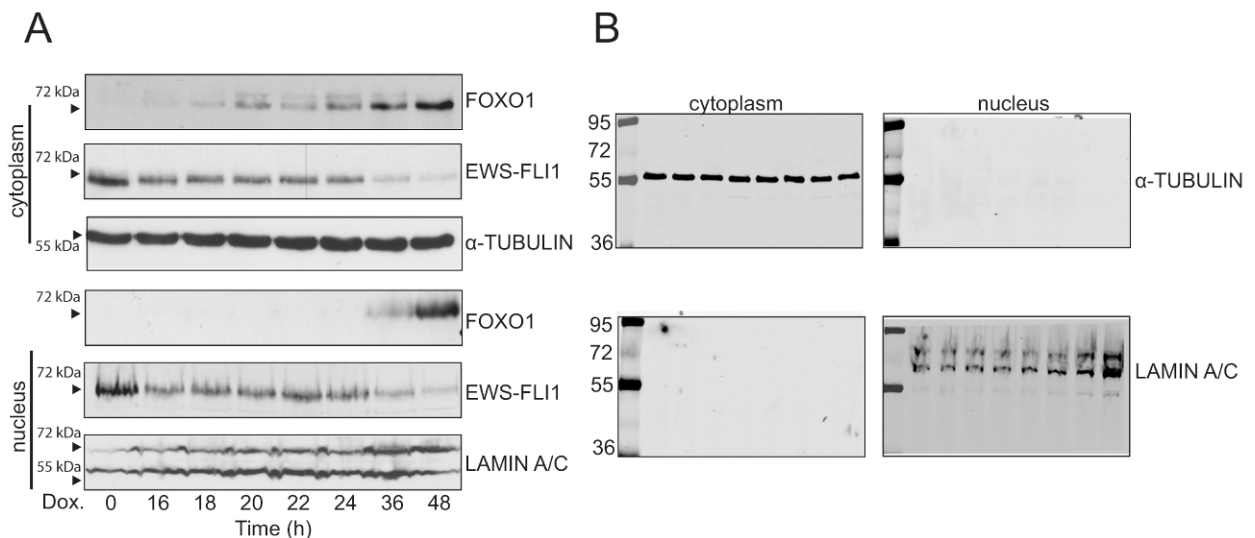
Figure 12: Kinetics of endogenous FOXO1 protein expression upon doxycycline induced EWS-FLI1 knockdown in A673sh cells.
(A) Down-regulation of EWS-FLI1 was already observed at 16h, the time when cytoplasmic FOXO1 induction became first detectable, while significant nuclear FOXO1 expression was first observed at 36h of doxycycline treatment with strongest expression at 48h. (B) To assess the purity of cytoplasmic/nuclear protein fractions, the same samples used in (A) were probed for Tubulin and Lamin A/C expression vice versa. The blots from (A) and (B) were processed in parallel.

Taken together, our findings suggest that EWS-FLI1 regulates FOXO1 not only at the transcriptional level but it also affects its subcellular localization thereby controlling the transcriptional activity of FOXO1.

3.4   CDK2 and AKT regulate FOXO1 activity in ES.

The subcellular localization of FOXO1 and FOXO3 transcription factors is known to be mainly regulated by posttranslational phosphorylation (27, 173). Mining the gene expression data upon knockdown of EWS-FLI1 in A673sh cells and in 5 additional ES cell lines (129), and of our EWS-FLI1 ChIP-seq data, we identified cyclin-dependent kinase 2 (CDK2), a well known negative regulator of FOXO1 transcriptional activity (27, 38, 174), among EWS-FLI1 induced genes (Figure 13).
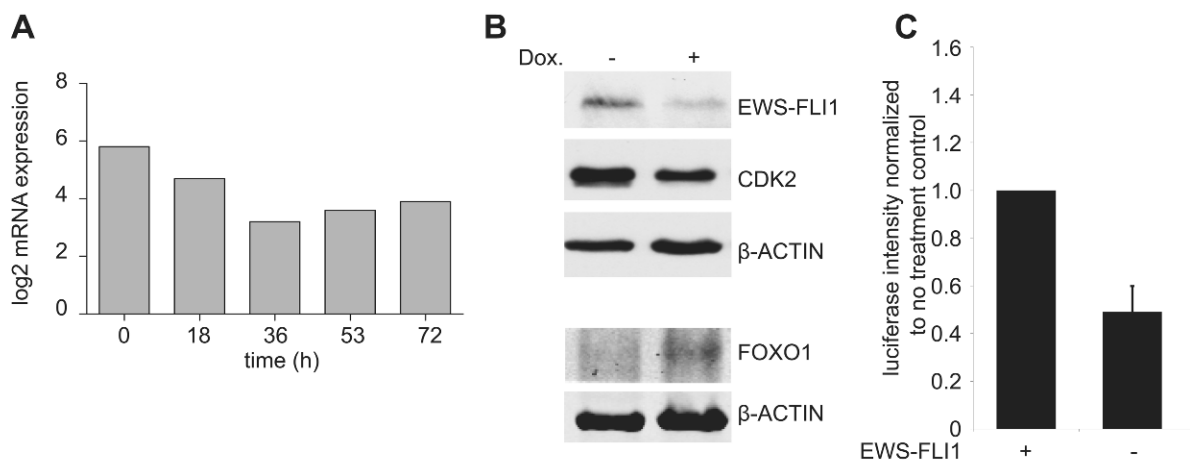
Figure 13: CDK2 is a EWS-FLI1 induced target.
(A) Kinetics of CDK2 mRNA expression in the EWS-FLI1 knockdown time-course of A673sh cells. X-Axis: interval after doxycycline induced EWS-FLI1 knockdown. Y-Axis: log2 CDK2 mRNA expression. (B) CDK2 and FOXO1 protein expression in A673sh cells upon 48 hours EWS-FLI1 knockdown. (C) Luciferase reporter gene assay testing CDK2 promoter responsiveness to EWS-FLI1knockdown. Y-axis: promoter activity of doxycycline treated relative to untreated cells (normalized for transfection efficiency and empty vector control transfections). Means and standard deviations of at least three independent experiments, each performed in triplicate, are shown.

Additionally, it has been reported that PI3K/AKT mediated phosphorylation negatively regulates FOXO1/3 nuclear localization and consequently activity (175, 176). To investigate whether CDK2 and/or AKT play a role in nuclear exclusion of FOXO1/3 downstream of EWS-FLI1, we treated A673sh cells with the inhibitors roscovitine and LY294002 alone, or in combination, to inhibit CDK2 and AKT activity, respectively (Figure 14A-B). Both inhibitors readily restored nuclear localization of ectopically expressed Flag-FOXO1 while Flag-FOXO3 remained in the cytoplasm. Coupled with the absence of nuclear translocation upon EWS-FLI1 knockdown, this result made

FOXO3 an unlikely candidate to participate in the gene regulatory network downstream of EWS-FLI1.
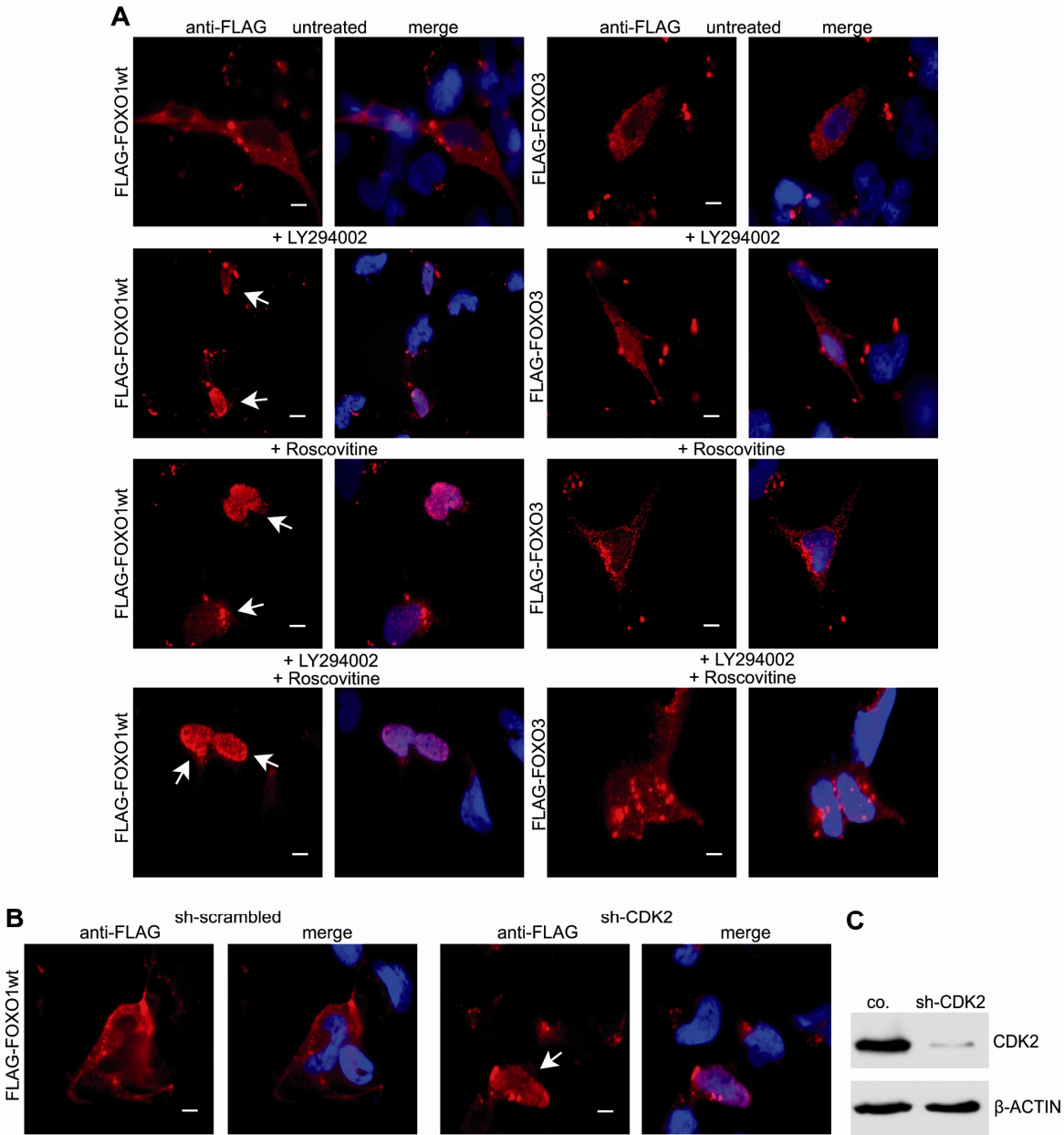
Figure 14: Nuclear localization of FOXO1 but not FOXO3 is tightly regulated by AKT and CDK2.
(A) Immunofluorescence analysis of A673sh cells transfected with either Flag-FOXO1wt or Flag-FOXO3 and treated with 40µM of the PI3K/AKT inhibitor LY294002 or 40µM of the canonical CDK2 inhibitor roscovitine, or a combination of both 48h post-transfection for 24h. Roscovitine and LY294002 treatments alone or in combination restore FOXO1 nuclear localization in the presence of EWS-FLI1, whereas FOXO3 remains in the cytoplasm. (B) Knockdown of endogenous CDK2 by shRNA-mediated RNA interference is sufficient to restore nuclear FOXO1 localization. A673sh cells were transfected with FLAG-FOXO1 and either shCDK2 or a scrambled shRNA control, and

immunofluorescence analysis was conducted 48h post-transfection. (C) Efficient CDK2 protein knockdown was monitored on the immunoblot. Results are representative of three experiments. Scale bars: 10μM

To test the importance of CDK2- and AKT-mediated phosphorylation for the transcriptional activity of FOXO1, we transiently transfected A673sh cells with phosphorylation-resistant FOXO1 mutants. We used Flag-FOXO1-T24A/S256A/S319A (Flag-FOXO1-AAA) and Flag-FOXO1-S249A/S298A in which AKT, respectively CDK2 specific phosphorylation sites were converted to alanine (38, 177). Both FOXO1 mutants localized to the nucleus but only Flag-FOXO1-AAA activated known FOXO1 target genes *GADD45a*, *BTG1*, and *CDKN1A*, despite the presence of EWS-FLI1 (Figure 15A-B).
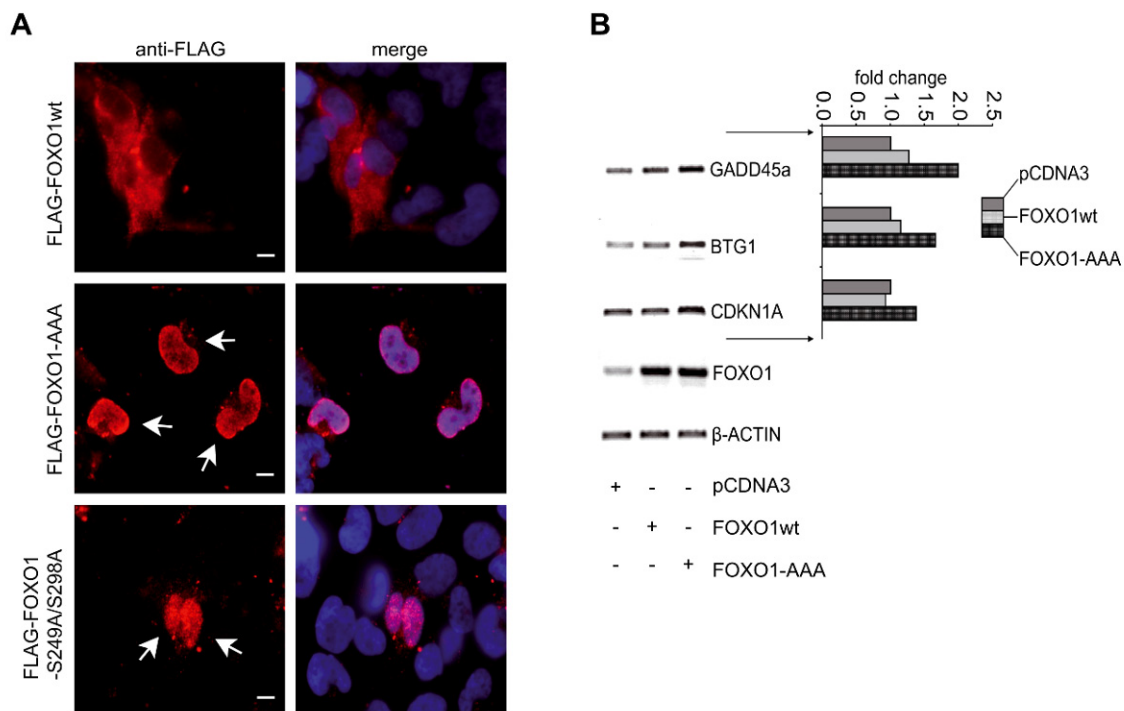
Figure 15: Nuclear localization and transcriptional activity of FOXO1 is rescued by mutation of inhibitory CDK2 and P-AKT phosphorylation sites.
(A) A673sh cells were transfected with Flag-FOXO1wt, an AKT-resistant (T24A/S256A/S319A, (AAA)) or a CDK2-resistant version of Flag-FOXO1 (S249A,S298A), and immunofluorescence analysis was performed 48h post-transfection. Cells were stained by anti-Flag antibody and visualized by red-fluorescent Alexa Fluor 594 goat anti–rabbit IgG antibody. (B) A673sh cells transfected with an AKT-resistant version of Flag-FOXO1 were analysed by RT-PCR for mRNA expression of canonical FOXO1 targets such as *GADD45a*, *BTG1* or *CDKN1A* and quantified using the image J software 1.37v. Results are representative of three experiments performed. β-Actin was used as internal

control. *GADD45a*, growth arrest and DNA damage inducible alpha (entrez gene number: ID:1647); *BTG1*, B-cell translocation gene 1, anti-proliferative (ID:694); *CDKN1A*, cyclin-dependent kinase inhibitor 1A (ID:1026). Scale bars: 10µM

Since treatment with roscovitine or mutation of residues S249 and S298 was sufficient to restore nuclear FOXO1 expression, we hypothesized that CDK2 played a central role in FOXO1 regulation downstream of EWS-FLI1. To test this, we performed knockdown experiments targeting endogenous CDK2 with specific shRNA in the presence of EWS-FLI1. As shown in Figure 14C, transiently transfected Flag-FOXO1wt was only found in the nucleus when endogenous CDK2 was concomitantly silenced. No influence on subcellular FOXO1 localization was observed using a scrambled shRNA control. These results confirm a rate-limiting role for CDK2 in nuclear FOXO1 exclusion in EWS-FLI1 expressing ES cells.

3.5 A repressive subsignature of EWS-FLI1 regulated genes is due to suppression of FOXO1.

To test for the contribution of FOXO1 inactivation to the EWS-FLI1 repressive transcriptional signature, the overlap between genes activated upon EWS-FLI1 knockdown and i) genes activated by ectopically expressed, nuclear directed FOXO1, and ii) genes re-activated after EWS-FLI1 knockdown with concomitant FOXO1 silencing were determined. In these experiments, 973 genes were found significantly (P<0.05, log2-foldchange>1) activated after EWS-FLI1 knockdown. Upon over-expression of AKT- or CDK2- phosphorylation resistant FOXO1 mutants, 208 and 184 genes, respectively, were up-regulated by FOXO1 (log2-foldchange>0.7). Of these, 94 and 58 genes respectively were also found up-regulated upon EWS-FLI1 knockdown. These overlaps are highly significant (P < 10-10, hypergeometric test). A double-knockdown of FOXO1 and EWS-FLI1 resulted in down-regulation of 306 genes (logFC<-0.7, P<0.05). The overlap of this gene set with 973 EWS-FLI1 repressed genes contained 94 genes (P < 10-10, hypergeometric test). Thus, a significant overlap between FOXO1 activated and EWS-FLI1 repressed genes was identified as measured by three different approaches (Figure 16A).
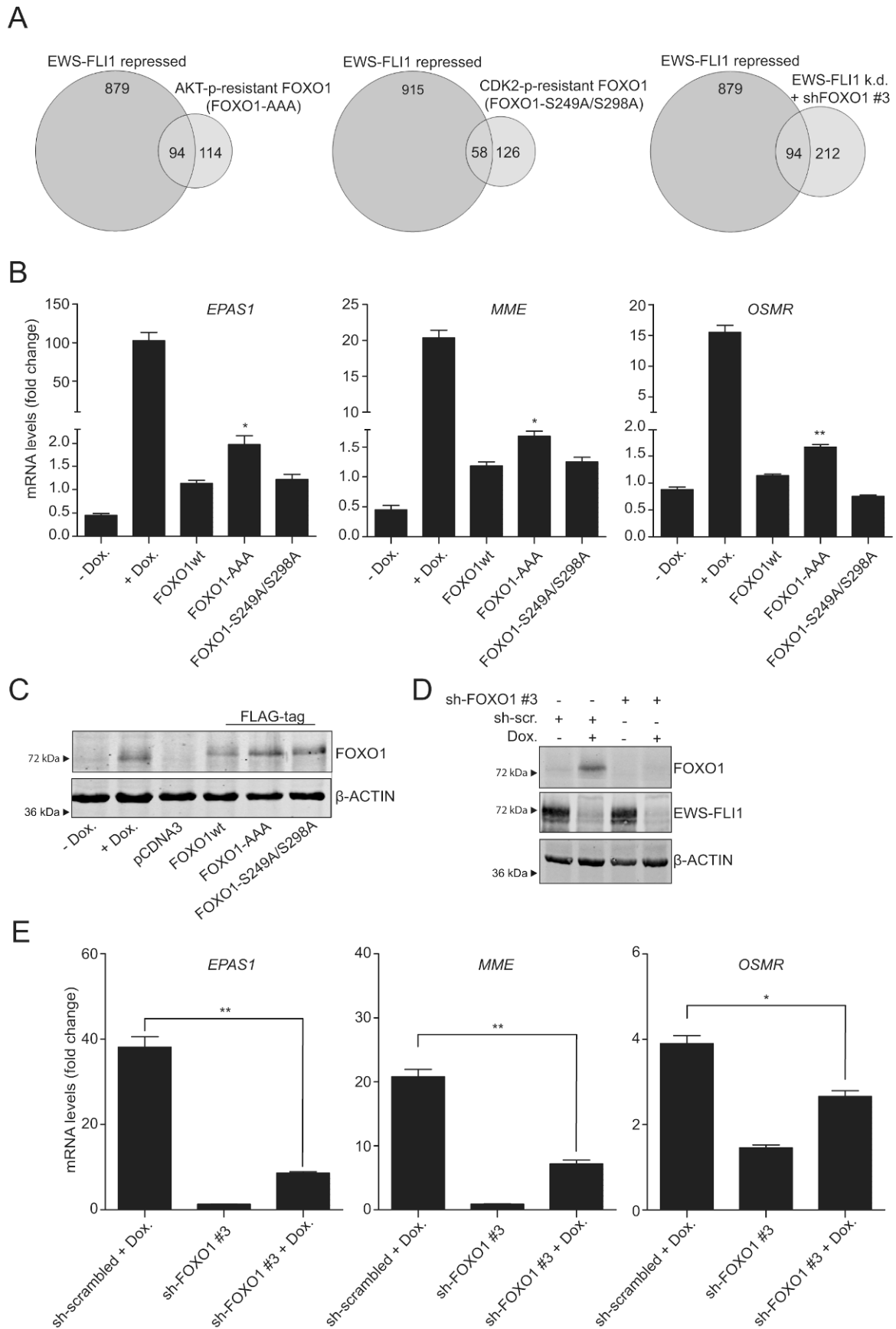
Figure 16: A subset of EWS-FLI1 repressed genes is regulated by FOXO1.

(A) Venn Diagramm showing the intersection between EWS-FLI1 repressed and FOXO1 activated genes. Over-expression of nuclear FOXO1 mutants (Flag-FOXO-T24A/S256A/S319A(AAA) (AKT-p-

resistant), Flag-FOXO-S249A/S29A (CDK2-p-resistant) led to reactivation of 94 and 58 EWS-FLI1 repressed genes, respectively, whereas silencing of reactivated endogenous FOXO1 under EWS-FLI1 knockdown conditions prohibited activation of 94 EWS-FLI1 repressed genes. (B) Validation of EWS-FLI1 repressed genes that can be reactivated by nuclear FOXO1. A673sh cells were transfected with AKT- or CDK2-phosphorylation-resistant versions of Flag-FOXO1, and mRNA expression of 3 genes representative of the overlap between EWS-FLI1 repressed and FOXO1 activated genes was measured by RT-qPCR. (C) Representative Western Blot for protein expression of endogenous FOXO1 upon inducible EWS-FLI1 knockdown as well as ectopically expressed wild-type and nuclear FOXO1 mutant, corresponding to B, showing similar levels of ectopically expressed and induced endogenous FOXO1. (D) Representative FOXO1 protein expression corresponding to E, showing specificity and efficiency of sh-RNA mediated FOXO1 silencing (shRNA #3). β-Actin was used as loading control. (E) In addition, knockdown of reactivated endogenous FOXO1 was used to demonstrate the dependency of EWS-FLI1 mediated repression on FOXO1 silencing. The mRNA expression was normalized to pCDNA3 empty vector control expression or to sh-scrambled control without doxycycline treatment, and statistical relevance was analysed using the unpaired t-test or one-sample t-test, respectively. B2M was used as internal control and doxycycline was applied for 72h. Results represent the mean ± SEM of two experiments performed. *p<0.05 and **p<0.01.

Validation of these results was performed by RT-qPCR on three arbitrarily chosen genes from the overlap of genes that were found significant in all three experimental settings (Figure 16B-C). In contrast to wild-type FOXO1, introduction of AKT-phosphorylation resistant FOXO1 significantly increased expression of *EPAS*1, *MME* and *OSMR* (Figure 16B and Figure 17E-F). In contrast, despite nuclear localization (Figure 15A), CDK2-phosphorylation resistant FOXO1 failed to reactivate these genes. This result may be explained by retention of intact AKT-mediated phosphorylation which is expected to lead to 14-3-3 binding and consequent FOXO1 dissociation from DNA (178-180). Reactivation of endogenous FOXO1 as a consequence of doxycycline-induced EWS-FLI1 knockdown led to the transcriptional induction of all three tested genes, which was largely abolished upon RNAi knockdown of FOXO1 (Figure 16D-E). Similar results were obtained using a second shRNA targeting endogenous FOXO1 (Figure 17B-D).
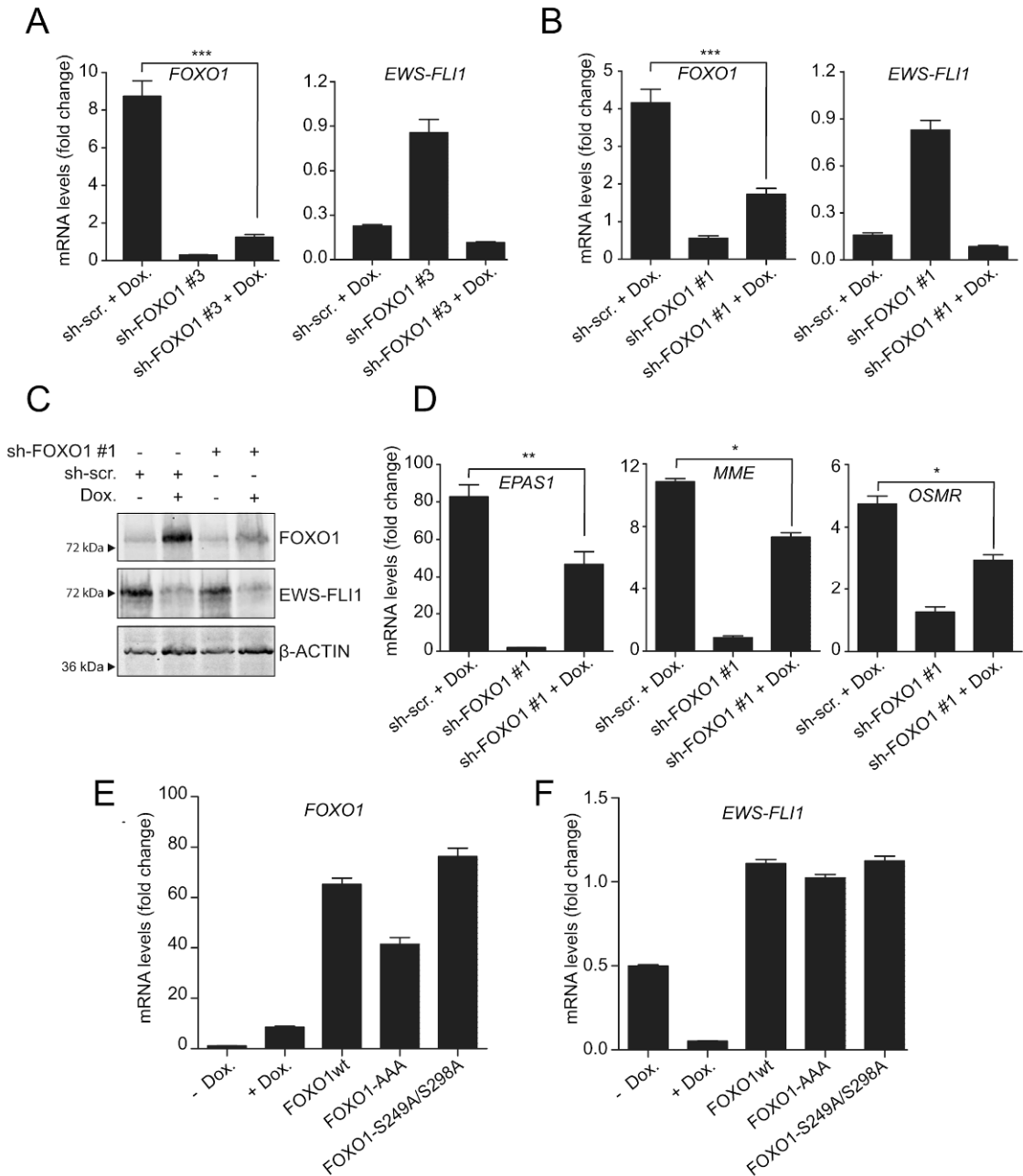
Figure 17: mRNA expression of endogenous FOXO1 and of EWS-FLI1 upon modulation of EWS-FLI1 and FOXO1 in A673sh cells (related to Figure 16 B and E).

(A-B) Doxycycline induced knockdown of EWS-FLI1 with concomitant FOXO1 silencing using two different FOXO1-shRNAs (#1, #3). (C) Representative FOXO1 protein expression showing specificity and efficiency of sh-RNA #1 mediated FOXO1 silencing and (D) comparable mRNA expression of the same genes (shown in Fig. 16E) upon knockdown of FOXO1 using shRNA #1. (E-F) FOXO1 and EWS-FLI1 mRNA expression upon ectopic expression of wild-type and mutant nuclear FOXO1. The mRNA expression was normalized to pCDNA3 empty vector control expression or to sh-scrambled control without doxycycline treatment. Statistical relevance was analysed using the unpaired t-test, B2M was used as internal control and doxycycline was applied for 72h. Results represent the mean ± SEM of two experiments performed. *$p < 0.05$, **$p < 0.01$ and ***$p < 0.001$.

This result demonstrates the dependency of reactivation of these EWS-FLI1 repressed genes on FOXO1 expression. Taken together, these data confirm our hypothesis that a repressive subsignature of EWS-FLI1 regulated genes is due to suppression of FOXO1.

3.6 Functional restoration of nuclear FOXO1 expression in ES results in impaired proliferation and reduced colony formation capability.

Since FOXO proteins are known to function as cell cycle regulators and, more specifically, can induce G1 arrest (22, 24), we asked whether restoration of nuclear FOXO1 functionally affects the proliferative activity of ES cells *in vitro*. A673sh and SK-N-MC cells were transfected with CDK2- and AKT-phosphorylation-resistant FOXO1 in the presence of EWS-FLI1. Control cells were transfected with empty vector or FOXO1wt. Proliferation of viable cells was monitored 4 days post transfection. As shown in Figure 18A-B, both A673sh and SK-N-MC exhibited significantly reduced proliferation upon restoration of nuclear FOXO1 compared to cells transfected with the empty vector control or FOXO1wt.

The ability of cells to grow under anchorage-independent conditions is considered a hallmark of oncogenic transformation (181). When seeded into soft agar, the number of colonies formed by A673sh and SK-N-MC cells after 2 weeks was also significantly reduced upon expression of nuclear FOXO1 compared to cytoplasmic FOXO1wt and to the empty-vector control (Figure 18C-D). Since colony sizes did not differ dramatically between control-transfectants (empty-vector, FOXO1wt) and cells expressing nuclear-targeted FOXO1, the observed significant reduction in colony number cannot be solely attributed to reduced proliferation but to decreased clonogenicity. Taken together, these results suggest that FOXO1 plays an important role in ES oncogenesis.
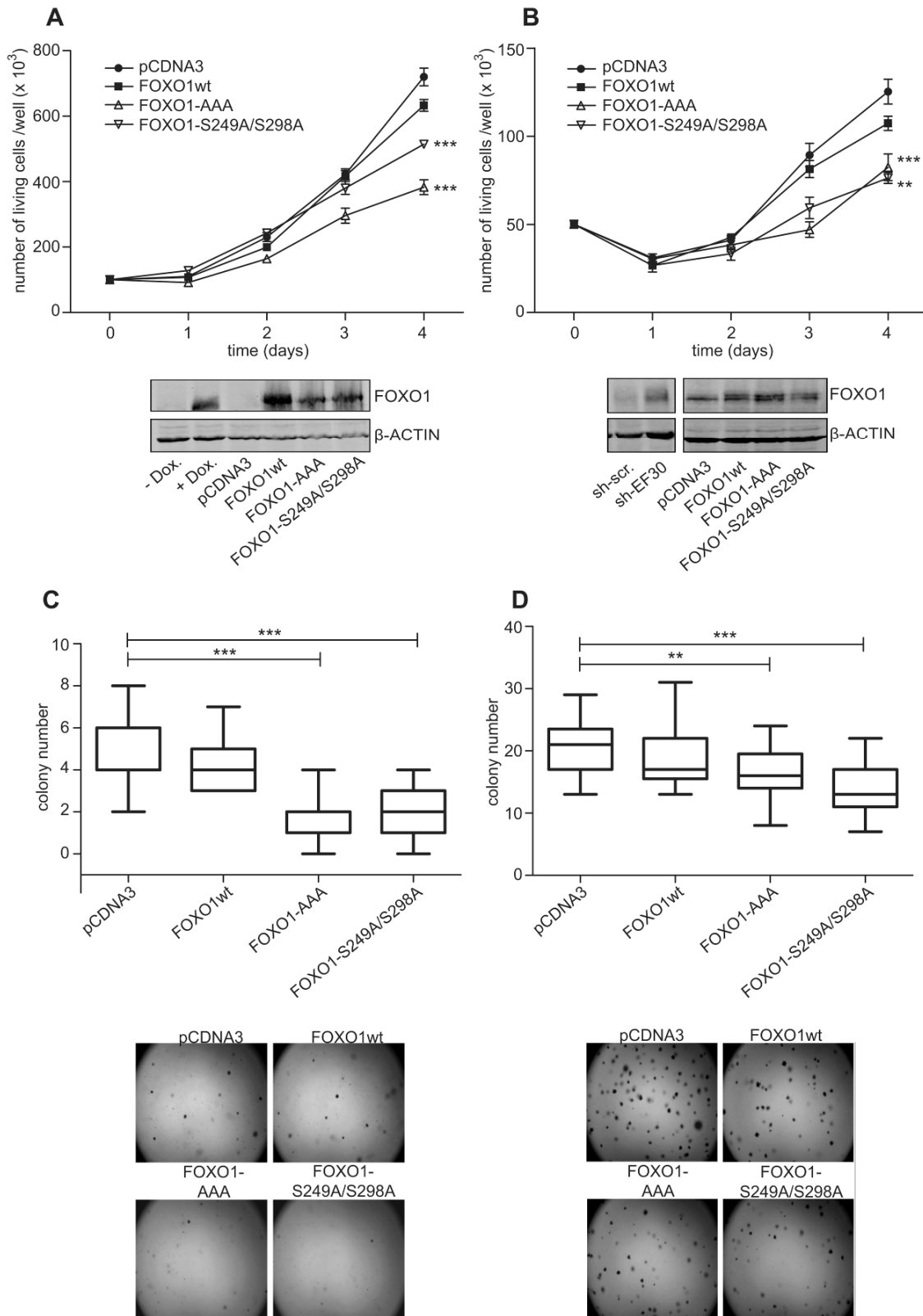
Figure 18: Functional restoration of nuclear FOXO1 expression in ES cells results in impaired proliferation and reduced soft agar colony formation capability.

A673sh (A, C) and SK-N-MC cells (B, D) were transfected with AKT- and CDK2- resistant FOXO1, or the empty vector control, or FOXO1wt. Experiments were performed in triplicates and one representative experiment of at least three is shown. (A) and (B) Anchorage-dependent growth.

Controls for FOXO1 protein expression are shown below the growth curves. (C) and (D) Clonogenicity of A673sh and SK-N-MC cells as studied by soft agar colony formation assays *in vitro*. The colony sizes (see corresponding pictures) were not found to be drastically different between controls (empty vector and FOXO1wt) and nuclear FOXO1 mutants, suggesting significantly reduced clonogenicity triggered by nuclear FOXO1. Colonies were counted 14 days after seeding. **p<0.01 and ***p<0.001.

3.7   Methylseleninic acid (MSA) can reactivate endogenous FOXO1 in a dose- and time-dependent manner.

Since we found endogenous FOXO1 to be negatively regulated by EWS-FLI1 at transcriptional and posttranslational levels in ES, a chemical compound, Methylseleninic acid (MSA), previously shown to reactivate FOXO1 in prostate cancer cells (150), was investigated for its potential to rescue FOXO1 activity in ES cells.
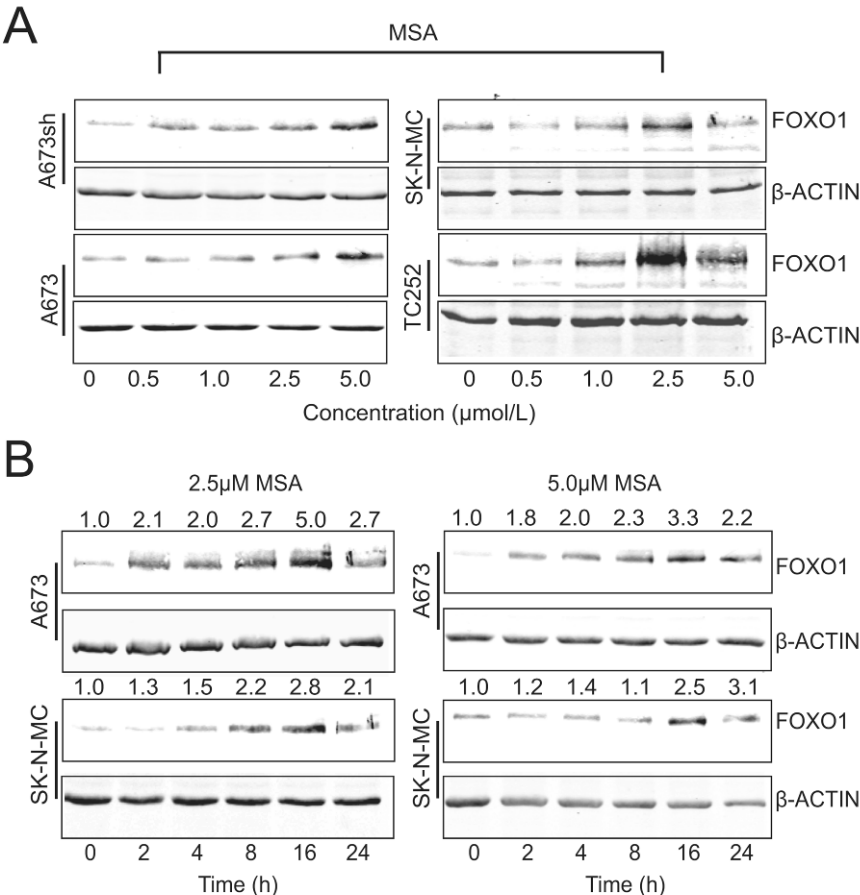
Figure 19: MSA reactivates FOXO1 expression.
MSA dose- (A) and time-dependent (B) FOXO1 protein induction as monitored by immuno blotting in different ES cell lines as indicated. Protein expression in (B) was quantified using the LICOR Odyssey® Infrared Imaging System.

Four different ES cell lines were treated with increasing MSA concentrations and the levels of endogenous FOXO1 protein were monitored by immunoblot analysis. As shown in Figure 19A, FOXO1 was induced in a concentration dependent manner with highest expression between 2.5 and 5µM MSA. FOXO1 protein expression peaked at 16h (Figure 19B) while mRNA levels were already induced between 2h and 4h of MSA treatment and declined gradually thereafter (Figure 20A-B).
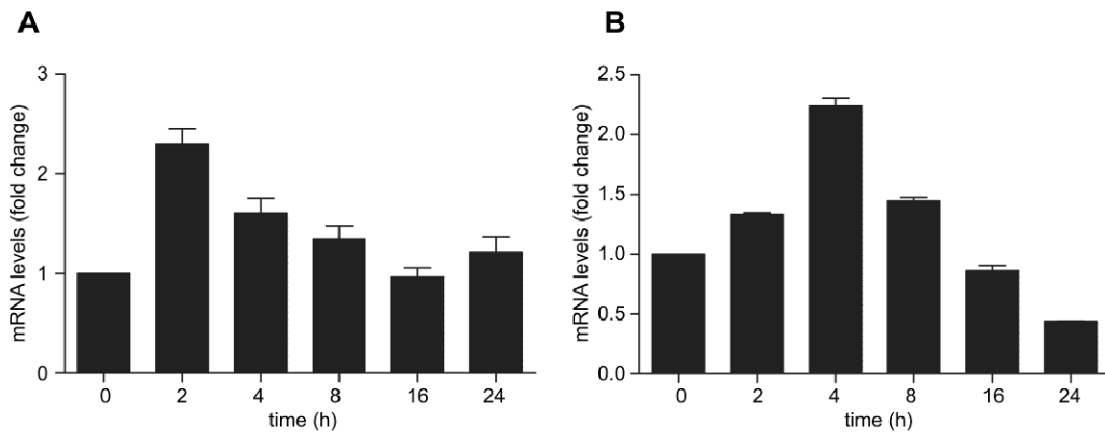
Figure 20: FOXO1 mRNA expression is induced early upon treatment with MSA.
Change of FOXO1 mRNA levels in (A) SK-N-MC and (B) A673 cells as a function of time measured by RT-qPCR. Shown are representative experiments of at least three, and the fold-induction was calculated in comparison to the untreated control and normalized to B2M.

These findings suggest that MSA not only induces FOXO1 protein expression but also regulates FOXO1 at the RNA level. As shown in Fig. 19B, quantification of FOXO1 protein expression revealed 3 to 5 fold induction upon MSA treatment which was comparable to FOXO1 protein levels after the EWS-FLI1 knockdown (3 to 6 fold, data not shown).

Notably, MSA treatments led to nuclear FOXO1 expression compared to the untreated control even in the presence of EWS-FLI1 *in vitro* and *in vivo* as shown for two different MSA treated tumours (MSA/1 and MSA/2) (Figure 21A-C).
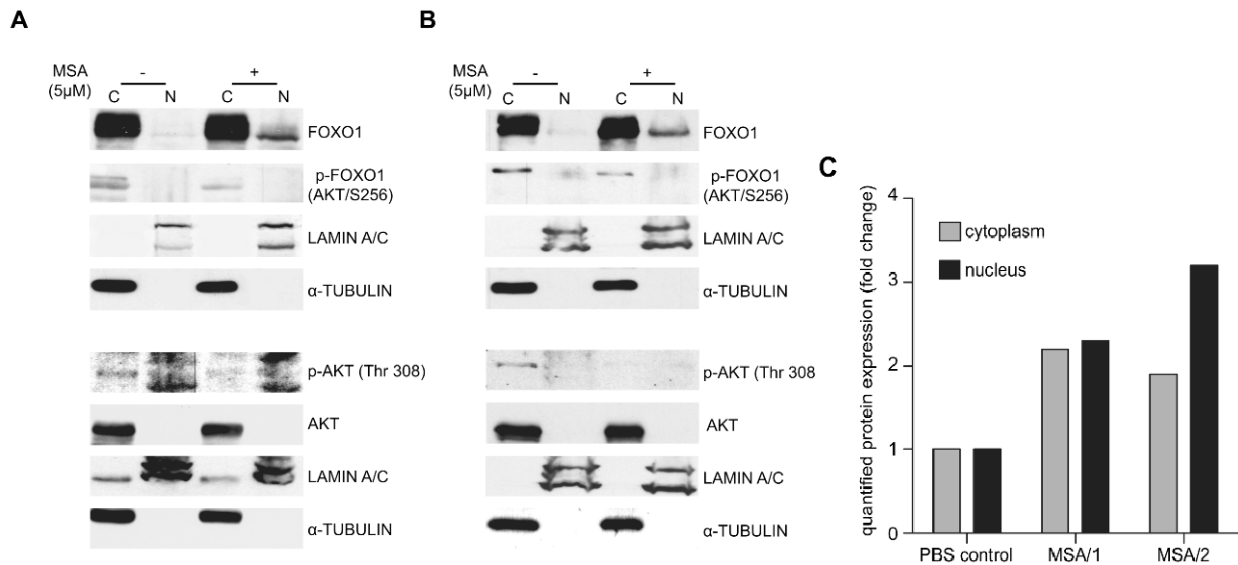
Figure 21: MSA induces expression of nuclear FOXO1 in the presence of EWS-FLI1 *in vitro* and *in vivo*.

The ES cell lines (A) SK-N-MC and (B) A673 were treated with 5µM MSA for 16h and subsequently processed to extract cytoplasmic and nuclear protein fractions. (C) Mice bearing orthotopic A673 tumors where treated with 2.5mg/kg MSA every second day for three times and further processed to generate cytoplasmic and nuclear protein fractions from fresh tumor tissues. Nuclear FOXO1 expression was elevated in MSA treated tumors (MSA/1 and MSA/2) compared to a PBS control. Protein expression was quantified using the LICOR Odyssey® Infrared Imaging System that allows linear quantification. Nuclear and cytoplasmic fractions were obtained using the NE-PER Nuclear and Cytoplasmic Extraction Reagent kit as described in materials and methods section 2.1.8. The protein samples were probed with FOXO1 specific, p-FOXO1 (AKT-S256) and P-AKT (Thr 308) antibodies. LaminA/C and α-Tubulin were used as nuclear and cytoplasmic loading controls, respectively.

This observation was accompanied by reduced cytoplasmic p-FOXO1 levels, presumably as a consequence of MSA induced reduction of P-AKT (151, 182) (Figure 21A-B).

3.8   MSA induces cell death which is dependent on FOXO1 expression.

To analyse the effect of MSA on ES cell survival, A673 and SK-N-MC cell lines were treated with different concentrations of MSA for 16h and subsequently processed for flow cytometric cell death analysis. The percentage of AnnexinV-FITC positive cells, representing the apoptotic sub-population, and DAPI positive necrotic cells were counted together to monitor overall cell death induction as shown in Figure 22A. At a final concentration of 5µM MSA, the proportion of drug-induced cell death approached 30-40% in both cell lines.

To clarify whether FOXO1 was involved in MSA induced cell death, we transiently transfected SK-N-MC and A673 ES cell lines with either sh-scrambled control or sh-RNA targeting endogenous FOXO1 (sh-FOXO1 #3) following MSA treatment (5µM) for 24h (Figure 22B and for control 22C-D). In both cell lines, induction of cell death as a function of AnnexinV-APC and DAPI positive cells was induced in sh-scrambled controls, whereas the knockdown of endogenously induced FOXO1 significantly reduced the MSA effect, suggesting that FOXO1 is at least partially involved in MSA induced cell death.
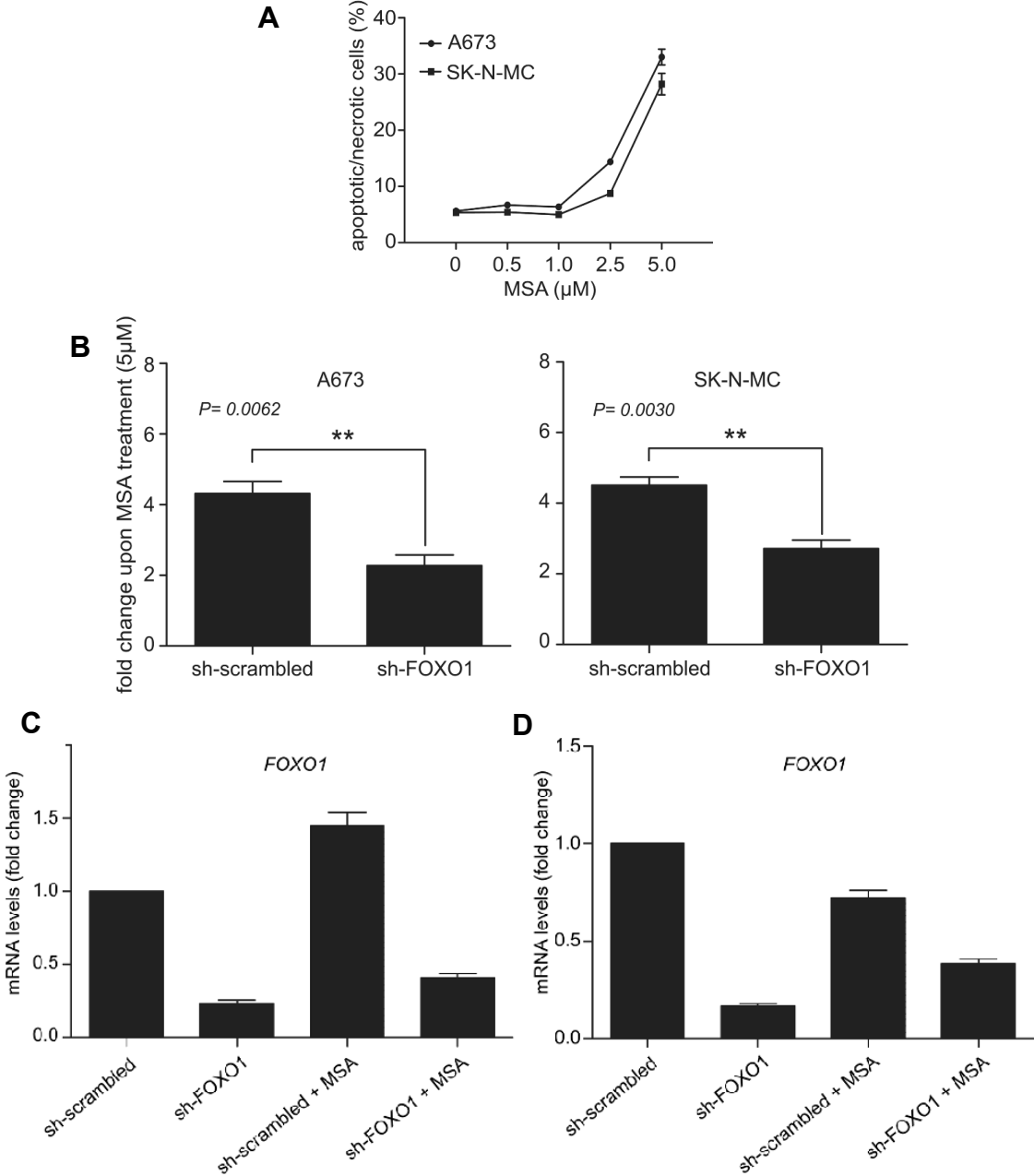
Figure 22: MSA induces ES cell death *in vitro*.

(A) MSA induces dose dependent cell death *in vitro* as measured by flow cytometry after 16h of treatment. (B) MSA induced cell death of A673 and SK-N-MC cells can be partially rescued by

transient knockdown of endogenous FOXO1. FOXO1 mRNA was readily reduced when ES cell lines (C) SK-N-MC and (D) A673 were transfected with sh-RNA targeting endogenous FOXO1 compared to the sh-scrambled control, as assessed by RT-qPCR. Results are representative of four experiments and the fold induction was calculated based on the untreated control, and B2M was used as internal control. Statistical analysis was done using the unpaired t test.

3.9 MSA reduces ES growth *in vivo*.

To assess the potential of MSA to reduce ES tumor growth in-vivo, we used an orthotopic mouse xenotransplantation model. 2×10^6 SK-N-MC cells were directly injected into the M. gastrocnemius of SCID/bg mice. Tumor formation was examined on a daily basis and treatments begun when tumors reached measurable sizes. A total of 14 mice per group (MSA or PBS) were treated with 2.5mg/kg MSA or the equivalent volume of PBS every second day for a time period of 2 weeks.
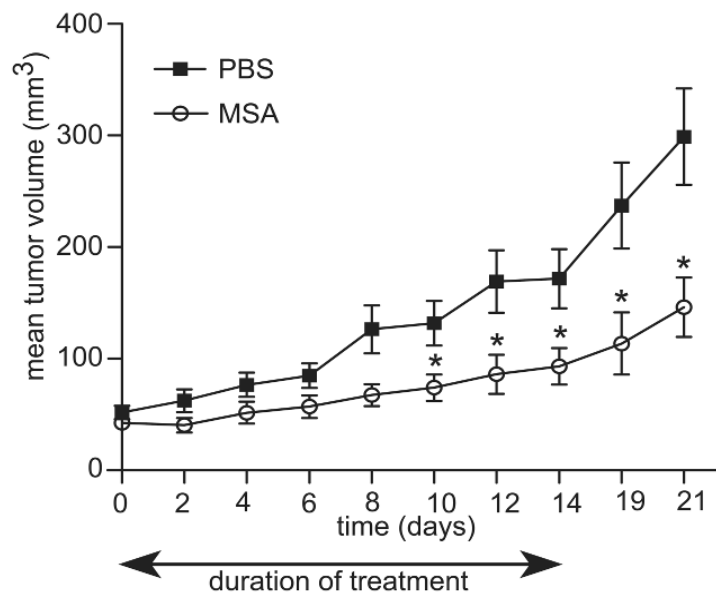
Figure 23: MSA reduces ES tumor growth *in vivo*.
MSA reduces ES tumor growth in vivo. After orthotopic injection of 2×10^6 SK-N-MC cells in the m. gastrocnemius, mice were either treated with 2.5mg/kg MSA (n=9) or PBS (n=12) every second day for 14 days. Tumor growth was further monitored until day 21. A distribution-free test for tumor-growth curve analyses revealed an overall significant difference between the MSA group versus the PBS group (P= 0.0403). Furthermore, significant differences were observed between the MSA group and the PBS group at different times as measured by Wilcoxon two sample test (day 10, P=0.04283; day 12, P=0.03604; day 14, P= 0.04283; day 19, P=0.02518; day 21, P=0.01565) *p<0.05.

Mice bearing tumors bigger than 100 mm^3 at day 0 were excluded from the analysis to avoid heterogeneity in MSA take-rate (183). Mice were observed for a period of 21 days after starting MSA treatments. As shown in Figure 23, tumor growth was significantly reduced in the MSA group compared to PBS control mice. Notably, the MSA mediated inhibitory growth effect on ES tumors persisted beyond the treatment period and tumor growth delay was accompanied by increased FOXO1 protein levels (Figure 24), suggesting a potent anti-tumorigenic activity of MSA.
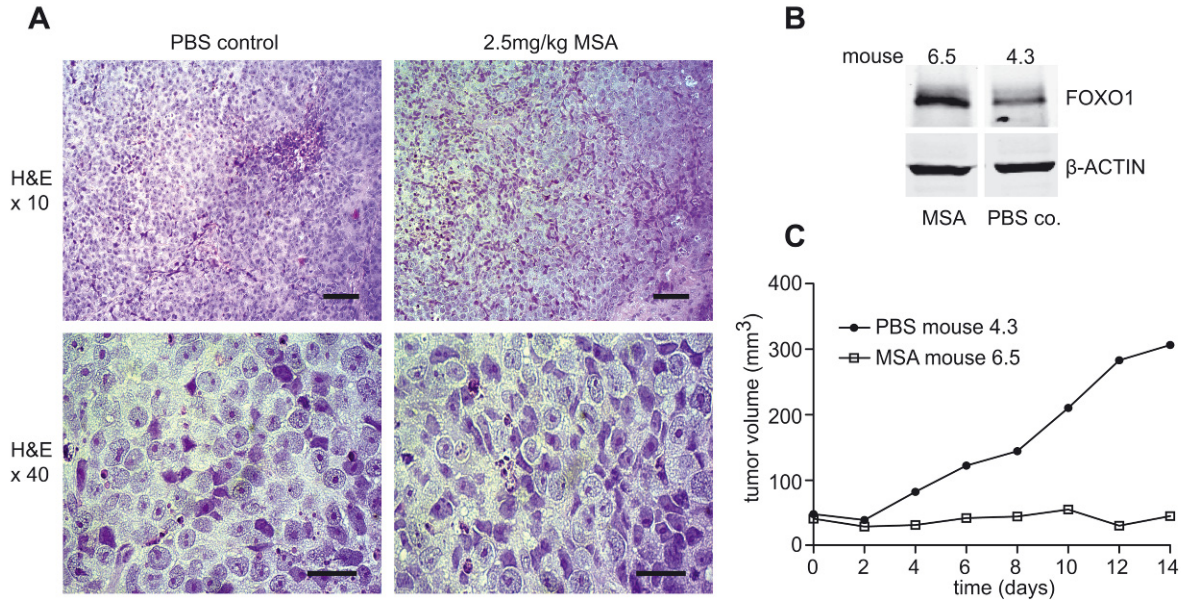
Figure 24: MSA induces FOXO1 expression and reduces ES tumor growth *in vivo*.
(A) Representative H&E stains of tumors from mice treated with PBS (mouse 4.3) or with 2.5mg/kg MSA (mouse 6.5) every second day for 2 weeks. Scale bar: 100 µm (first row); 20 µm (second row). (B) Immunoblot analysis on the tumors from A showed that MSA treatments induced FOXO1 expression compared to the PBS control. (C) Tumor volume over time from mice shown in A and B. Whereas PBS treatments led to exponential tumor growth, MSA treatments prohibited ES tumor growth consistent with induced FOXO1 expression.

4 Discussion

Because of its specificity to ES and its proven involvement in ES oncogenesis and progression (141, 184, 185), EWS-FLI1 is considered to be the ideal therapeutic target for future ES treatment strategies (124). Unfortunately, it has been difficult to therapeutically target nuclear transcription factors. Consequently, intervention with the downstream transcriptional network of EWS-FLI1 may be an alternative option to treat ES. However, the mechanisms of transcriptional regulation by EWS-FLI1 are only partially understood. So far, very little is known about mechanisms of EWS-FLI1 mediated gene repression, even though there is evidence that part of its repressive signature can be assigned to the activation of transcriptional repressors such as NKX2.2 or NR0B1 (156, 157). Moreover, it has been recently shown that EWS-FLI1 can mediate gene repression via transcriptional and posttranscriptional mechanisms (158).

Here we report that EWS-FLI1 exerts a significant part of its transcriptional repression activity via inhibition of the forkhead transcription factor FOXO1. Our *in vitro* data show that FOXO1 is tightly regulated in a multilayered manner by EWS-FLI1 mediated transcriptional repression and inhibitory phosphorylation by EWS-FLI1 induced CDK2 and AKT (summarized in Figure 25).

Figure 25: The transcriptional activity of FOXO1 is regulated in a multilayered manner.
EWS-FLI1 not only represses the transcription of FOXO1 but also affects P-AKT levels and regulates CDK2 activity, thus regulating FOXO1 transcriptional activity on a post-translational level. Blocking the PI3K-AKT signaling pathway with the canonical PI3K inhibitor LY294002 or by blocking active CDK2
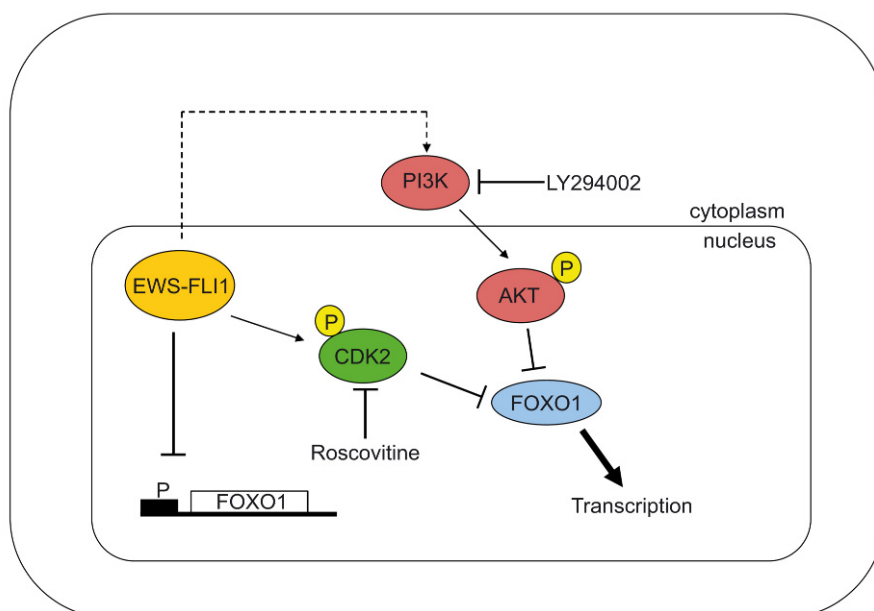
with roscovitine can overcome the repressive effect of EWS-FLI1 as shown for ectopically expressed FOXO1wt.

There is ample experimental evidence that AKT and CDK2 regulate the subcellular localization of FOXO1 independently of each other. In ES, the PI3K pathway is known to be an essential pro-survival pathway (186) which can be activated by growth factors such as IGF-1. It was previously shown that insulin-like growth factor binding protein-3 (IGFBP-3) is directly suppressed by EWS-FLI1 which at least partially enables ES cells to strongly activate this signaling pathway (130). Treatment with recombinant IGFBP-3 drastically decreases levels of phosphorylated AKT in ES cells (130) as a consequence of reduced IGF-1 levels and subsequently decreased phosphorylation of IGF-1R and p-AKT (163). Consistent with these findings, our immunofluorescence analysis revealed that by using a phosphorylation-resistant version of FOXO1, AKT mediated nuclear exclusion was abrogated. On the other hand, CDK2 was reported to functionally interact with FOXO1 leading to phosphorylation at two specific serine residues (S249/S298) followed by nuclear exclusion (38). Interestingly, ChIP-seq analysis and reporter gene assays identified CDK2 as a EWS-FLI1 induced target, suggesting an important role for CDK2 in FOXO1 repression by EWS-FLI1. Here, we show that knockdown of CDK2 was sufficient to drive ectopically expressed FOXO1 into the nucleus of ES cells even in the presence of active PI3K/AKT signaling. This finding is supported by nuclear localization of a CDK2-resistant FOXO1 mutant (S249A/S298A). While AKT phosphorylation at residues T24 and S256 causes binding of chaperon protein 14-3-3 (176, 187), potentially masking the nuclear localization signal (NLS) and causing dissociation of FOXO1 from DNA (178, 187), CDK2 phosphorylation at S249 does not affect 14-3-3 binding (38) but increases the negative charge of an adjacent stretch of three arginines within the NLS (38), which was previously demonstrated to play a major role in FOXO3 nuclear localization (49). However, the CDK2-phosphorylation-resistant version (S249A/S298A) of FOXO1 is still exposed to AKT-mediated phosphorylation thus allowing for 14-3-3 mediated destabilization of FOXO1 on DNA. Therefore, it was not unexpected that over-expression of CDK2-mutant FOXO1 did not re-activate EWS-FLI1 repressed genes to the same extent as AKT phosphorylation resistant FOXO1. The latter was capable of reactivating about 10% of EWS-FLI1 repressed genes as opposed to only 6% reactivated by CDK2-

resistant FOXO1. FOXO1 suppression by RNAi prohibited the activation of a similar number of genes by EWS-FLI1 knockdown as by the AKT resistant mutant.

FOXO1 was demonstrated to be involved in cellular differentiation (reviewed in (35)), and more specifically to function as an early molecular regulator in the differentiation of mesenchymal cells into osteoblasts (188). Along these lines, Tirode et al. reported previously that long-term inhibition of EWS-FLI1 enables differentiation of ES cells into the osteogenic lineage when treated with a suitable differentiation cocktail (98). Thus, reactivation of FOXO1 may represent an appropriate tool to induce differentiation in ES. Consistent with FOXO1-induced regulation of proliferation via induction of cell cycle arrest (189-191), our *in vitro* assays revealed reduced proliferative ability of ES cells upon restoration of nuclear FOXO1. In addition, nuclear FOXO1 decreased the clonogenicity of ES cells in soft agar, suggesting that FOXO1 plays an important role in ES oncogenesis.

Since our results identify the tumor suppressor FOXO1 as a potent negative regulator of cell proliferation and anchorage-independent growth *in vitro*, we hypothesized that reactivation of endogenous FOXO1 in the presence of EWS-FLI1 may constitute a potentially promising therapeutic strategy for ES. As a proof of principle, we chose to interrogate a small molecule, MSA, previously demonstrated to reactivate FOXO1 in prostate cancer cells, for its activity in ES cells *in vitro* and *in vivo*.

Selenium, as an essential component of the human diet, has long been discussed as a potential agent for cancer prevention (192-195). In a randomized, double-blinded, placebo-controlled human study (Nutritional Prevention of Cancer Trial (NPC)), more than 1300 patients were treated with a daily dose of 200µg selenized yeast as source for nutritional selenium supplementation in order to reduce the risk of recurrent non-melanoma skin cancer (192). Interestingly, the NPC study revealed a significant protective effect of selenium supplementation on the overall incidence of prostate cancer, especially in patients with a low baseline of plasma selenium concentrations (193, 194). This effect was largely attributed to selenite in the yeast, which is rapidly excreted via feces and urine. Based on the findings of NPC, the Selenium and Vitamin E Cancer Prevention Trial (SELECT) was initiated but prematurely terminated in 2008 because it failed to reduce prostate cancer incidence (196). These contradictory findings of the NPC and SELECT studies have been discussed as possibly arising from the use of different selenium formulations. Selenomethionine, used in SELECT, was suggested to be ineffective due to its rapid

incorporation into proteins which limits its bio availability in the plasma where it has been proposed to exert its anti-cancer activity (197). In contrast, mono-methylated forms of selenium, methylseleninic acid (MSA) and methylselenocysteine (MSC), which are rapidly metabolized to methylselenol, have been proposed to be active against a variety of cancers (198). MSA was shown to be more effective than MSC or Selenite in a prostate cancer xenograft model (199, 200). Moreover, it was demonstrated to act synergistically with several established chemotherapeutic agents including Doxorubicin and Etoposide, two components of standard chemotherapy in ES patients (201).

We found that ES cell-lines were highly sensitive to MSA treatment. MSA was previously shown to be involved in induction of apoptosis by different mechanisms (202, 203). We here demonstrate that cell death induction in ES was at least partially dependent on MSA-induced FOXO1 activity. We also observed anti-tumor activity in an orthotopic ES xenograft model which was accompanied by elevated FOXO1 protein levels consistent with our hypothesis that FOXO1 activation downstream of EWS-FLI1 confers a therapeutic benefit. However, the mechanism of FOXO1 reactivation by MSA remains elusive. MSA was demonstrated to reduce IGF1R levels and, consequently, phospho-AKT levels in a mouse mammary hyperplastic epithelial cell-line (204) providing a possible explanation for the post-translational FOXO1-inducing activity of the drug. A study in prostate cancer cells revealed that MSA treatment results in decreased expression of genes involved in metabolism, angiogenesis, certain transcription factors and, interestingly, signal transduction (ERK and AKT), which was significantly higher in tumor cells than in non-tumor cells (205).

High selenium doses are often associated with intoxication, and the MSA concentration used in this study (2.5mg/kg) represents the highest tolerated dose in SCID/bg mice (data not shown). For potential clinical use, we envision combination of low-dose methylated selenium in combination with other standard chemotherapeutic agents, since it was reported that MSA synergizes with conventional drugs such as etoposide and doxorubicin, which are frequently used in the treatment of Ewing sarcoma (205).

Taken together, our results imply that FOXO1 acts as a tumor suppressor in ES, and identify FOXO1 reactivation as a promising strategy for a future ES specific therapy.

References

1. Stratton, M.R. 2011. Exploring the genomes of cancer cells: progress and promise. *Science* 331:1553-1558.

2. Stratton, M.R., Campbell, P.J., and Futreal, P.A. 2009. The cancer genome. *Nature* 458:719-724.

3. Hanahan, D., and Weinberg, R.A. 2000. The hallmarks of cancer. *Cell* 100:57-70.

4. Schinzel, A.C., and Hahn, W.C. 2008. Oncogenic transformation and experimental models of human cancer. *Front Biosci* 13:71-84.

5. Beerenwinkel, N., Antal, T., Dingli, D., Traulsen, A., Kinzler, K.W., Velculescu, V.E., Vogelstein, B., and Nowak, M.A. 2007. Genetic progression and the waiting time to cancer. *PLoS Comput Biol* 3:e225.

6. Sjoblom, T., Jones, S., Wood, L.D., Parsons, D.W., Lin, J., Barber, T.D., Mandelker, D., Leary, R.J., Ptak, J., Silliman, N., et al. 2006. The consensus coding sequences of human breast and colorectal cancers. *Science* 314:268-274.

7. Futreal, P.A., Coin, L., Marshall, M., Down, T., Hubbard, T., Wooster, R., Rahman, N., and Stratton, M.R. 2004. A census of human cancer genes. *Nat Rev Cancer* 4:177-183.

8. Jones, S., Chen, W.D., Parmigiani, G., Diehl, F., Beerenwinkel, N., Antal, T., Traulsen, A., Nowak, M.A., Siegel, C., Velculescu, V.E., et al. 2008. Comparative lesion sequencing provides insights into tumor evolution. *Proc Natl Acad Sci U S A* 105:4283-4288.

9. Bardeesy, N., and DePinho, R.A. 2002. Pancreatic cancer biology and genetics. *Nat Rev Cancer* 2:897-909.

10. O'Hagan, R.C., Chang, S., Maser, R.S., Mohan, R., Artandi, S.E., Chin, L., and DePinho, R.A. 2002. Telomere dysfunction provokes regional amplification and deletion in cancer genomes. *Cancer Cell* 2:149-155.

11. Artandi, S.E., Chang, S., Lee, S.L., Alson, S., Gottlieb, G.J., Chin, L., and DePinho, R.A. 2000. Telomere dysfunction promotes non-reciprocal translocations and epithelial cancers in mice. *Nature* 406:641-645.

12. Gisselsson, D., Jonson, T., Petersen, A., Strombeck, B., Dal Cin, P., Hoglund, M., Mitelman, F., Mertens, F., and Mandahl, N. 2001. Telomere dysfunction

triggers extensive DNA fragmentation and evolution of complex chromosome abnormalities in human malignant tumors. *Proc Natl Acad Sci U S A* 98:12683-12688.

13.   Bignell, G.R., Santarius, T., Pole, J.C., Butler, A.P., Perry, J., Pleasance, E., Greenman, C., Menzies, A., Taylor, S., Edkins, S., et al. 2007. Architectures of somatic genomic rearrangement in human cancer amplicons at sequence-level resolution. *Genome Res* 17:1296-1303.

14.   Stephens, P.J., Greenman, C.D., Fu, B., Yang, F., Bignell, G.R., Mudie, L.J., Pleasance, E.D., Lau, K.W., Beare, D., Stebbings, L.A., et al. 2011. Massive genomic rearrangement acquired in a single catastrophic event during cancer development. *Cell* 144:27-40.

15.   Kopnin, B.P. 2000. Targets of oncogenes and tumor suppressors: key for understanding basic mechanisms of carcinogenesis. *Biochemistry (Mosc)* 65:2-27.

16.   Touw, I.P., and Erkeland, S.J. 2007. Retroviral insertion mutagenesis in mice as a comparative oncogenomics tool to identify disease genes in human leukemia. *Mol Ther* 15:13-19.

17.   Soda, M., Choi, Y.L., Enomoto, M., Takada, S., Yamashita, Y., Ishikawa, S., Fujiwara, S., Watanabe, H., Kurashina, K., Hatanaka, H., et al. 2007. Identification of the transforming EML4-ALK fusion gene in non-small-cell lung cancer. *Nature* 448:561-566.

18.   Tomlins, S.A., Rhodes, D.R., Perner, S., Dhanasekaran, S.M., Mehra, R., Sun, X.W., Varambally, S., Cao, X., Tchinda, J., Kuefer, R., et al. 2005. Recurrent fusion of TMPRSS2 and ETS transcription factor genes in prostate cancer. *Science* 310:644-648.

19.   Myatt, S.S., and Lam, E.W. 2007. The emerging roles of forkhead box (Fox) proteins in cancer. *Nat Rev Cancer* 7:847-859.

20.   Weigel, D., Jurgens, G., Kuttner, F., Seifert, E., and Jackle, H. 1989. The homeotic gene fork head encodes a nuclear protein and is expressed in the terminal regions of the Drosophila embryo. *Cell* 57:645-658.

21.   Maiese, K., Chong, Z.Z., Shang, Y.C., and Hou, J. 2009. A "FOXO" in sight: targeting Foxo proteins from conception to cancer. *Med Res Rev* 29:395-418.

22. Nakamura, N., Ramaswamy, S., Vazquez, F., Signoretti, S., Loda, M., and Sellers, W.R. 2000. Forkhead transcription factors are critical effectors of cell death and cell cycle arrest downstream of PTEN. *Mol Cell Biol* 20:8969-8982.

23. Seoane, J., Le, H.V., Shen, L., Anderson, S.A., and Massague, J. 2004. Integration of Smad and forkhead pathways in the control of neuroepithelial and glioblastoma cell proliferation. *Cell* 117:211-223.

24. Schmidt, M., Fernandez de Mattos, S., van der Horst, A., Klompmaker, R., Kops, G.J., Lam, E.W., Burgering, B.M., and Medema, R.H. 2002. Cell cycle inhibition by FoxO forkhead transcription factors involves downregulation of cyclin D. *Mol Cell Biol* 22:7842-7852.

25. Greer, E.L., and Brunet, A. 2005. FOXO transcription factors at the interface between longevity and tumor suppression. *Oncogene* 24:7410-7425.

26. Modur, V., Nagarajan, R., Evers, B.M., and Milbrandt, J. 2002. FOXO proteins regulate tumor necrosis factor-related apoptosis inducing ligand expression. Implications for PTEN mutation in prostate cancer. *J Biol Chem* 277:47928-47937.

27. Huang, H., and Tindall, D.J. 2007. Dynamic FoxO transcription factors. *J Cell Sci* 120:2479-2487.

28. Tzivion, G., Dobson, M., and Ramakrishnan, G. 2011. FoxO transcription factors; Regulation by AKT and 14-3-3 proteins. *Biochim Biophys Acta* 1813:1938-1945.

29. Clark, K.L., Halay, E.D., Lai, E., and Burley, S.K. 1993. Co-crystal structure of the HNF-3/fork head DNA-recognition motif resembles histone H5. *Nature* 364:412-420.

30. Maiese, K., Chong, Z.Z., Hou, J., and Shang, Y.C. 2009. The "O" class: crafting clinical care with FoxO transcription factors. *Adv Exp Med Biol* 665:242-260.

31. Tsai, K.L., Sun, Y.J., Huang, C.Y., Yang, J.Y., Hung, M.C., and Hsiao, C.D. 2007. Crystal structure of the human FOXO3a-DBD/DNA complex suggests the effects of post-translational modification. *Nucleic Acids Res* 35:6984-6994.

32. Gilley, J., Coffer, P.J., and Ham, J. 2003. FOXO transcription factors directly activate bim gene expression and promote apoptosis in sympathetic neurons. *J Cell Biol* 162:613-622.

33. Furuyama, T., Nakazawa, T., Nakano, I., and Mori, N. 2000. Identification of the differential distribution patterns of mRNAs and consensus binding sequences for mouse DAF-16 homologues. *Biochem J* 349:629-634.

34. Biggs, W.H., 3rd, Meisenhelder, J., Hunter, T., Cavenee, W.K., and Arden, K.C. 1999. Protein kinase B/Akt-mediated phosphorylation promotes nuclear exclusion of the winged helix transcription factor FKHR1. *Proc Natl Acad Sci U S A* 96:7421-7426.

35. Accili, D., and Arden, K.C. 2004. FoxOs at the crossroads of cellular metabolism, differentiation, and transformation. *Cell* 117:421-426.

36. Xuan, Z., and Zhang, M.Q. 2005. From worm to human: bioinformatics approaches to identify FOXO target genes. *Mech Ageing Dev* 126:209-215.

37. Burgering, B.M., and Kops, G.J. 2002. Cell cycle and death control: long live Forkheads. *Trends Biochem Sci* 27:352-360.

38. Huang, H., Regan, K.M., Lou, Z., Chen, J., and Tindall, D.J. 2006. CDK2-dependent phosphorylation of FOXO1 as an apoptotic response to DNA damage. *Science* 314:294-297.

39. Brunet, A., Park, J., Tran, H., Hu, L.S., Hemmings, B.A., and Greenberg, M.E. 2001. Protein kinase SGK mediates survival signals by phosphorylating the forkhead transcription factor FKHRL1 (FOXO3a). *Mol Cell Biol* 21:952-965.

40. Woods, Y.L., Rena, G., Morrice, N., Barthel, A., Becker, W., Guo, S., Unterman, T.G., and Cohen, P. 2001. The kinase DYRK1A phosphorylates the transcription factor FKHR at Ser329 in vitro, a novel in vivo phosphorylation site. *Biochem J* 355:597-607.

41. Essers, M.A., Weijzen, S., de Vries-Smits, A.M., Saarloos, I., de Ruiter, N.D., Bos, J.L., and Burgering, B.M. 2004. FOXO transcription factor activation by oxidative stress mediated by the small GTPase Ral and JNK. *EMBO J* 23:4802-4812.

42. Wang, M.C., Bohmann, D., and Jasper, H. 2005. JNK extends life span and limits growth by antagonizing cellular and organism-wide responses to insulin signaling. *Cell* 121:115-125.

43. Van Der Heide, L.P., Hoekman, M.F., and Smidt, M.P. 2004. The ins and outs of FoxO shuttling: mechanisms of FoxO translocation and transcriptional regulation. *Biochem J* 380:297-309.

44. Sunayama, J., Tsuruta, F., Masuyama, N., and Gotoh, Y. 2005. JNK antagonizes Akt-mediated survival signals by phosphorylating 14-3-3. *J Cell Biol* 170:295-304.

45. Lehtinen, M.K., Yuan, Z., Boag, P.R., Yang, Y., Villen, J., Becker, E.B., DiBacco, S., de la Iglesia, N., Gygi, S., Blackwell, T.K., et al. 2006. A conserved MST-FOXO signaling pathway mediates oxidative-stress responses and extends life span. *Cell* 125:987-1001.

46. Graves, J.D., Gotoh, Y., Draves, K.E., Ambrose, D., Han, D.K., Wright, M., Chernoff, J., Clark, E.A., and Krebs, E.G. 1998. Caspase-mediated activation and induction of apoptosis by the mammalian Ste20-like kinase Mst1. *EMBO J* 17:2224-2234.

47. Huang, H., Regan, K.M., Wang, F., Wang, D., Smith, D.I., van Deursen, J.M., and Tindall, D.J. 2005. Skp2 inhibits FOXO1 in tumor suppression through ubiquitin-mediated degradation. *Proc Natl Acad Sci U S A* 102:1649-1654.

48. Sutterluty, H., Chatelain, E., Marti, A., Wirbelauer, C., Senften, M., Muller, U., and Krek, W. 1999. p45SKP2 promotes p27Kip1 degradation and induces S phase in quiescent cells. *Nat Cell Biol* 1:207-214.

49. Brunet, A., Kanai, F., Stehn, J., Xu, J., Sarbassova, D., Frangioni, J.V., Dalal, S.N., DeCaprio, J.A., Greenberg, M.E., and Yaffe, M.B. 2002. 14-3-3 transits to the nucleus and participates in dynamic nucleocytoplasmic transport. *J Cell Biol* 156:817-828.

50. van der Horst, A., de Vries-Smits, A.M., Brenkman, A.B., van Triest, M.H., van den Broek, N., Colland, F., Maurice, M.M., and Burgering, B.M. 2006. FOXO4 transcriptional activity is regulated by monoubiquitination and USP7/HAUSP. *Nat Cell Biol* 8:1064-1073.

51. Li, M., Luo, J., Brooks, C.L., and Gu, W. 2002. Acetylation of p53 inhibits its ubiquitination by Mdm2. *J Biol Chem* 277:50607-50611.

52. Brunet, A., Sweeney, L.B., Sturgill, J.F., Chua, K.F., Greer, P.L., Lin, Y., Tran, H., Ross, S.E., Mostoslavsky, R., Cohen, H.Y., et al. 2004. Stress-dependent regulation of FOXO transcription factors by the SIRT1 deacetylase. *Science* 303:2011-2015.

53. Frescas, D., Valenti, L., and Accili, D. 2005. Nuclear trapping of the forkhead transcription factor FoxO1 via Sirt-dependent deacetylation promotes expression of glucogenetic genes. *J Biol Chem* 280:20589-20595.

54. Kitamura, Y.I., Kitamura, T., Kruse, J.P., Raum, J.C., Stein, R., Gu, W., and Accili, D. 2005. FoxO1 protects against pancreatic beta cell failure through NeuroD and MafA induction. *Cell Metab* 2:153-163.

55. Daitoku, H., Hatta, M., Matsuzaki, H., Aratani, S., Ohshima, T., Miyagishi, M., Nakajima, T., and Fukamizu, A. 2004. Silent information regulator 2 potentiates Foxo1-mediated transcription through its deacetylase activity. *Proc Natl Acad Sci U S A* 101:10042-10047.

56. Dansen, T.B., and Burgering, B.M. 2008. Unravelling the tumor-suppressive functions of FOXO proteins. *Trends Cell Biol* 18:421-429.

57. Mercado, G.E., and Barr, F.G. 2007. Fusions involving PAX and FOX genes in the molecular pathogenesis of alveolar rhabdomyosarcoma: recent advances. *Curr Mol Med* 7:47-61.

58. So, C.W., and Cleary, M.L. 2003. Common mechanism for oncogenic activation of MLL by forkhead family proteins. *Blood* 101:633-639.

59. Medema, R.H., Kops, G.J., Bos, J.L., and Burgering, B.M. 2000. AFX-like Forkhead transcription factors mediate cell-cycle regulation by Ras and PKB through p27kip1. *Nature* 404:782-787.

60. Bouchard, C., Marquardt, J., Bras, A., Medema, R.H., and Eilers, M. 2004. Myc-induced proliferation and transformation require Akt-mediated phosphorylation of FoxO proteins. *EMBO J* 23:2830-2840.

61. Yang, H., Zhao, R., Yang, H.Y., and Lee, M.H. 2005. Constitutively active FOXO4 inhibits Akt activity, regulates p27 Kip1 stability, and suppresses HER2-mediated tumorigenicity. *Oncogene* 24:1924-1935.

62. Hu, M.C., Lee, D.F., Xia, W., Golfman, L.S., Ou-Yang, F., Yang, J.Y., Zou, Y., Bao, S., Hanada, N., Saso, H., et al. 2004. IkappaB kinase promotes tumorigenesis through inhibition of forkhead FOXO3a. *Cell* 117:225-237.

63. Hwangbo, D.S., Gershman, B., Tu, M.P., Palmer, M., and Tatar, M. 2004. Drosophila dFOXO controls lifespan and regulates insulin signalling in brain and fat body. *Nature* 429:562-566.

64. Kenyon, C., Chang, J., Gensch, E., Rudner, A., and Tabtiang, R. 1993. A C. elegans mutant that lives twice as long as wild type. *Nature* 366:461-464.

65. Paik, J.H., Kollipara, R., Chu, G., Ji, H., Xiao, Y., Ding, Z., Miao, L., Tothova, Z., Horner, J.W., Carrasco, D.R., et al. 2007. FoxOs are lineage-restricted

redundant tumor suppressors and regulate endothelial cell homeostasis. *Cell* 128:309-323.

66. Bouchard, C., Lee, S., Paulus-Hock, V., Loddenkemper, C., Eilers, M., and Schmitt, C.A. 2007. FoxO transcription factors suppress Myc-driven lymphomagenesis via direct activation of Arf. *Genes Dev* 21:2775-2787.

67. Teleman, A.A., Hietakangas, V., Sayadian, A.C., and Cohen, S.M. 2008. Nutritional control of protein biosynthetic capacity by insulin via Myc in Drosophila. *Cell Metab* 7:21-32.

68. Tsai, W.B., Chung, Y.M., Takahashi, Y., Xu, Z., and Hu, M.C. 2008. Functional interaction between FOXO3a and ATM regulates DNA damage response. *Nat Cell Biol* 10:460-467.

69. Yalcin, S., Zhang, X., Luciano, J.P., Mungamuri, S.K., Marinkovic, D., Vercherat, C., Sarkar, A., Grisotto, M., Taneja, R., and Ghaffari, S. 2008. Foxo3 is essential for the regulation of ataxia telangiectasia mutated and oxidative stress-mediated homeostasis of hematopoietic stem cells. *J Biol Chem* 283:25692-25705.

70. Warburg, O. 1956. On the origin of cancer cells. *Science* 123:309-314.

71. Mammucari, C., Milan, G., Romanello, V., Masiero, E., Rudolf, R., Del Piccolo, P., Burden, S.J., Di Lisi, R., Sandri, C., Zhao, J., et al. 2007. FoxO3 controls autophagy in skeletal muscle in vivo. *Cell Metab* 6:458-471.

72. Amaravadi, R.K., Yu, D., Lum, J.J., Bui, T., Christophorou, M.A., Evan, G.I., Thomas-Tikhonenko, A., and Thompson, C.B. 2007. Autophagy inhibition enhances therapy-induced apoptosis in a Myc-induced model of lymphoma. *J Clin Invest* 117:326-336.

73. Maclean, K.H., Dorsey, F.C., Cleveland, J.L., and Kastan, M.B. 2008. Targeting lysosomal degradation induces p53-dependent cell death and prevents cancer in mouse models of lymphomagenesis. *J Clin Invest* 118:79-88.

74. Forsythe, J.A., Jiang, B.H., Iyer, N.V., Agani, F., Leung, S.W., Koos, R.D., and Semenza, G.L. 1996. Activation of vascular endothelial growth factor gene transcription by hypoxia-inducible factor 1. *Mol Cell Biol* 16:4604-4613.

75. Harris, A.L. 2002. Hypoxia--a key regulatory factor in tumour growth. *Nat Rev Cancer* 2:38-47.

76. Paik, J.H. 2006. FOXOs in the maintenance of vascular homoeostasis. *Biochem Soc Trans* 34:731-734.

77. Hosaka, T., Biggs, W.H., 3rd, Tieu, D., Boyer, A.D., Varki, N.M., Cavenee, W.K., and Arden, K.C. 2004. Disruption of forkhead transcription factor (FOXO) family members in mice reveals their functional diversification. *Proc Natl Acad Sci U S A* 101:2975-2980.

78. Tang, T.T., and Lasky, L.A. 2003. The forkhead transcription factor FOXO4 induces the down-regulation of hypoxia-inducible factor 1 alpha by a von Hippel-Lindau protein-independent mechanism. *J Biol Chem* 278:30125-30135.

79. Bakker, W.J., Harris, I.S., and Mak, T.W. 2007. FOXO3a is activated in response to hypoxic stress and inhibits HIF1-induced apoptosis via regulation of CITED2. *Mol Cell* 28:941-953.

80. Emerling, B.M., Weinberg, F., Liu, J.L., Mak, T.W., and Chandel, N.S. 2008. PTEN regulates p300-dependent hypoxia-inducible factor 1 transcriptional activity through Forkhead transcription factor 3a (FOXO3a). *Proc Natl Acad Sci U S A* 105:2622-2627.

81. Stiller, C.A., Bielack, S.S., Jundt, G., and Steliarova-Foucher, E. 2006. Bone tumours in European children and adolescents, 1978-1997. Report from the Automated Childhood Cancer Information System project. *Eur J Cancer* 42:2124-2135.

82. Ewing, J. 1972. Classics in oncology. Diffuse endothelioma of bone. James Ewing. Proceedings of the New York Pathological Society, 1921. *CA Cancer J Clin* 22:95-98.

83. Denny, C.T. 1998. Ewing's sarcoma--a clinical enigma coming into focus. *J Pediatr Hematol Oncol* 20:421-425.

84. Paulussen, M., Frohlich, B., and Jurgens, H. 2001. Ewing tumour: incidence, prognosis and treatment options. *Paediatr Drugs* 3:899-913.

85. Kimber, C., Michalski, A., Spitz, L., and Pierro, A. 1998. Primitive neuroectodermal tumours: anatomic location, extent of surgery, and outcome. *J Pediatr Surg* 33:39-41.

86. Sankar, S., and Lessnick, S.L. 2011. Promiscuous partnerships in Ewing's sarcoma. *Cancer Genet* 204:351-365.

87. Grier, H.E. 1997. The Ewing family of tumors. Ewing's sarcoma and primitive neuroectodermal tumors. *Pediatr Clin North Am* 44:991-1004.

88. Kovar, H. 1998. Ewing's sarcoma and peripheral primitive neuroectodermal tumors after their genetic union. *Curr Opin Oncol* 10:334-342.

89. Turc-Carel, C., Philip, I., Berger, M.P., Philip, T., and Lenoir, G.M. 1984. Chromosome study of Ewing's sarcoma (ES) cell lines. Consistency of a reciprocal translocation t(11;22)(q24;q12). *Cancer Genet Cytogenet* 12:1-19.

90. Whang-Peng, J., Triche, T.J., Knutsen, T., Miser, J., Douglass, E.C., and Israel, M.A. 1984. Chromosome translocation in peripheral neuroepithelioma. *N Engl J Med* 311:584-585.

91. Bernstein, M., Kovar, H., Paulussen, M., Randall, R.L., Schuck, A., Teot, L.A., and Juergens, H. 2006. Ewing's sarcoma family of tumors: current management. *Oncologist* 11:503-519.

92. Terrier, P., Llombart-Bosch, A., and Contesso, G. 1996. Small round blue cell tumors in bone: prognostic factors correlated to Ewing's sarcoma and neuroectodermal tumors. *Semin Diagn Pathol* 13:250-257.

93. Linabery, A.M., and Ross, J.A. 2008. Childhood and adolescent cancer survival in the US by race and ethnicity for the diagnostic period 1975-1999. *Cancer* 113:2575-2596.

94. Randall, R.L., Lessnick, S.L., Jones, K.B., Gouw, L.G., Cummings, J.E., Cannon-Albright, L., and Schiffman, J.D. 2010. Is There a Predisposition Gene for Ewing's Sarcoma? *J Oncol* 2010:397632.

95. Lahl, M., Fisher, V.L., and Laschinger, K. 2008. Ewing's sarcoma family of tumors: an overview from diagnosis to survivorship. *Clin J Oncol Nurs* 12:89-97.

96. Wang, C.C., and Schulz, M.D. 1953. Ewing's sarcoma; a study of fifty cases treated at the Massachusetts General Hospital, 1930-1952 inclusive. *N Engl J Med* 248:571-576.

97. Dahlin, D.C., Coventry, M.B., and Scanlon, P.W. 1961. Ewing's sarcoma. A critical analysis of 165 cases. *J Bone Joint Surg Am* 43-A:185-192.

98. Tirode, F., Laud-Duval, K., Prieur, A., Delorme, B., Charbord, P., and Delattre, O. 2007. Mesenchymal stem cell features of Ewing tumors. *Cancer Cell* 11:421-429.

99. Riggi, N., Cironi, L., Provero, P., Suva, M.L., Kaloulis, K., Garcia-Echeverria, C., Hoffmann, F., Trumpp, A., and Stamenkovic, I. 2005. Development of Ewing's sarcoma from primary bone marrow-derived mesenchymal progenitor cells. *Cancer Res* 65:11459-11468.

100. Meltzer, P.S. 2007. Is Ewing's sarcoma a stem cell tumor? *Cell Stem Cell* 1:13-15.

101. Riggi, N., Suva, M.L., Suva, D., Cironi, L., Provero, P., Tercier, S., Joseph, J.M., Stehle, J.C., Baumer, K., Kindler, V., et al. 2008. EWS-FLI-1 expression triggers a Ewing's sarcoma initiation program in primary human mesenchymal stem cells. *Cancer Res* 68:2176-2185.

102. Cavazzana, A.O., Magnani, J.L., Ross, R.A., Miser, J., and Triche, T.J. 1988. Ewing's sarcoma is an undifferentiated neuroectodermal tumor. *Prog Clin Biol Res* 271:487-498.

103. Lipinski, M., Braham, K., Philip, I., Wiels, J., Philip, T., Goridis, C., Lenoir, G.M., and Tursz, T. 1987. Neuroectoderm-associated antigens on Ewing's sarcoma cell lines. *Cancer Res* 47:183-187.

104. Staege, M.S., Hutter, C., Neumann, I., Foja, S., Hattenhorst, U.E., Hansen, G., Afar, D., and Burdach, S.E. 2004. DNA microarrays reveal relationship of Ewing family tumors to both endothelial and fetal neural crest-derived cells and define novel targets. *Cancer Res* 64:8213-8221.

105. von Levetzow, C., Jiang, X., Gwye, Y., von Levetzow, G., Hung, L., Cooper, A., Hsu, J.H., and Lawlor, E.R. 2011. Modeling initiation of Ewing sarcoma in human neural crest cells. *PLoS One* 6:e19305.

106. Riggi, N., Suva, M.L., and Stamenkovic, I. 2009. Ewing's sarcoma origin: from duel to duality. *Expert Rev Anticancer Ther* 9:1025-1030.

107. Torchia, E.C., Boyd, K., Rehg, J.E., Qu, C., and Baker, S.J. 2007. EWS/FLI-1 induces rapid onset of myeloid/erythroid leukemia in mice. *Mol Cell Biol* 27:7918-7934.

108. Codrington, R., Pannell, R., Forster, A., Drynan, L.F., Daser, A., Lobato, N., Metzler, M., and Rabbitts, T.H. 2005. The Ews-ERG fusion protein can initiate neoplasia from lineage-committed haematopoietic cells. *PLoS Biol* 3:e242.

109. McCormack, M.P., Forster, A., Drynan, L., Pannell, R., and Rabbitts, T.H. 2003. The LMO2 T-cell oncogene is activated via chromosomal translocations

or retroviral insertion during gene therapy but has no mandatory role in normal T-cell development. *Mol Cell Biol* 23:9003-9013.

110. Lin, P.P., Pandey, M.K., Jin, F., Xiong, S., Deavers, M., Parant, J.M., and Lozano, G. 2008. EWS-FLI1 induces developmental abnormalities and accelerates sarcoma formation in a transgenic mouse model. *Cancer Res* 68:8968-8975.

111. Delattre, O., Zucman, J., Plougastel, B., Desmaze, C., Melot, T., Peter, M., Kovar, H., Joubert, I., de Jong, P., Rouleau, G., et al. 1992. Gene fusion with an ETS DNA-binding domain caused by chromosome translocation in human tumours. *Nature* 359:162-165.

112. Turc-Carel, C., Aurias, A., Mugneret, F., Lizard, S., Sidaner, I., Volk, C., Thiery, J.P., Olschwang, S., Philip, I., Berger, M.P., et al. 1988. Chromosomes in Ewing's sarcoma. I. An evaluation of 85 cases of remarkable consistency of t(11;22)(q24;q12). *Cancer Genet Cytogenet* 32:229-238.

113. Rossow, K.L., and Janknecht, R. 2001. The Ewing's sarcoma gene product functions as a transcriptional activator. *Cancer Res* 61:2690-2695.

114. Petermann, R., Mossier, B.M., Aryee, D.N., Khazak, V., Golemis, E.A., and Kovar, H. 1998. Oncogenic EWS-Fli1 interacts with hsRPB7, a subunit of human RNA polymerase II. *Oncogene* 17:603-610.

115. Araya, N., Hirota, K., Shimamoto, Y., Miyagishi, M., Yoshida, E., Ishida, J., Kaneko, S., Kaneko, M., Nakajima, T., and Fukamizu, A. 2003. Cooperative interaction of EWS with CREB-binding protein selectively activates hepatocyte nuclear factor 4-mediated transcription. *J Biol Chem* 278:5427-5432.

116. Bertolotti, A., Melot, T., Acker, J., Vigneron, M., Delattre, O., and Tora, L. 1998. EWS, but not EWS-FLI-1, is associated with both TFIID and RNA polymerase II: interactions between two members of the TET family, EWS and hTAFII68, and subunits of TFIID and RNA polymerase II complexes. *Mol Cell Biol* 18:1489-1497.

117. Melet, F., Motro, B., Rossi, D.J., Zhang, L., and Bernstein, A. 1996. Generation of a novel Fli-1 protein by gene targeting leads to a defect in thymus development and a delay in Friend virus-induced erythroleukemia. *Mol Cell Biol* 16:2708-2718.

118. Brown, L.A., Rodaway, A.R., Schilling, T.F., Jowett, T., Ingham, P.W., Patient, R.K., and Sharrocks, A.D. 2000. Insights into early vasculogenesis revealed

by expression of the ETS-domain transcription factor Fli-1 in wild-type and mutant zebrafish embryos. *Mech Dev* 90:237-252.

119. Hart, A., Melet, F., Grossfeld, P., Chien, K., Jones, C., Tunnacliffe, A., Favier, R., and Bernstein, A. 2000. Fli-1 is required for murine vascular and megakaryocytic development and is hemizygously deleted in patients with thrombocytopenia. *Immunity* 13:167-177.

120. Graves, B.J., and Petersen, J.M. 1998. Specificity within the ets family of transcription factors. *Adv Cancer Res* 75:1-55.

121. Sharrocks, A.D. 2001. The ETS-domain transcription factor family. *Nat Rev Mol Cell Biol* 2:827-837.

122. May, W.A., Gishizky, M.L., Lessnick, S.L., Lunsford, L.B., Lewis, B.C., Delattre, O., Zucman, J., Thomas, G., and Denny, C.T. 1993. Ewing sarcoma 11;22 translocation produces a chimeric transcription factor that requires the DNA-binding domain encoded by FLI1 for transformation. *Proc Natl Acad Sci U S A* 90:5752-5756.

123. May, W.A., Lessnick, S.L., Braun, B.S., Klemsz, M., Lewis, B.C., Lunsford, L.B., Hromas, R., and Denny, C.T. 1993. The Ewing's sarcoma EWS/FLI-1 fusion gene encodes a more potent transcriptional activator and is a more powerful transforming gene than FLI-1. *Mol Cell Biol* 13:7393-7398.

124. Uren, A., and Toretsky, J.A. 2005. Ewing's sarcoma oncoprotein EWS-FLI1: the perfect target without a therapeutic agent. *Future Oncol* 1:521-528.

125. Kovar, H. 2005. Context matters: the hen or egg problem in Ewing's sarcoma. *Semin Cancer Biol* 15:189-196.

126. Erkizan, H.V., Kong, Y., Merchant, M., Schlottmann, S., Barber-Rotenberg, J.S., Yuan, L., Abaan, O.D., Chou, T.H., Dakshanamurthy, S., Brown, M.L., et al. 2009. A small molecule blocking oncogenic protein EWS-FLI1 interaction with RNA helicase A inhibits growth of Ewing's sarcoma. *Nat Med* 15:750-756.

127. Chansky, H.A., Barahmand-Pour, F., Mei, Q., Kahn-Farooqi, W., Zielinska-Kwiatkowska, A., Blackburn, M., Chansky, K., Conrad, E.U., 3rd, Bruckner, J.D., Greenlee, T.K., et al. 2004. Targeting of EWS/FLI-1 by RNA interference attenuates the tumor phenotype of Ewing's sarcoma cells in vitro. *J Orthop Res* 22:910-917.

128. Kovar, H., Aryee, D.N., Jug, G., Henockl, C., Schemper, M., Delattre, O., Thomas, G., and Gadner, H. 1996. EWS/FLI-1 antagonists induce growth inhibition of Ewing tumor cells in vitro. *Cell Growth Differ* 7:429-437.

129. Kauer, M., Ban, J., Kofler, R., Walker, B., Davis, S., Meltzer, P., and Kovar, H. 2009. A molecular function map of Ewing's sarcoma. *PLoS One* 4:e5415.

130. Prieur, A., Tirode, F., Cohen, P., and Delattre, O. 2004. EWS/FLI-1 silencing and gene profiling of Ewing cells reveal downstream oncogenic pathways and a crucial role for repression of insulin-like growth factor binding protein 3. *Mol Cell Biol* 24:7275-7283.

131. Smith, R., Owen, L.A., Trem, D.J., Wong, J.S., Whangbo, J.S., Golub, T.R., and Lessnick, S.L. 2006. Expression profiling of EWS/FLI identifies NKX2.2 as a critical target gene in Ewing's sarcoma. *Cancer Cell* 9:405-416.

132. Fuchs, B., Inwards, C.Y., and Janknecht, R. 2004. Vascular endothelial growth factor expression is up-regulated by EWS-ETS oncoproteins and Sp1 and may represent an independent predictor of survival in Ewing's sarcoma. *Clin Cancer Res* 10:1344-1353.

133. Tirado, O.M., Mateo-Lozano, S., Villar, J., Dettin, L.E., Llort, A., Gallego, S., Ban, J., Kovar, H., and Notario, V. 2006. Caveolin-1 (CAV1) is a target of EWS/FLI-1 and a key determinant of the oncogenic phenotype and tumorigenicity of Ewing's sarcoma cells. *Cancer Res* 66:9937-9947.

134. Hahm, K.B. 1999. Repression of the gene encoding the TGF-beta type II receptor is a major target of the EWS-FLI1 oncoprotein. *Nat Genet* 23:481.

135. Nakatani, F., Tanaka, K., Sakimura, R., Matsumoto, Y., Matsunobu, T., Li, X., Hanada, M., Okada, T., and Iwamoto, Y. 2003. Identification of p21WAF1/CIP1 as a direct target of EWS-Fli1 oncogenic fusion protein. *J Biol Chem* 278:15105-15115.

136. Richter, G.H., Plehm, S., Fasan, A., Rossler, S., Unland, R., Bennani-Baiti, I.M., Hotfilder, M., Lowel, D., von Luettichau, I., Mossbrugger, I., et al. 2009. EZH2 is a mediator of EWS/FLI1 driven tumor growth and metastasis blocking endothelial and neuro-ectodermal differentiation. *Proc Natl Acad Sci U S A* 106:5324-5329.

137. Siligan, C., Ban, J., Bachmaier, R., Spahn, L., Kreppel, M., Schaefer, K.L., Poremba, C., Aryee, D.N., and Kovar, H. 2005. EWS-FLI1 target genes recovered from Ewing's sarcoma chromatin. *Oncogene* 24:2512-2524.

138. Welford, S.M., Hebert, S.P., Deneen, B., Arvand, A., and Denny, C.T. 2001. DNA binding domain-independent pathways are involved in EWS/FLI1-mediated oncogenesis. *J Biol Chem* 276:41977-41984.

139. Jaishankar, S., Zhang, J., Roussel, M.F., and Baker, S.J. 1999. Transforming activity of EWS/FLI is not strictly dependent upon DNA-binding activity. *Oncogene* 18:5592-5597.

140. Lessnick, S.L., Braun, B.S., Denny, C.T., and May, W.A. 1995. Multiple domains mediate transformation by the Ewing's sarcoma EWS/FLI-1 fusion gene. *Oncogene* 10:423-431.

141. Bailly, R.A., Bosselut, R., Zucman, J., Cormier, F., Delattre, O., Roussel, M., Thomas, G., and Ghysdael, J. 1994. DNA-binding and transcriptional activation properties of the EWS-FLI-1 fusion protein resulting from the t(11;22) translocation in Ewing sarcoma. *Mol Cell Biol* 14:3230-3241.

142. Guillon, N., Tirode, F., Boeva, V., Zynovyev, A., Barillot, E., and Delattre, O. 2009. The oncogenic EWS-FLI1 protein binds in vivo GGAA microsatellite sequences with potential transcriptional activation function. *PLoS One* 4:e4932.

143. Kim, S., Denny, C.T., and Wisdom, R. 2006. Cooperative DNA binding with AP-1 proteins is required for transformation by EWS-Ets fusion proteins. *Mol Cell Biol* 26:2467-2478.

144. Ramakrishnan, R., Fujimura, Y., Zou, J.P., Liu, F., Lee, L., Rao, V.N., and Reddy, E.S. 2004. Role of protein-protein interactions in the antiapoptotic function of EWS-Fli-1. *Oncogene* 23:7087-7094.

145. Nakajima, T., Uchida, C., Anderson, S.F., Lee, C.G., Hurwitz, J., Parvin, J.D., and Montminy, M. 1997. RNA helicase A mediates association of CBP with RNA polymerase II. *Cell* 90:1107-1112.

146. Hartman, T.R., Qian, S., Bolinger, C., Fernandez, S., Schoenberg, D.R., and Boris-Lawrie, K. 2006. RNA helicase A is necessary for translation of selected messenger RNAs. *Nat Struct Mol Biol* 13:509-516.

147. Toretsky, J.A., Erkizan, V., Levenson, A., Abaan, O.D., Parvin, J.D., Cripe, T.P., Rice, A.M., Lee, S.B., and Uren, A. 2006. Oncoprotein EWS-FLI1 activity is enhanced by RNA helicase A. *Cancer Res* 66:5574-5581.

148. Magnaghi-Jaulin, L., Masutani, H., Robin, P., Lipinski, M., and Harel-Bellan, A. 1996. SRE elements are binding sites for the fusion protein EWS-FLI-1. *Nucleic Acids Res* 24:1052-1058.

149. Watson, D.K., Robinson, L., Hodge, D.R., Kola, I., Papas, T.S., and Seth, A. 1997. FLI1 and EWS-FLI1 function as ternary complex factors and ELK1 and SAP1a function as ternary and quaternary complex factors on the Egr1 promoter serum response elements. *Oncogene* 14:213-221.

150. Knoop, L.L., and Baker, S.J. 2000. The splicing factor U1C represses EWS/FLI-mediated transactivation. *J Biol Chem* 275:24865-24871.

151. Knoop, L.L., and Baker, S.J. 2001. EWS/FLI alters 5'-splice site selection. *J Biol Chem* 276:22317-22322.

152. Sanchez, G., Bittencourt, D., Laud, K., Barbier, J., Delattre, O., Auboeuf, D., and Dutertre, M. 2008. Alteration of cyclin D1 transcript elongation by a mutated transcription factor up-regulates the oncogenic D1b splice isoform in cancer. *Proc Natl Acad Sci U S A* 105:6004-6009.

153. Yang, L., Chansky, H.A., and Hickstein, D.D. 2000. EWS.Fli-1 fusion protein interacts with hyperphosphorylated RNA polymerase II and interferes with serine-arginine protein-mediated RNA splicing. *J Biol Chem* 275:37612-37618.

154. Chansky, H.A., Hu, M., Hickstein, D.D., and Yang, L. 2001. Oncogenic TLS/ERG and EWS/Fli-1 fusion proteins inhibit RNA splicing mediated by YB-1 protein. *Cancer Res* 61:3586-3590.

155. Bachmaier, R., Aryee, D.N., Jug, G., Kauer, M., Kreppel, M., Lee, K.A., and Kovar, H. 2009. O-GlcNAcylation is involved in the transcriptional activity of EWS-FLI1 in Ewing's sarcoma. *Oncogene* 28:1280-1284.

156. Owen, L.A., Kowalewski, A.A., and Lessnick, S.L. 2008. EWS/FLI mediates transcriptional repression via NKX2.2 during oncogenic transformation in Ewing's sarcoma. *PLoS One* 3:e1965.

157. Kinsey, M., Smith, R., Iyer, A.K., McCabe, E.R., and Lessnick, S.L. 2009. EWS/FLI and its downstream target NR0B1 interact directly to modulate transcription and oncogenesis in Ewing's sarcoma. *Cancer Res* 69:9047-9055.

158. France, K.A., Anderson, J.L., Park, A., and Denny, C.T. 2011. Oncogenic fusion protein EWS/FLI1 down-regulates gene expression by both transcriptional and posttranscriptional mechanisms. *J Biol Chem* 286:22750-22757.

159. Burdach, S., Plehm, S., Unland, R., Dirksen, U., Borkhardt, A., Staege, M.S., Muller-Tidow, C., and Richter, G.H. 2009. Epigenetic maintenance of stemness and malignancy in peripheral neuroectodermal tumors by EZH2. *Cell Cycle* 8:1991-1996.

160. Ban, J., Jug, G., Mestdagh, P., Schwentner, R., Kauer, M., Aryee, D.N., Schaefer, K.L., Nakatani, F., Scotlandi, K., Reiter, M., et al. 2011. Hsa-mir-145 is the top EWS-FLI1-repressed microRNA involved in a positive feedback loop in Ewing's sarcoma. *Oncogene* 30:2173-2180.

161. McKinsey, E.L., Parrish, J.K., Irwin, A.E., Niemeyer, B.F., Kern, H.B., Birks, D.K., and Jedlicka, P. 2011. A novel oncogenic mechanism in Ewing sarcoma involving IGF pathway targeting by EWS/Fli1-regulated microRNAs. *Oncogene* 30:4910-4920.

162. Kovar, H. 2010. Downstream EWS/FLI1 - upstream Ewing's sarcoma. *Genome Med* 2:8.

163. Pear, W.S., Miller, J.P., Xu, L., Pui, J.C., Soffer, B., Quackenbush, R.C., Pendergast, A.M., Bronson, R., Aster, J.C., Scott, M.L., et al. 1998. Efficient and rapid induction of a chronic myelogenous leukemia-like myeloproliferative disease in mice receiving P210 bcr/abl-transduced bone marrow. *Blood* 92:3780-3792.

164. Kovar, H., Auinger, A., Jug, G., Aryee, D., Zoubek, A., Salzer-Kuntschik, M., and Gadner, H. 1993. Narrow spectrum of infrequent p53 mutations and absence of MDM2 amplification in Ewing tumours. *Oncogene* 8:2683-2690.

165. Kovar, H., Jug, G., Aryee, D.N., Zoubek, A., Ambros, P., Gruber, B., Windhager, R., and Gadner, H. 1997. Among genes involved in the RB dependent cell cycle regulatory cascade, the p16 tumor suppressor gene is frequently lost in the Ewing family of tumors. *Oncogene* 15:2225-2232.

166. Stemberger, J., Witt, V., Printz, D., Geyeregger, R., and Fritsch, G. 2010. Novel single-platform multiparameter FCM analysis of apoptosis: Significant differences between wash and no-wash procedure. *Cytometry A* 77:1075-1081.

167. Winter, G.E., Rix, U., Lissat, A., Stukalov, A., Mullner, M.K., Bennett, K.L., Colinge, J., Nijman, S.M., Kubicek, S., Kovar, H., et al. 2011. An integrated chemical biology approach identifies specific vulnerability of Ewing's sarcoma

to combined inhibition of Aurora kinases A and B. *Mol Cancer Ther* 10:1846-1856.

168. Gentleman, R.C., Carey, V.J., Bates, D.M., Bolstad, B., Dettling, M., Dudoit, S., Ellis, B., Gautier, L., Ge, Y., Gentry, J., et al. 2004. Bioconductor: open software development for computational biology and bioinformatics. *Genome Biol* 5:R80.

169. Wettenhall, J.M., and Smyth, G.K. 2004. limmaGUI: a graphical user interface for linear modeling of microarray data. *Bioinformatics* 20:3705-3706.

170. Koziol, J.A., Maxwell, D.A., Fukushima, M., Colmerauer, M.E., and Pilch, Y.H. 1981. A distribution-free test for tumor-growth curve analyses with application to an animal tumor immunotherapy experiment. *Biometrics* 37:383-390.

171. Yang, L., Hu, H.M., Zielinska-Kwiatkowska, A., and Chansky, H.A. 2010. FOXO1 is a direct target of EWS-Fli1 oncogenic fusion protein in Ewing's sarcoma cells. *Biochem Biophys Res Commun* 402:129-134.

172. Su, A.I., Wiltshire, T., Batalov, S., Lapp, H., Ching, K.A., Block, D., Zhang, J., Soden, R., Hayakawa, M., Kreiman, G., et al. 2004. A gene atlas of the mouse and human protein-encoding transcriptomes. *Proc Natl Acad Sci U S A* 101:6062-6067.

173. Weidinger, C., Krause, K., Klagge, A., Karger, S., and Fuhrer, D. 2008. Forkhead box-O transcription factor: critical conductors of cancer's fate. *Endocr Relat Cancer* 15:917-929.

174. Huang, H., and Tindall, D.J. 2007. CDK2 and FOXO1: a fork in the road for cell fate decisions. *Cell Cycle* 6:902-906.

175. Kops, G.J., de Ruiter, N.D., De Vries-Smits, A.M., Powell, D.R., Bos, J.L., and Burgering, B.M. 1999. Direct control of the Forkhead transcription factor AFX by protein kinase B. *Nature* 398:630-634.

176. Brunet, A., Bonni, A., Zigmond, M.J., Lin, M.Z., Juo, P., Hu, L.S., Anderson, M.J., Arden, K.C., Blenis, J., and Greenberg, M.E. 1999. Akt promotes cell survival by phosphorylating and inhibiting a Forkhead transcription factor. *Cell* 96:857-868.

177. Tang, E.D., Nunez, G., Barr, F.G., and Guan, K.L. 1999. Negative regulation of the forkhead transcription factor FKHR by Akt. *J Biol Chem* 274:16741-16746.

178. Cahill, C.M., Tzivion, G., Nasrin, N., Ogg, S., Dore, J., Ruvkun, G., and Alexander-Bridges, M. 2001. Phosphatidylinositol 3-kinase signaling inhibits DAF-16 DNA binding and function via 14-3-3-dependent and 14-3-3-independent pathways. *J Biol Chem* 276:13402-13410.

179. Obsil, T., Ghirlando, R., Anderson, D.E., Hickman, A.B., and Dyda, F. 2003. Two 14-3-3 binding motifs are required for stable association of Forkhead transcription factor FOXO4 with 14-3-3 proteins and inhibition of DNA binding. *Biochemistry* 42:15264-15272.

180. Silhan, J., Vacha, P., Strnadova, P., Vecer, J., Herman, P., Sulc, M., Teisinger, J., Obsilova, V., and Obsil, T. 2009. 14-3-3 protein masks the DNA binding interface of forkhead transcription factor FOXO4. *J Biol Chem* 284:19349-19360.

181. Li, Q.X., Yu, D.H., Liu, G., Ke, N., McKelvy, J., and Wong-Staal, F. 2008. Selective anticancer strategies via intervention of the death pathways relevant to cell transformation. *Cell Death Differ* 15:1197-1210.

182. Sanchez, G., Delattre, O., Auboeuf, D., and Dutertre, M. 2008. Coupled alteration of transcription and splicing by a single oncogene: boosting the effect on cyclin D1 activity. *Cell Cycle* 7:2299-2305.

183. Kelland, L.R. 2004. Of mice and men: values and liabilities of the athymic nude mouse model in anticancer drug development. *Eur J Cancer* 40:827-836.

184. Beauchamp, E., Bulut, G., Abaan, O., Chen, K., Merchant, A., Matsui, W., Endo, Y., Rubin, J.S., Toretsky, J., and Uren, A. 2009. GLI1 is a direct transcriptional target of EWS-FLI1 oncoprotein. *J Biol Chem* 284:9074-9082.

185. Lessnick, S.L., Dacwag, C.S., and Golub, T.R. 2002. The Ewing's sarcoma oncoprotein EWS/FLI induces a p53-dependent growth arrest in primary human fibroblasts. *Cancer Cell* 1:393-401.

186. Hotfilder, M., Sondermann, P., Senss, A., van Valen, F., Jurgens, H., and Vormoor, J. 2005. PI3K/AKT is involved in mediating survival signals that rescue Ewing tumour cells from fibroblast growth factor 2-induced cell death. *Br J Cancer* 92:705-710.

187. Zhao, X., Gan, L., Pan, H., Kan, D., Majeski, M., Adam, S.A., and Unterman, T.G. 2004. Multiple elements regulate nuclear/cytoplasmic shuttling of FOXO1: characterization of phosphorylation- and 14-3-3-dependent and -independent mechanisms. *Biochem J* 378:839-849.

188. Teixeira, C.C., Liu, Y., Thant, L.M., Pang, J., Palmer, G., and Alikhani, M. 2010. Foxo1, a novel regulator of osteoblast differentiation and skeletogenesis. *J Biol Chem* 285:31055-31065.

189. Furukawa-Hibi, Y., Yoshida-Araki, K., Ohta, T., Ikeda, K., and Motoyama, N. 2002. FOXO forkhead transcription factors induce G(2)-M checkpoint in response to oxidative stress. *J Biol Chem* 277:26729-26732.

190. Nowak, K., Killmer, K., Gessner, C., and Lutz, W. 2007. E2F-1 regulates expression of FOXO1 and FOXO3a. *Biochim Biophys Acta* 1769:244-252.

191. Jacobsen, E.A., Ananieva, O., Brown, M.L., and Chang, Y. 2006. Growth, differentiation, and malignant transformation of pre-B cells mediated by inducible activation of v-Abl oncogene. *J Immunol* 176:6831-6838.

192. Clark, L.C., Combs, G.F., Jr., Turnbull, B.W., Slate, E.H., Chalker, D.K., Chow, J., Davis, L.S., Glover, R.A., Graham, G.F., Gross, E.G., et al. 1996. Effects of selenium supplementation for cancer prevention in patients with carcinoma of the skin. A randomized controlled trial. Nutritional Prevention of Cancer Study Group. *JAMA* 276:1957-1963.

193. Clark, L.C., Dalkin, B., Krongrad, A., Combs, G.F., Jr., Turnbull, B.W., Slate, E.H., Witherington, R., Herlong, J.H., Janosko, E., Carpenter, D., et al. 1998. Decreased incidence of prostate cancer with selenium supplementation: results of a double-blind cancer prevention trial. *Br J Urol* 81:730-734.

194. Duffield-Lillico, A.J., Reid, M.E., Turnbull, B.W., Combs, G.F., Jr., Slate, E.H., Fischbach, L.A., Marshall, J.R., and Clark, L.C. 2002. Baseline characteristics and the effect of selenium supplementation on cancer incidence in a randomized clinical trial: a summary report of the Nutritional Prevention of Cancer Trial. *Cancer Epidemiol Biomarkers Prev* 11:630-639.

195. Duffield-Lillico, A.J., Slate, E.H., Reid, M.E., Turnbull, B.W., Wilkins, P.A., Combs, G.F., Jr., Park, H.K., Gross, E.G., Graham, G.F., Stratton, M.S., et al. 2003. Selenium supplementation and secondary prevention of nonmelanoma skin cancer in a randomized trial. *J Natl Cancer Inst* 95:1477-1481.

196. Lippman, S.M., Klein, E.A., Goodman, P.J., Lucia, M.S., Thompson, I.M., Ford, L.G., Parnes, H.L., Minasian, L.M., Gaziano, J.M., Hartline, J.A., et al. 2009. Effect of selenium and vitamin E on risk of prostate cancer and other cancers: the Selenium and Vitamin E Cancer Prevention Trial (SELECT). *JAMA* 301:39-51.

197. Combs, G.F., Jr., Clark, L.C., and Turnbull, B.W. 2001. An analysis of cancer prevention by selenium. *Biofactors* 14:153-159.

198. Ip, C. 1998. Lessons from basic research in selenium and cancer prevention. *J Nutr* 128:1845-1854.

199. Ip, C., Thompson, H.J., Zhu, Z., and Ganther, H.E. 2000. In vitro and in vivo studies of methylseleninic acid: evidence that a monomethylated selenium metabolite is critical for cancer chemoprevention. *Cancer Res* 60:2882-2886.

200. Li, G.X., Lee, H.J., Wang, Z., Hu, H., Liao, J.D., Watts, J.C., Combs, G.F., Jr., and Lu, J. 2008. Superior in vivo inhibitory efficacy of methylseleninic acid against human prostate cancer over selenomethionine or selenite. *Carcinogenesis* 29:1005-1012.

201. Juliger, S., Goenaga-Infante, H., Lister, T.A., Fitzgibbon, J., and Joel, S.P. 2007. Chemosensitization of B-cell lymphomas by methylseleninic acid involves nuclear factor-kappaB inhibition and the rapid generation of other selenium species. *Cancer Res* 67:10984-10992.

202. Wu, Y., Zhang, H., Dong, Y., Park, Y.M., and Ip, C. 2005. Endoplasmic reticulum stress signal mediators are targets of selenium action. *Cancer Res* 65:9073-9079.

203. Dong, Y., Zhang, H., Hawthorn, L., Ganther, H.E., and Ip, C. 2003. Delineation of the molecular basis for selenium-induced growth arrest in human prostate cancer cells by oligonucleotide array. *Cancer Res* 63:52-59.

204. Zhu, Z., Jiang, W., Ganther, H.E., and Thompson, H.J. 2002. Mechanisms of cell cycle arrest by methylseleninic acid. *Cancer Res* 62:156-164.

205. Gonzalez-Moreno, O., Segura, V., Serrano, D., Nguewa, P., de las Rivas, J., and Calvo, A. 2007. Methylseleninic acid enhances the effect of etoposide to inhibit prostate cancer growth in vivo. *Int J Cancer* 121:1197-1204.

Acknowledgments

Curriculum Vitae

Surname: **Niedan**

Forename: **Stephan**

Address: Steingasse 6/3/21 1030 Vienna

Date of Birth: 26.06.1984

Place of Birth: Vienna, Austria

Citizenship: Austria

Email Address: stephan.niedan@ccri.at

WORK EXPERIENCE

Since March 2008   Research position at the Children's Cancer Research Institute (CCRI), Vienna, Austria, Group Heinrich Kovar

May-July 2007:   Trainee position at the Children's Cancer Research Institute (CCRI)
St. Anna Kinderkrebsforschung Vienna - Group Heinrich Kovar: Molecular Biology

Project: *"CXCR4 and metastasis in Ewing's Sarcoma"*

Project*: "Cloning of a regulatory sequence within Jag1 intron 2"*

March-April 2007:   Trainee position at the Max F. Perutz Laboratories, Vienna; - Group Friedrich Propst: Membranes and the cytoskeleton

Project: *"The MAP1B- cytoskeletal protein"*

October-November 2007: Trainee position at the Max F. Perutz Laboratories, Vienna; - Group Markus Teige: Cell Signalling

Project: *"Salt tolerance in A. thaliana"*

PROFESSIONAL EXPERIENCE

16.08- 22.9.2006:	Internship at Ökopharm GmbH, Tamsweg Austria*;*
	HPLC, inductively-coupled-plasma mass-spectrometry (ICP-MS), Microbiology and quality assurance
04.07- 04.08.2005	Internship at Adler Pharma und Vertrieb GmbH, Zell am See - Schüttdorf, Austria*;*
	Microbiology and quality assurance
02.08- 31.08.2004:	Internship at Adler Pharma GmbH, Zell am See - Schüttdorf, Austria*;*
	Microbiology and quality assurance
01.10- 31.12.2002:	Internship at Adler Apotheke KG, Zell am See - Schüttdorf, Austria; *Practical pharmaceutical laboratory* work

UNIVERSITY EDUCATION

Since December 2009	PhD thesis supervised by Dr. Heinrich Kovar at the Children's Cancer Research Institute (CCRI), St. Anna Kinderkrebsforschung, Vienna.
	Topic: "*Mechanisms of EWS-FLI1 driven gene regulation in Ewing´s sarcoma.*"
02.04.2009:	Diploma examination in Genetics, Molecular Medicine and Cell Biology, passed with honors.
March 2008-	
February 2009:	Master thesis supervised by Dr. Heinrich Kovar and Dr. Dave Aryee at the Children's Cancer Research Institute (CCRI), St. Anna Kinderkrebsforschung, Vienna.
	Topic: "*Role of hypoxia and hypoxia inducible factors (HIFs) in cells of Ewing's Sarcoma Family Tumors.*"

| 2003-2009: | Graduate studies in Molecular Biology at the University of Vienna |

MILITARY SERVICE

| 07.01- 05.09.2003: | Military Service, St. Johann i.Pongau, Austria |

EDUCATION

| 1994 – 2002: | Grammar School "Bundes Realgymnasium", with focus on biology, chemistry and physics. Zell am See, Salzburg, Austria |
| *1990 – 1994*: | Primary school in Zell am See, Salzburg, Austria |

SPECIAL SKILLS

Computer platforms	MacOs X, Windows 7/XP/2000
Office distributions	Microsoft Office, Keynote & Pages 09
Graphical distributions	Adobe Photoshop & Illustrator, Gimp, ImageJ, GraphPad Prism
Languages	German (native) and English (fluent in spoken and written)
Driving licence	B

| **AWARDS** | AACR Pezcoller-Scholar-in-Training Award for travel support recognizing outstanding proffered papers by early-career scientists in Europe; AACR Annual Meeting 2012, Chicago |

PUBLICATIONS

Niedan S, Kauer M, Aryee DNT, Meier A, Kofler R, Schwentner R, Poetschger U, Kontny U, Kovar H.
Reactivation of FOXO1 expression as a novel therapeutic strategy for Ewing sarcoma (submitted).

Kovar H, Alonso J, Aman P, Aryee DNT, Jozef Ban, Burchill SA, Burdach S, De Alava E, Delattre O, Dirksen U, Fourtouna A, Fulda S, Helman LJ, Herrero-Martin D, Hogendoorn PCW, Kontny U, Lawlor ER, Lessnick SL, Llombart-Bosch A, Metzler M, Moriggl R, **Niedan S**, Potratz J, Redini F, Richter GHS, Riedmann LT, Rossig C, Schäfer BW, Schwentner R, Scotlandi K, Sorensen PH, Staege MS, Tirode F, Toretsky J, Ventura S, Eggert A, Ladenstein R. (2012), *The First European Interdisciplinary Ewing Sarcoma Research Summit*
Front Oncol. 2012;2:54. Epub 2012 May 29. PMID:22662320

Krapf G, **Niedan S**, Morak M, Kaindl U, Fuka G, Sturtzel C, Aryee DN and Panzer-Gruemayer ER.
ETV6/RUNX1 fusion protein activates the hypoxia pathway thereby enhancing its nuclear localized protein and transactivation activity.
(Manuscript in preparation)

Niedan S, Kauer M, Jug G, Walker RL, Meltzer PS, Kontny U, Kovar H.
Re-activation of EWS-FLI1 suppressed FOXO1 expression as a novel therapeutic strategy for Ewing´s sarcoma.
AACR annual meeting 2012, Chicago, USA, oral presentation

Herrero-Martin D, Fourtouna A, **Niedan S**, Riedmann LT, Schwentner R, Aryee DN.
Factors affecting EWS-FLI1 activity in Ewing's Sarcoma
Sarcoma. 2011;2011:352580. Epub 2011 Nov 10. PMID:22135504

Niedan S, Kauer M, Jug G, Walker RL, Meltzer PS, Kovar H.
A repressive EWS-FLI1 subsignature is the result of FOXO1 suppression and nuclear exclusion. EMBO meeting 2011, Vienna, Austria, poster presentation

Niedan S, Kauer M, Jug G, Walker RL, Meltzer PS, Kovar H.

A repressive EWS-FLI1 subsignature is the result of FOXO1 suppression and nuclear exclusion.

AACR 102nd annual meeting 2011, Orlando, USA, poster presentation

Aryee DN, **Niedan S**, Kauer M, Schwentner R, Bennani-Baiti IM, Ban J, Muehlbacher K, Kreppel M, Walker RL, Meltzer P, Poremba C, Kofler R, Kovar H.

Hypoxia modulates EWS-FLI1 transcriptional signature and enhances the malignant properties of Ewing's sarcoma cells in vitro.

Cancer Res. 2010 May 15;70(10):4015-23. Epub 2010 May 4. PMID:20442286

Kauer M, Jug G, **Niedan S**, Walker RL, Meltzer PS, Kovar H.

A new repressive network module in Ewing's Sarcoma

AACR 101st annual meeting 2010, Washington, USA, poster presentation

Aryee DN, **Niedan S**, Kauer M, Muehlbacher K, Walker RL, Meltzer PS, Poremba C, Kofler R, Kovar H.

Hypoxia modulates EWS-FLI1 transcriptional signature and enhances invasiveness and anchorage-independent growth of Ewing's sarcoma cells in-vitro.

AACR 101st annual meeting 2010, Washington, USA, poster presentation

Aryee DN, **Niedan S,** Muehlbacher K, Kauer M, Ban J, Bennani-Baiti IM, Kovar H.

HIF-1α mediates hypoxia modulation of EWS-FLI1 expression in Ewing's sarcoma family tumors.

AACR 100th annual meeting 2009, Denver, USA, poster presentation